Doctoral Dissertation (Shinshu University)

Electrochemiluminescence and sonochemiluminescence of lucigenin and their applications in antioxidative capacity analysis

(抗酸化能分析を志向するルシゲニンの電気化学発光と

超音波化学発光に関する研究)

2016 年　9 月

Masanori Matsuoka

CONTENTS

Chapter 1 Introduction

1.1 Superoxide anion radical and the analytical techniques for its assays 2

1.2 Chemiluminescence methods 4

1.3 The objectives of this study 9

Chapter 2 Electrochemiluminescence of lucigenin (Luc^{2+}) and its application for the evaluation of antioxidant capacity against superoxide anion radicals

2.1 Introduction 18

2.2 Experimental section

2.2.1 Reagents 20

2.2.2 Instrumentation 21

2.3 Results and discussion

2.3.1 Cathodic ECL of Luc^{2+} on GC Electrodes 25

2.3.2 Quenching of the ECL signals by SOD 30

2.3.3 Quenching of the ECL signals by phenolic compounds 32

2.3.4 Evaluation of antioxidant capacity of phenolic compounds against superoxide anion radicals 36

2.3.5 Comparison with the other methods 38

2.4 Conclusions 49

Chapter 3 Sonochemiluminescence (SCL) of lucigenin

3.1 Introduction 56

3.2 Experimental section

3.2.1 Reagents 57

3.2.2 Instrumentation 58

3.3 Results and discussion

3.3.1 SCL of Luc^{2+} using alcohol as coreactant 62

3.3.2 Effect of output power and frequency 67

3.3.3 Effect of concentration of 2-propanol and solution pH 69

3.3.4 SCL of Luc^{2+} using amine as coreactant 71
3.3.5 Fluorescence probe used for detection of superoxide anion radicals .. 74
3.3.6 Calibration using hypoxanthine and xanthine oxidase 77
3.3.7 Observation of SCL using a sonochemical microreactor 82
3.3.8 Possible pathways and spectroscopic properties of Luc^{2+} SCL system 83
3.4 Conclusions 88

Chapter 4 Antioxidant capacity analysis based on SCL
4.1 Introduction 96
4.2 Experimental section
4.2.1 Reagents 97
4.2.2 Instruments 98
4.2.3 Measurement of the $O_2 \cdot^-$ scavenging properties of samples 98
4.3 Results and discussion
4.3.1 Features of SCL profiles 99
4.3.2 Quenching of the SCL signals 101
4.3.3 Kinetic aspects involved in Luc^{2+} SCL system 104
4.4 Conclusions 108

Chapter 5 Conclusions and future prospects 111

List of publications 115

Acknowledgements 118

Chapter 1

Introduction

1.1 Superoxide anion radical and the analytical techniques for its assays

Reactive oxygen species (ROS) is a term used to describe a number of reactive molecules and free radicals derived from molecular oxygen [1, 2]. Molecular oxygen, with a redox potential of −0.16 V (for an oxygen concentration of 1 atm at pH 7 in the standard state), is a poor oxidant and is fairly benign to biomolecules. However, the electronic structure of oxygen has two unpaired electrons in separate orbitals in its outer shell, making it especially prone to radical formation.

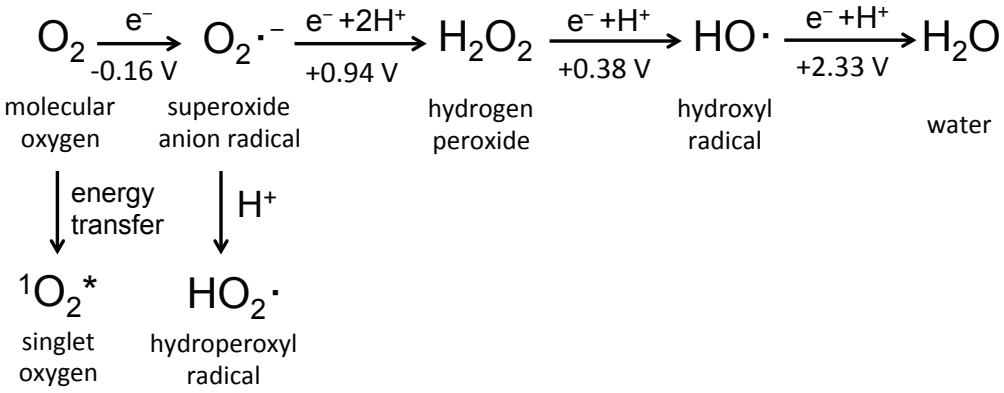

Scheme 1-1 Formation scheme of ROS through electron-transfer reactions

As shown in Scheme 1-1, the one-electron reduction of oxygen results in the formation of the superoxide radical anion ($O_2 \cdot^-$). Moreover, $O_2 \cdot^-$ can be protonated to the hydroperoxyl radical ($HO_2 \cdot$) at low pH ($pK_a = 4.8$); however, in an aqueous solution, $O_2 \cdot^-$ favors dismutation, which leads to the formation of hydrogen peroxide (H_2O_2). Both oxygen species are precursors of the most powerful oxidant ·OH, which has a redox potential of +2.33 V. These oxygen

species could potentially be involved in the production of an energetically richer form of molecular oxygen known as singlet oxygen ($^1O_2$). Therefore, ROS is a collective term that includes the oxygen radicals such as $O_2\cdot^-$, H_2O_2, $\cdot OH$, ozone (O_3), and $^1O_2$ [3,4].

As excessive amounts of ROS formation in the human body can attack biological macromolecules and give rise to protein, lipid, and DNA damage, antioxidants have recently attracted considerable attention because of their tissue-protecting effects via the neutralization of ROS. Currently, there is a strong demand from the food industry to replace synthetic additives, including antioxidants, with natural additives. This requires reliable methods for the evaluation of the antioxidative activity of such additives; indeed, numerous such analytical methods have been reported for measuring the antioxidant activity in terms of the ability to scavenge free radicals [5, 6]. Electron spin resonance (ESR) spectrometry is the only analytical technique that can specifically detect free radicals including ROS. However, ESR is insensitive to the detection of reactive, short-lived free radicals with lifetimes varying from 10^{-9} s for the hydroxyl radical to several seconds for the peroxyl radical at transient concentrations below 10^{-8} M. To overcome this problem, spin trapping has yet to be developed to the stage where short-lived radicals can be trapped by a certain compound (the spin trap) to form radical-adducts [7, 8] that are considerably longer-lived than the original species. Nevertheless, to date, applications are limited owing mainly to the sensitivity problem. Other problems include the specialist nature and relatively

large size and cost of the equipment and instrumentation.

Over the past few years, there has been significant interest in developing an indirect detection method for ROS. Various methods, such as spectrophotometry [9, 10], fluorometry [11, 12], high performance liquid chromatography [13, 14], electrochemistry [15-17], and chemiluminescence [18, 19], have been reported for the detection of ROS after coupling with the appropriate chemical probes. Among them, chemiluminescence is of particular interest because the instrumentation is relatively simple but has high sensitivity and a wide dynamic range.

1.2 Chemiluminescence methods

Chemiluminescence (CL) is the emission of light as the result of a chemical reaction. Two chemicals (A and B) react to form an excited (high-energy) intermediate (P*), which breaks down releasing some of its energy as photons of light to reach its ground state.

$$A + B \rightarrow P^* + \text{other products} \qquad (1\text{-}1)$$

$$P^* \rightarrow P + h\nu \quad \text{(luminescence)} \qquad (1\text{-}2)$$

Using certain specialty CL probes, CL has become a useful method for the detection of free radicals and ROS. Luminol (3-aminophthalhydrazide) has received the most attention as a solution CL reagent for antioxidant capacity analysis (although it lacks specificity) [20, 21]. Lucigenin (N,N'-Dimethyl-9,9'-biacridinium dinitrate, Luc^{2+}) is the second most popular solution CL reagent, but it is specific to $O_2\cdot^-$.

1.2.1 Chemiluminescence of lucigenin for $O_2\cdot^-$ detection

Luc^{2+} is known to produce strong CL in the presence of hydrogen peroxide and reducing agents in alkaline solution. Although the reactions undergone by Luc^{2+} are quite complex, the CL mechanism generally seems to involve three reaction steps, as illustrated in Scheme 1-2. To detect $O_2\cdot^-$, Luc^{2+} must first be reduced by one electron to produce the lucigenin cation radical ($Luc\cdot^+$). $Luc\cdot^+$ then reacts with $O_2\cdot^-$ and yields an extremely unstable dioxetane-type intermediate (Luc(OO)). The decomposition of this intermediate provides an excited state of N-methyl-acridone (NMA∗), which is the primary emitter, emitting at ca. 452 nm [22].

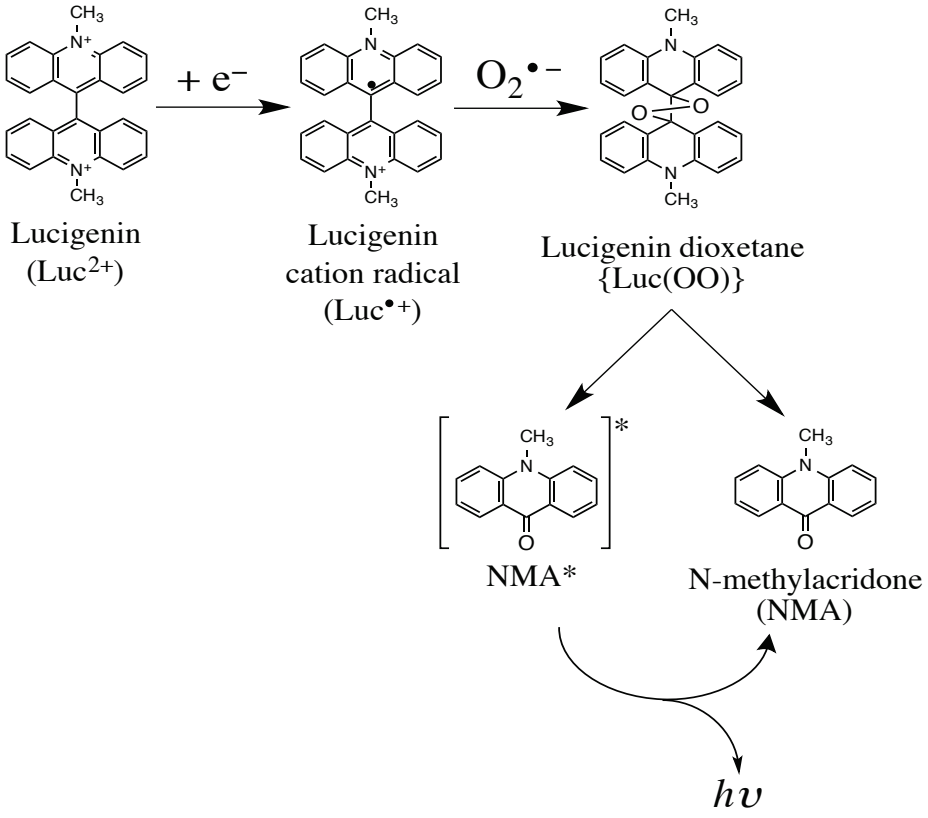

Scheme 1-2 Chemiluminescence reaction of Luc^{2+} with $O_2\cdot^-$

1.2.2 Electrochemiluminescence

Electrochemiluminescence or electrogenerated chemiluminescence (ECL) is a phenomenon where light emission arises from a high energy electron transfer reaction between electrogenerated species. The first detailed ECL study concerning the production of light during electrolysis of aromatic hydrocarbons in non-aqueous solvents was reported by Hercules in 1964 [23]. ECL can be generated by ion annihilation when the ECL emitters (R) are electrochemically oxidized and reduced to sufficiently stable radical cations ($R^{\cdot+}$) and anions ($R^{\cdot-}$), respectively. The radical ions produced are annihilated by the oppositely charged radical ions to generate the excited state species (R*), as shown in the following.

$$R - e \rightarrow R^{\bullet+} \quad (1\text{-}3)$$

$$R + e \rightarrow R^{\bullet-} \quad (1\text{-}4)$$

$$R^{\bullet+} + R^{\bullet-} \rightarrow R + R^{*} \quad (1\text{-}5)$$

$$R^{*} \rightarrow R + h\nu \quad (1\text{-}6)$$

Depending on the energy available in the ion annihilation, the produced R* could be the lowest excited singlet state species ($^1R^*$).

If stable $R^{\bullet-}$ or $R^{\bullet+}$ cannot be produced at the electrode surface, ECL can still be generated when a suitable co-reactant (C) is present, as illustrated in Fig. 1-1. A co-reactant (C) is a compound that can produce a reactive intermediate (a strong reducing or oxidizing agent) by a reaction following the electrochemical or chemical electron transfer reaction [24]. Employing a co-reactant is useful, especially when either $R^{\bullet+}$ or $R^{\bullet-}$ is not stable enough for ECL reaction, or when

the ECL solvent has a narrow potential window such that $R^{\bullet+}$ or $R^{\bullet-}$ cannot be formed. In an aqueous solvent, the use of a co-reactant is very important because water has a narrow potential window; many organic compounds have low solubility, and many radical ions of organic emitters are unstable in an aqueous solvent.

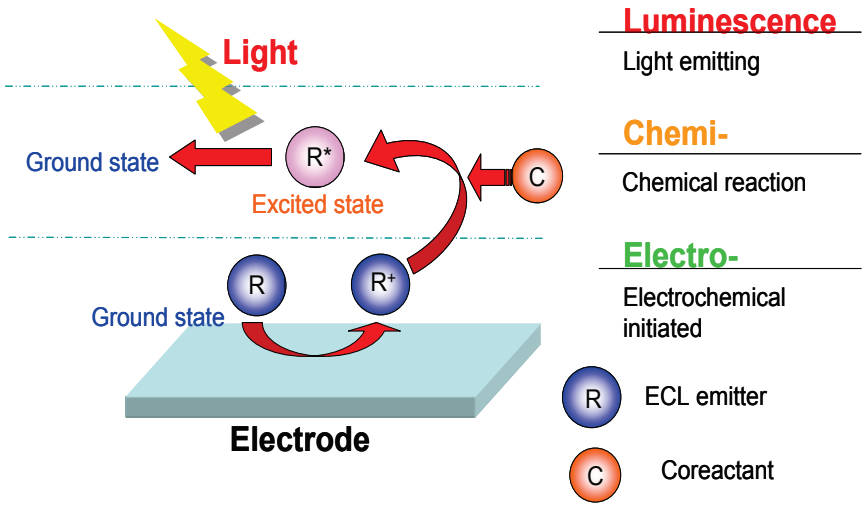

Figure 1-1 Schematic of ECL reaction with a co-reactant

1.2.3 Sonochemiluminescence

The passing of ultrasound through a liquid causes micro-sized gas bubbles to oscillate and, under appropriate conditions, the bubbles undergo a large change in volume and collapse in a near adiabatic process. This is commonly referred to as acoustic cavitation, which is always accompanied by a violent collapse that leads to high pressures (~100 MPa) and temperatures (~5000 K) within and around the bubbles [25]. These bubbles behave as "individual hot-spot microreactors" in which water vapor is cleaved into H and OH radicals to produce

different kinds of reactive species such as ·OH, H·, and H_2O_2 in aqueous solutions according to equations 1-7 to 1-10, where ‘)))’ denotes ultrasonic irradiation.

$$H_2O \;))) \; \cdot OH + H\cdot \qquad (1\text{-}7)$$

$$2\cdot OH \rightarrow H_2O_2 \qquad (1\text{-}8)$$

$$H\cdot + H_2O_2 \rightarrow \cdot OH + H_2O \qquad (1\text{-}9)$$

$$\cdot OH + H_2O_2 \rightarrow \cdot OOH + H_2O \qquad (1\text{-}10)$$

Both ·OH and H· have been detected in ESR spin trapping experiments [26, 27]. These species are capable of initializing the secondary chemical reactions in the ultrasonic field. It is well known that an alkaline luminol solution emits light when irradiated with ultrasound of sufficient intensity (Fig. 1-2). This phenomenon is called sonochemiluminescence (SCL), which is believed to arise from CL reactions with the oxidants produced within the bubbles, such as ·OH, $O_2\cdot^-$, and H_2O_2 [28].

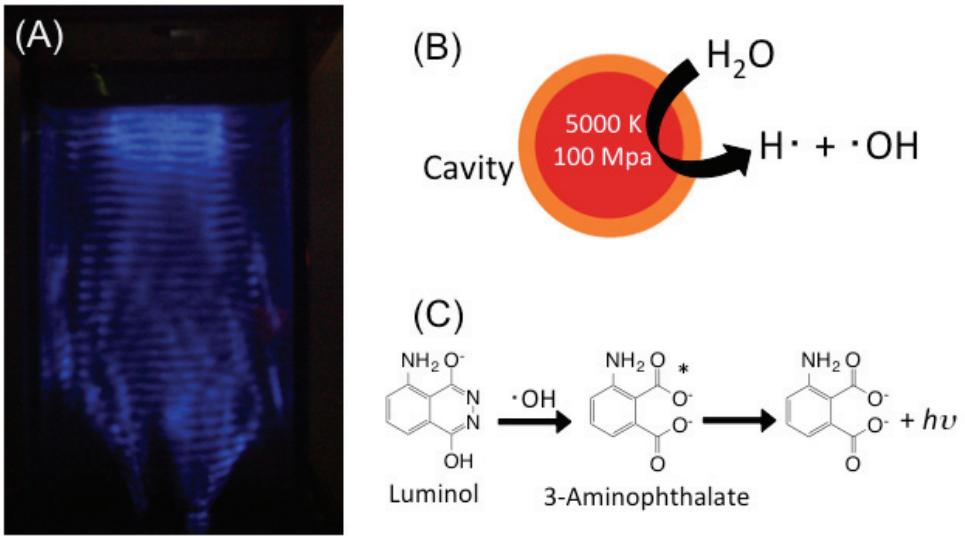

Figure 1-2 (A) Photograph of SCL observed in 50 μM luminol solution (pH 11) upon 490 kHz ultrasound irradiation; (B) Pyrolysis of water in a cavitational bubble; (C) Initialization of the luminol CL reaction.

Although the SCL of luminol has been used to quantify cavitation activity [28, 29], details of the reaction mechanism, including the number and nature of the reactive intermediates that lead to SCL, have not been fully determined.

1.3 Objectives of this study

As described above, recent interest in antioxidants due to their health benefits has led to the development of a number of antioxidant activity assays. Plant foods are rich sources of natural antioxidants such as phenolic acids and flavonoids, which can break the ROS through reaction with the phenolic hydroxyl group and consequently inhibit oxidative damage from the ROS. Antioxidant activity is the rate constant of the reaction between a unique antioxidant and a given free radical. Lucigenin CL coupled with an enzymatic system has been

proposed for the evaluation of antioxidant activity against $O_2\cdot^-$. The hypoxanthine/xanthine oxidase system can release $O_2\cdot^-$, which can then be detected by Luc^{2+} CL [19, 30]. When an antioxidant is present in the assay mixture, it scavenges the $O_2\cdot^-$ and quenches the production of light, as shown in Fig. 1-3 (A). Nevertheless, it was reported that some flavonoids may inhibit radical formation by interfering with the enzyme [31]; furthermore, the validity of Luc^{2+} for detecting biological $O_2\cdot^-$ has recently been questioned in several enzymatic systems because $O_2\cdot^-$ production decreased due to competition between the one-electron reduction of oxygen and Luc^{2+} [32]. Therefore, the development of analytical protocols based on non-enzymatic reactions is greatly desired.

A system for the determination of antioxidant activity has two components: 1) a generator of free radicals, e.g., ROS, and 2) a detector that allows for quantification of the generated species and indicates changes in the measured signal as a response to the presence of antioxidative compounds. In this study, novel determination systems in which $O_2\cdot^-$ was electrochemically or sonochemically generated were developed based on ECL and SCL in enzyme-free systems, as illustrated in Fig. 1-3 (B) and (C). Both ECL and SCL potentially provide the following benefits for the evaluation of antioxidant activity toward $O_2\cdot^-$.

1) *In situ* and reagentless ROS generation. The reagents of the SCL system can thus be greatly simplified, and mechanical mixing, which is necessary in most CL measurements, is avoided.

2) ECL has some advantages over CL because the ECL reaction occurs only in the diffusion layer adjacent to the electrode. ECL can be more selective than CL because the generation of excited states can be selectively controlled by varying the electrode potentials.

3) The automatic SCL device consists of a CL analyzer and an ultrasonic wave control device. The SCL produced by the irradiation of ultrasound results in highly reproducible, sensitive, and rapid measurements.

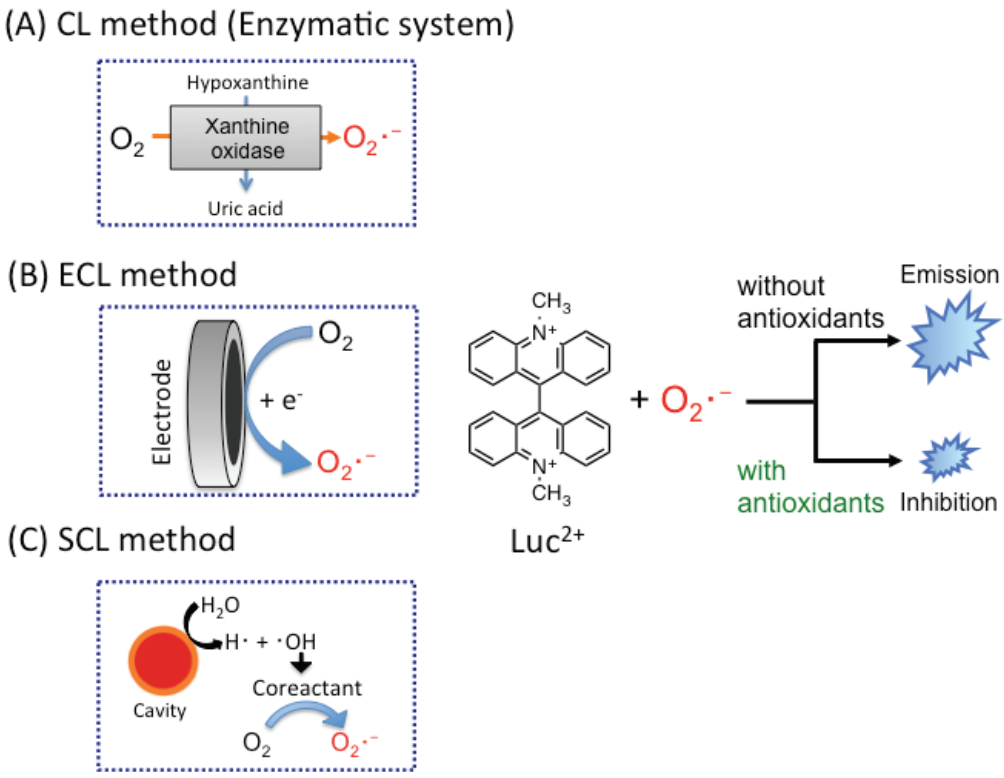

Figure 1-3 Schematic diagram of the generation of a superoxide anion radical in the CL, ECL, SCL methods, and the validation of antioxidation capacity from the inhibition of light emission.

In this thesis, fundamental studies on ECL and SCL systems for Luc^{2+} were carried out for the purpose of developing a reliable analytical tool for antioxidant activity evaluation. This study provides chemical information about such methods and clarifies the reaction mechanisms, scavenging efficiency, and kinetic scavenging rates of antioxidants. Moreover, the study will aid the identification of reactive species and the quantification of the extent of antioxidant scavenging through various assays. It will also increase the comparability and understanding of results and bring a more rational basis to the evaluation of these assays.

In this dissertation, Chapter 2 describes the ECL behavior of Luc^{2+} at a glassy carbon electrode in aqueous solution. It is the first report of a novel and non-enzymatic method for studying the free radical-scavenging properties of phenolic compounds toward $O_2\cdot^-$ using a cathodic ECL of Luc^{2+}. Chapter 3 describes the SCL behavior of Luc^{2+} in aqueous solutions irradiated with 500 kHz ultrasound. The evidence for $O_2\cdot^-$ production is examined and the most likely pathways for SCL are proposed. In Chapter 4, attention is focused on the introduction of SCL into the field of analytical chemistry. The Luc^{2+} SCL system is applied to the analysis of the antioxidant capacity of selected phenolic compounds and flavonoids. The kinetics of the reaction of $O_2\cdot^-$ with antioxidants within this system are discussed.

References

[1] J.F. Turrens, Mitochondrial formation of reactive oxygen species, *J. Physiol.* **552** (2003) 335.

[2] F. Muller, The nature and mechanism of superoxide production by the electron transport chain: Its relevance to aging, *J. Am. Aging Assoc.*, **23** (2000) 227.

[3] O. Hirayama, M. Takagi, K. Hukumoto, S. Katoh: Evaluation of Antioxidant Activity by Chemiluminescence, *Anal. Biochem.*, **247** (1997) 237.

[4] S.R. Georgetti, R. Casagrande, V.M. Di Mambro, A.E. Azzolini, M.J. Fonseca, Evaluation of the antioxidant activity of different flavonoids by the chemiluminescence method, *AAPS PharmSci.* **5** (2003) E20.

[5] E. Niki, H. Shimaski, M. Mino, Antioxidantism-Free Radical and Biological Defense, Gakkai Syuppan Center, Tokyo (1994)

[6] C.M. Liyana-Pathirana, F. Shahidi, C. Alasalvar, Antioxidant activity of cherry laurel fruit (Laurocerasus officinalis Roem.) and its concentrated juice, *Food Chemistry*, **99**, 121–128(2006).

[7] M. L. Vicente, J. A. Empis, N. Deighton, S. M. Glidewell, B. A. Goodman and C. C. Rowlands, Use of EPR and ENDOR spectroscopy in conjunction with the spin trapping technique to study the high-temperature oxidative degradation of fatty acid methyl esters, *J. Chem. Soc.*, *Perkin Trans.*, **2** (1998) 449.

[8] P. T. Gardner, D. B. McPhail and G. G. Duthie, Electron spin resonance spectroscopic assessment of the antioxidant potential of teas in aqueous and organic media, *J. Sci. Food Agric*., **76** (1998) 257.

[9] J. M. McCord and I. Fridovich, Superoxide dismutase an enzymic function for erytherocuprein (hemocuprein), *J. Biol. Chem.*, **244** (1969) 6049.

[10] C. Beauchamp and I. Fridovich, Superoxide dismutase: Improved assays and

an assay applicable to acrylamide gels**,** *Anal. Biochem*., **44** (1971) 276.

[11] B. Ou, M. Hampsch-Woodill, J. Flanagan, E. K. Deemer, R.L. Prior, D. Huang, Novel fluorometric assay for hydroxyl radical prevention capacity using fluorescein as the probe, *J Agric Food Chem.* **50** (2002) 2772.

[12] R. H. Bisby, R. Brooke, S. Navaratnam, Effect of antioxidant oxidation potential in the oxygen radical absorption capacity (ORAC) assay, *Food Chem.*,**108** (2008) 1002.

[13] I. I. Koleva , H. A. G. Niederländer, and T. A. van Beek, An On-Line HPLC Method for Detection of Radical Scavenging Compounds in Complex Mixtures, *Anal. Chem.*, **72** (2000) 2323.

[14] Dapkevicius, Airidas; van Beek, Teris A.; Niederlaender, Harm A. G.; de Groot, Aede, Online Detection of Antioxidative Activity in High-Performance Liquid Chromatography Eluates by Chemiluminescence, *Anal. Chem.*, **71** (1999) 736.

[15] O. Korbut, M. Bučková, J. Labuda and P. Gründler, Voltammetric Detection of Antioxidative Properties of Flavonoids Using Electrically Heated DNA Modified Carbon Paste Electrode, *Sensors*, **3** (2003) 1.

[16] S. Gorjanović, D. Komes, F. T. Pastor, A. Belščak-Cvitanović, L. Pezo, I. Hečimović, and D..Sužnjević, Antioxidant capacity of teas and herbal infusions: polarographic assessment, *J Agric Food Chem*. **60** (2012) 9573.

[17] J. Liu , C. Roussel , G. Lagger , P. Tacchini , and H. H. Girault, Antioxidant Sensors Based on DNA-Modified Electrodes, *Anal. Chem.*, **77** (2005) 7687.

[18] X. Huang, Y. Zhou, M. Ma, Z. Cai, and T. Li, Chemiluminescence Evaluation of Antioxidant Activity and Prevention of DNA Damage Effect of Peptides Isolated from Soluble Eggshell Membrane Protein Hydrolysate, *J. Agric. Food Chem.*, **58** (2010) 12137.

[19] S. Yamaguchi, N. Kishikawa, K. Ohyama, Y. Ohba, M. Kohno, T. Matsuda,

A. Takadate, K. Nakashima and N. Kuroda, Evaluation of chemiluminescence reagents for selective detection of reactive oxygen species, *Anal. Chim. Acta*, **665** (2010) 74.

[20] Aldo Roda (Ed), Chemiluminescence and Bioluminescence: Past, Present and Future, Royal Society of Chemistry, page 2011 - 590

[21] Total antioxidant activity measured by chemiluminescence methods, *Methods in Enzymology, Oxidants and Antioxidants Part A*, **299** (1999) 3.

[22] R. Maskiewicz, D. Sogah and T. C. Bruice, Chemiluminescent Reactions of Lucigenin. 1. Reactions of Lucigenin with Hydrogen Peroxide, *J. Am. Chem. Soc.*, **101** (1979) 5347.

[23] D. M. Hercules, Chemiluminescence Resulting from Electrochemically Generated Species, *Science*, **145** (1964) 808.

[24] A.J. Bard (Ed), Electrogenerated Chemiluminescence, Dekker, New York, 2004.

[25] K. S. Suslick, Sonochemistry, *Science*, **247** (1990) 1439.

[26] K. Makino, M. M. Mossoba and P. Riesz, Chemical Effects of Ultrasound on Aqueous Solutions. Evidence for ·OH and ·H by Spin Trapping, *J. Am. Chem. Soc.*, **104** (1982) 3537.

[27] K. Makino, M. M. Mossoba and P. Riesz, Chemical Effects of Ultrasound on Aqueous Solutions. Formation of Hydroxyl Radicals and Hydrogen Atoms, *J. Phys. Chem.*, **87** (1983) 1369.

[28] H. N. McMurray and B. P. Wilson, Mechanistic and Spatial Study of Ultrasonically Induced Luminol Chemiluminescence, *J. Phys. Chem. A*, **103** (1999) 3955.

[29] T. Tuziuti, K. Yasui, T. Kozuka, A. Towata and Y. Iida, Enhancement of sonochemical reaction rate by addition of micrometer-sized air bubbles, *J. Phys. Chem. A*, **110** (2006) 10720.

[30] J. Storch and E. Ferber, Detergent-amplified chemiluminescence of lucigenin for determination of superoxide anion production by NADPH oxidase and xanthine oxidase, *Anal. Biochem.,* **169** (1988) 262.

[31] P. Cos, L. Ying, M. Calomme, J. P. Hu, K. Cimanga, B. V. Poel, L. Pieters, A. J. Vlietinck and D. V. Berghe, Structure-activity relationship and classification of flavonoids as inhibitors of xanthine oxidase and superoxide scavengers, *J. Nat. Prod.*, **61** (1998) 71.

[32] Y. Li, H. Zhu, P. Kuppusamy, V. Roubaud, J. L. Zweier, and M. A. Trush, Validation of lucigenin (bis-N-methylacridinium) as a chemilumigenic probe for detecting superoxide anion radical production by enzymatic and cellular systems, *J. Biol. Chem.*, **273** (1998) 2015.

Chapter 2

Electrochemiluminescence of lucigenin and its application for the evaluation of antioxidant capacity against superoxide anion radicals

2.1 Introduction

Phenolic compounds such as flavonoids (e.g., quercetin and rutin) and hydroxycinnamic acid derivatives (e.g., caffeic acid) are known to possess free-radical scavenging properties. They can scavenge harmful reactive oxygen species (ROS) via the donation of electrons with more or less efficiency. Additionally, they have gained much interest as natural antioxidants. [1-3] As the presence of these compounds in foods may prevent the development of many diseases, including atherosclerosis and cancer, in the last few years, there has been significant interest toward developing new methods for estimating the total antioxidant capacity of these compounds and elucidating the relationship between their chemical structure and antioxidant activity. [4, 5] ROS are various forms of activated oxygen, including superoxide anion radicals ($O_2{\cdot}^-$), hydroxyl radicals (·OH), and nonfree radical species (H_2O_2). Because different ROS have their own characteristics in terms of generation mechanism, lifetime, and chemical reactivity, the development of a method capable of evaluating the antioxidant capacity toward a certain ROS is necessary.

Note that $O_2{\cdot}^-$ is formed by the one-electron reduction of dioxygen (O_2), which is abundantly present in nature. It appears to be a particularly interesting species because it has a longer lifetime than ·OH; moreover, its various possible reaction pathways make $O_2{\cdot}^-$ a good candidate for probing mechanisms. [6] A few analytical methods have been developed to determine scavenging capacity, specifically of $O_2{\cdot}^-$. These assays are generally based on $O_2{\cdot}^-$ generation using an enzyme system, for example, the hypoxanthine/xanthine oxidase system. The inhibition reaction by the antioxidant

substrate is usually measured by spectrophotometry, [7] amperometry, [8] and chemiluminescent techniques. [9] Nevertheless, since some flavonoids (like quercetin) may inhibit radical formation by interfering with the enzyme, [10] the development of analytical protocols based on non-enzymatic reactions is greatly desired.

Recently, M. L. Abasq *et al.* proposed an electrochemical method with a non-enzymatic reaction for evaluating the antioxidant capacities of some phenolic compounds. [11, 12] The method was based on the kinetics of the reaction of the antioxidant phenols with $O_2{\cdot}^-$. A cyclic voltammetric technique was used to generate $O_2{\cdot}^-$ by the reduction of molecular oxygen in aprotic media. In the same experiment, the consumption of the radical was directly measured by the anodic current decay of the superoxide anion radical oxidation in the presence of increasing concentrations of antioxidant substrate. However, the approach was only applicable in aprotic media. [12]

The electrogenerated chemiluminescence (ECL) of lucigenin (Luc^{2+}) has been studied in both aqueous and non-aqueous media at solid electrodes. In the cathodic process, the coupling reaction between an *in situ* electrogenerated radical species, such as one-electron reduced lucigenin ($Luc{\cdot}^+$) and $O_2{\cdot}^-$, would lead to the formation of a dioxetane-type intermediate and ultimately to the generation of chemiluminescence in neutral or relatively weak alkaline solutions (pH 7–10). [13-16] Lucigenin ECL has been used for a diverse range of analytical applications, including the detection of $O_2{\cdot}^-$ production, [17-19] riboflavin, and isatin, based on the enhancement of ECL signals. [20,21] If an antioxidant is added into the Luc^{2+}/O_2 system, ECL intensity is inhibited and the degree of ECL decrease depends on both the antioxidant capacity and the

concentration. Until now, however, the use of ECL in an antioxidant capacity study has not been well investigated. Herein, we report our original results evaluating the antioxidant capacity of phenolic compounds, specifically against $O_2^{\cdot -}$, using cathodic ECL of Luc^{2+}. In terms of its application, ECL may have more promise than protocols based on enzymatic reaction because it mitigates problems that are due to the inhibition of enzyme activity by phenolic compounds.

2.2 Experimental section

2.2.1 Reagents

All reagents were of analytical grade and used as received. Lucigenin (bis-N-methylacridiniumnitrate), hypoxanthine, xanthine oxidase from Buttermilk and superoxide dismutase (SOD) of bovine erythrocytes (5140 U/mg) were purchased from Nacalai Tesque (Kyoto, Japan). 2,2-diphenyl-1-picrylhydrazyl radical (DPPH) and N-methylaciridone (NMA) were purchased from Tokyo chemical Industry Co. (Tokyo, Japan). Methanol was purchased from Wako Pure Chemical Industries (Osaka, Japan). The phenolic compounds, catechol, 2,3-dihydroxy benzoic acid (2,3-DHBA), 2,4-dihydroxy benzoic acid (2,4-DHBA) and salicylic acid were purchased from Wako Pure Chemical Industries; 2,5-dihydroxy benzoic acid (2,5-DHBA) was purchased from Alfa Aesar (Lancashire, United Kingdom); protocatechuic acid, catechin and rutin were purchased from Nacalai Tesque; caffeic acid and quercetin were purchased from Tokyo Chemical Industry Co. Surfactants, Triton X-100 was purchased from Nacalai tesque; Tween 20 was purchased from Tokyo Chemical Industry Co.; CTAB was purchased

from Wako Pure Chemical Industries. A solution containing 0.1 M of KNO_3 was used as a supporting electrolyte in this study. The stock solution of DPPH was prepared by dissolving 24.0 mg DPPH into 100 mL of methanol and stored in a freezer. Working solution of DPPH was prepared by mixing 10 mL of stock solution and 45 mL methanol (0.44 g L^{-1} DPPH). All solutions were prepared with distilled water purified by a WS200 distillation system (Yamato Scientific Co., Tokyo, Japan).

2.2.2 Instruments

The ECL measurement was performed with an EG&G/PAR 263A potentiostat / galvanostat. The measurements were conducted in an electrochemical cell by using a salt-bridge system to separate the working and counter electrodes. Pt wire was served as the counter electrode and Ag/AgCl reference electrode (RE-1, BAS Japan) was used. A glassy carbon disk (Tokai Carbon Co., Tokyo, Japan) with diameter of 3 mm was used as a working electrode. Before measurement, the working electrode was polished with 0.3 μm of alumina slurry, sonicated in an ultrasound bath, and finally rinsed with water. The light emission from the electrode surface was measured by H7732-10 PMT photosensor module equipped with a C7319 signal preamplifier unit (Hamamatsu Photonics, Japan). C7169 power supply unit (Hamamatsu Photonics, Japan) was used for driving the photosensor module. The electrode surface of the working electrode was 0.5 mm distance from the optical window. The dissolved oxygen was measured with a polarographic oxygen sensor (Model DO-5509, LUTRON Electronic, Taiwan). ECL spectra were measured using an USBFL-2000 spectrometer (Ocean Optics, USA).

The CL measurements were performed by a flow-injection system using micro mixing cell as shown in Fig. 2.2. A SPE-1 syringe pump (AS ONE, Japan) was used as a flow pump with flow rate of 150 μL min^{-1}. The solution of 50 μM hypoxanthine contained with surfactant was injected into the flow. The emission from the mixing cell was measured by PMT module. The light emission measurement system was the same as ECL system. Absorption spectra were measured by UV-2550 UV-Visible spectrophotometer (Shimadzu).

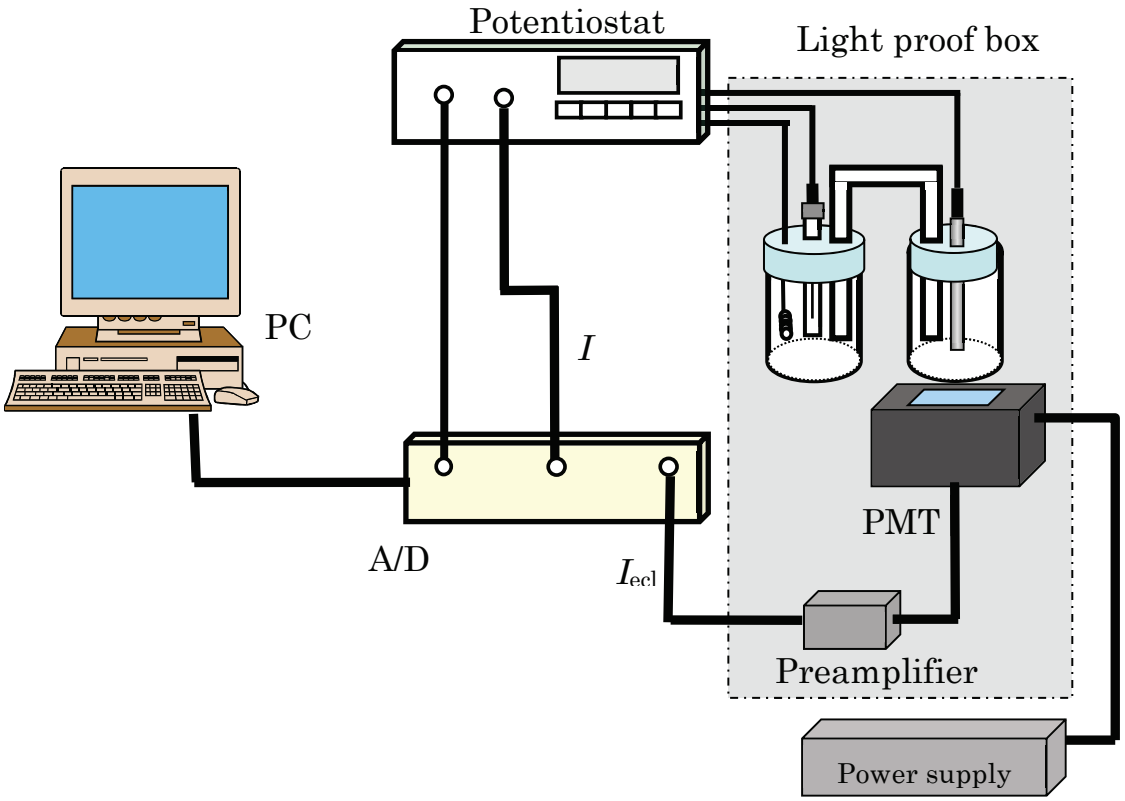

Figure. 2-1 The ECL measurement system.

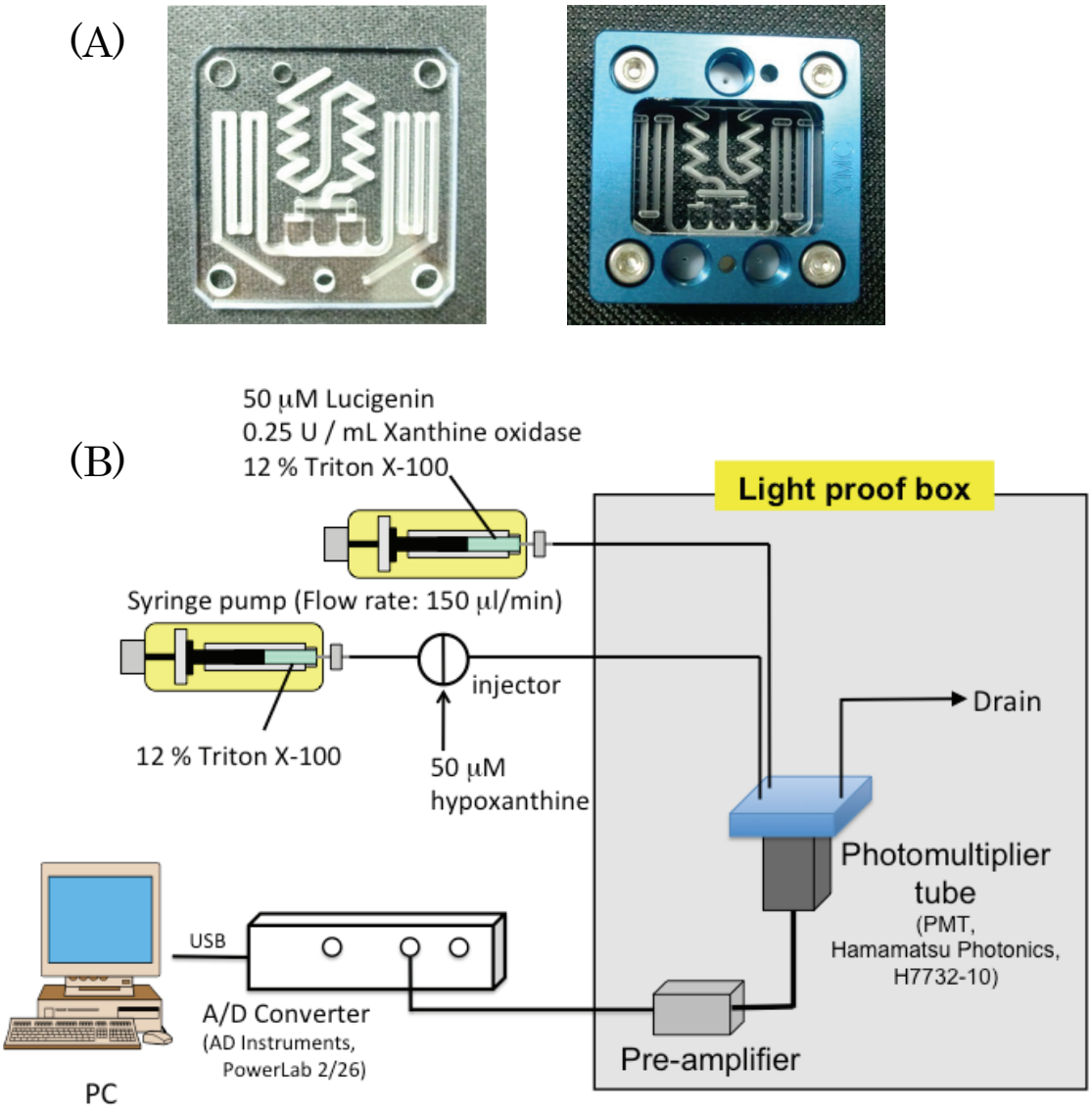

Figure 2-2 (A) A mixing cell used for CL detection. (B) Schematic diagram of Luc^{2+}-HX/XOD CL system.

2.3 Results and discussion

2.3.1 Cathodic ECL of Luc^{2+} on GC electrodes

Figure 2-3 shows the simultaneous linear sweep voltammograms (A) and corresponding ECL responses (B) of 50 μM Luc^{2+} in 0.1 M KNO_3 aqueous solution (Ar or O_2−saturated) on the GC electrode. The blue curves are the responses measured in an O_2-free (Ar-saturated) solution, whereas the red curves are the responses in an O_2-saturated solution. In the absence of O_2, a reduction peak was observed at -0.3 V vs. Ag/AgCl (Fig.2-3 (a)). This could be due to the reduction of Luc^{2+}. The electrode reaction involved a one-electron reduction of Luc^{2+} to produce an intermediate radical, $Luc^{\cdot +}$, and was subsequently reduced to Luc^0 at the electrode surface. [15, 16] The produced $Luc^{\cdot +}$ and Luc^0 could be confirmed at about +0.35 V (Fig. 2-4 II), +0.65 V (Fig. 2-4 III) *vs*. Ag/AgCl in a subsequent anodic potential scan in a cyclic voltammogram (Fig. 2-4), respectively. (peak I is reduction of Luc^{2+}) However, there was no ECL response that could be observed during the reduction process of Luc^{2+} in the absence of O_2 (Fig. 2-3 (c)). In the O_2 saturated solution, a much lager reductive wave appeared at around –0.6 V *vs*. Ag/AgCl, which is attributed to the O_2 reduction, as is shown in Fig. 2-3 (b). The electrochemical reduction steps for O_2 involve a one-electron reduction of O_2 to $O_2^{\cdot -}$, and the subsequent one-electron reduction to produce of H_2O_2. [22, 23] A distinct ECL signal was detected at the electrode potential coinciding with the reduction potential of O_2, as can be seen in Fig. 2-3 (d).

The cathodic ECL of Luc^{2+} has been studied, and was suggested to involve 3 reaction steps: (1) a one-electron reduction of Luc^{2+} to produce radical $Luc^{\cdot +}$; (2) $Luc^{\cdot +}$

then reacts with a superoxide anion radical ($O_2\cdot^-$) and yields an extremely unstable dioxetane-type intermediate; (3) the decomposition of this intermediate provides an excited state of N-methylacridone (*NMA); (4) which will be the primary emitter, emitting at ca. 452 nm. [13-16] It is worthy of note that the ECL spectrum with a broad band at 510 nm was observed in our experiment. This fact suggests that the light emission originated from the excited triplet state $^*Luc^{2+}$ through the energy-transfer process from *NMA to Luc^{2+}, since Luc^{2+} fluoresced at 510 nm. The ECL reaction scheme for the Luc^{2+}/O_2 system is summarized in Scheme 2-1.

Fig. 2-5 shows the effect of the dissolved oxygen concentration on the Luc^{2+} ECL responses. The ECL intensity decreased with the decrease of dissolved oxygen, and nearly no ECL peak was observed in an Ar saturated solution. This means that the ECL signal is proportional to the $O_2\cdot^-$ concentration *in situ* generated at the electrode surface. The influence of hydrogen peroxide (H_2O_2) on the Luc^{2+} cathodic ECL process was examined, as is shown in Fig. 2-6. It can be seen that the co-existing H_2O_2 up to a concentration level of 200 μM has almost no influence on the ECL response. Consequently, we had confirmed the ECL specifically responded to the $O_2\cdot^-$ concentration level at the electrode surface.

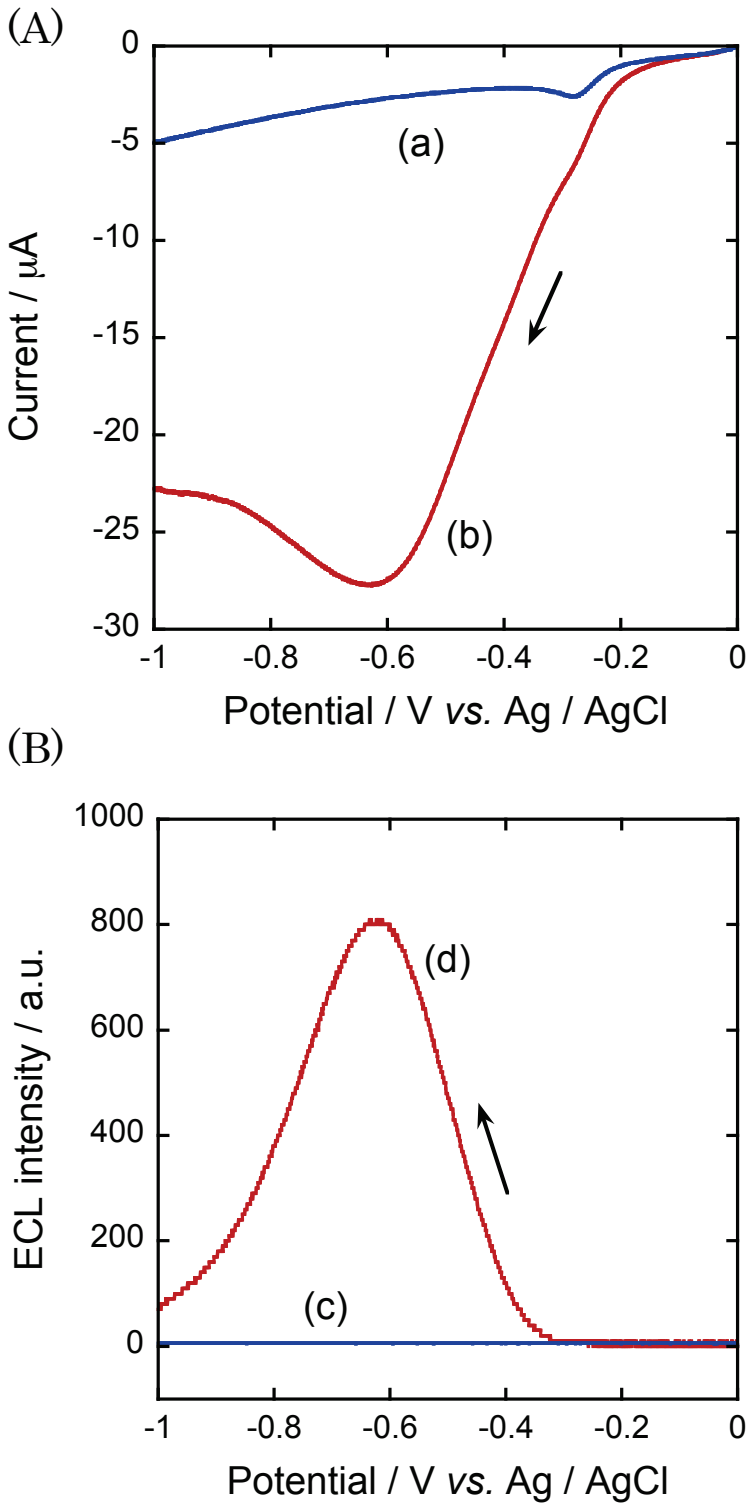

Figure 2-3 (A) linear sweep voltammograms and (B) the corresponding ECL responses of 50 μM Luc^{2+} in 0.1 M KNO_3 with Ar ((a), (c)) or O_2 saturated ((b), (d)) on the GC electrode. The Scan rate was 50 mV s^{-1}. The arrow stands for the potential sweep direction.

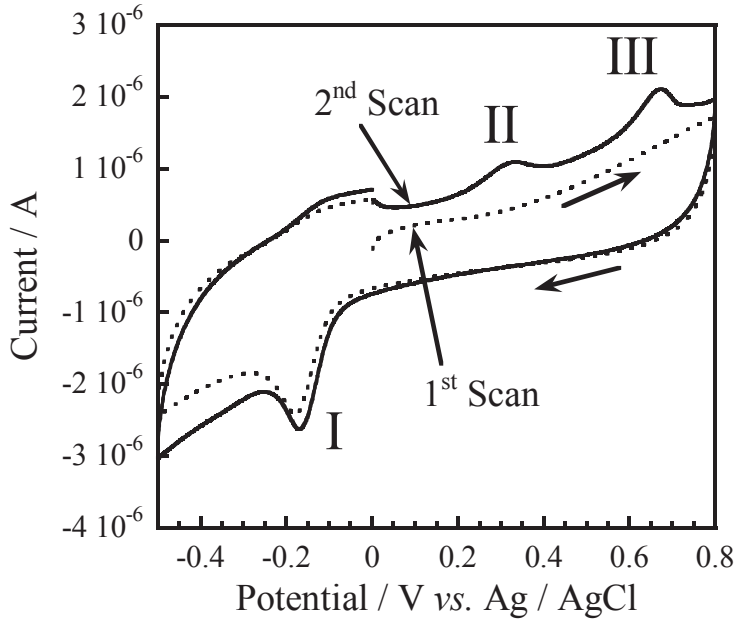

Figure 2-4 Cyclic voltammograms of 50 μM lucigenin in 0.1 M KNO_3 saturated with Ar. Dotted line: the first scan; solid line: the second scan. Arrows show the sweep direction. Scan rate was 50 mV s^{-1}.

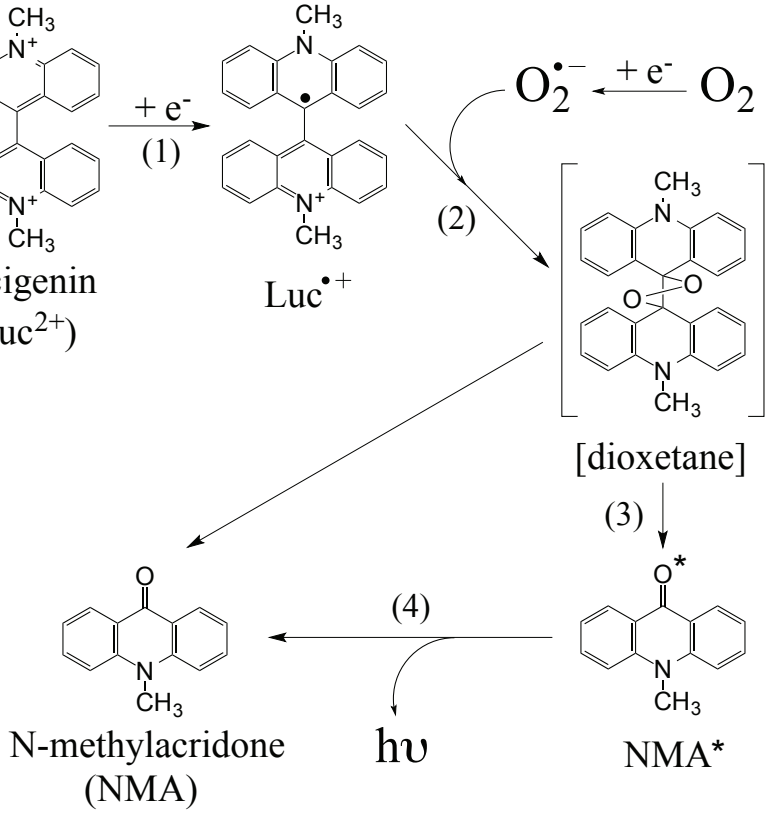

Scheme 2-1 Possible pathways of Luc^{2+}/O_2 cathodic ECL system.

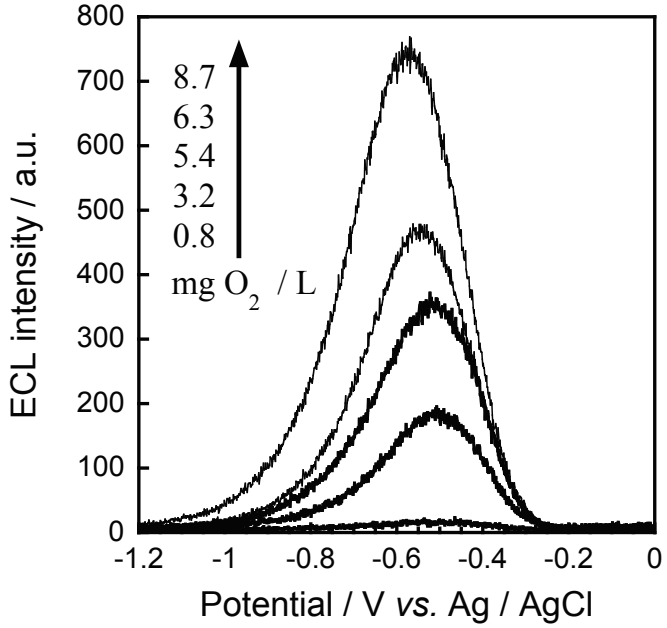

Figure 2-5 Effect of the dissolved oxygen on the cathodic ECL responses. Scan rate is 50 mV s^{-1}. Electrolytic solution: 50 μM lucigenin in 0.1 M KNO_3. The concentrations of dissolved oxygen were measured with a polarographic oxygen sensor.

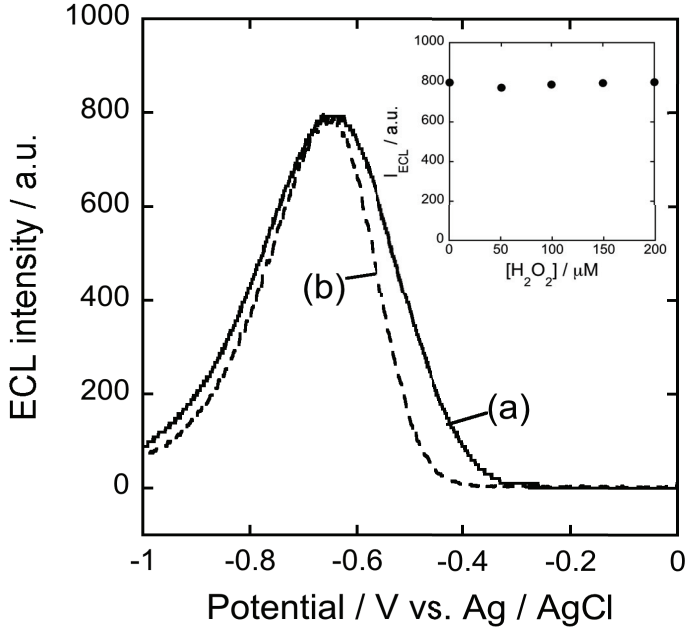

Figure 2-6 Effect of H_2O_2 on cathodic Luc^{2+} ECL. Solid line (a): without H_2O_2; dotted line (b): in the presence of 200 μM H_2O_2. Inset: the dependence of H_2O_2 concentration on the ECL intensity.

2.3.2 Quenching of the ECL signals by SOD

In Figure 2-7, it was found that the intensity of the ECL signal was inhibited by about 60% upon the addition of 0.1 U mL^{-1} of superoxide dismutase (SOD). SOD was discovered by McCord and Fridovich in 1968, [24, 25] and is known as one of the most important antioxidative enzymes that can catalyze the dismutation of $O_2 \cdot^-$ into hydrogen peroxide and molecular oxygen. The antioxidant activity of SOD can be evaluated from an ECL inhibition rate (%), which can be calculated from the following equation:

$$\text{ECL inhibition rate } (\%) = \frac{I_{\text{ECL}}^0 - I_{\text{ECL}}}{I_{\text{ECL}}^0} \times 100\% \qquad (2\text{-}1)$$

where $I_{\text{ECL}}{}^0$ is the ECL intensity measured without SOD, and I_{ECL} is that measured in the presence of SOD. Figure 2-8 shows that an increase in the concentrations of SOD enhances the scavenging activity against $O_2 \cdot^-$, and therefore increases the ECL inhibition rate (%). The intensity of Luc^{2+} ECL is almost all inhibited by addition of 5 U mL^{-1} SOD. This is an evidence that Luc^{2+} ECL originates from $O_2 \cdot^-$ and supports the reaction mechanism supposed in section 2.3.1.

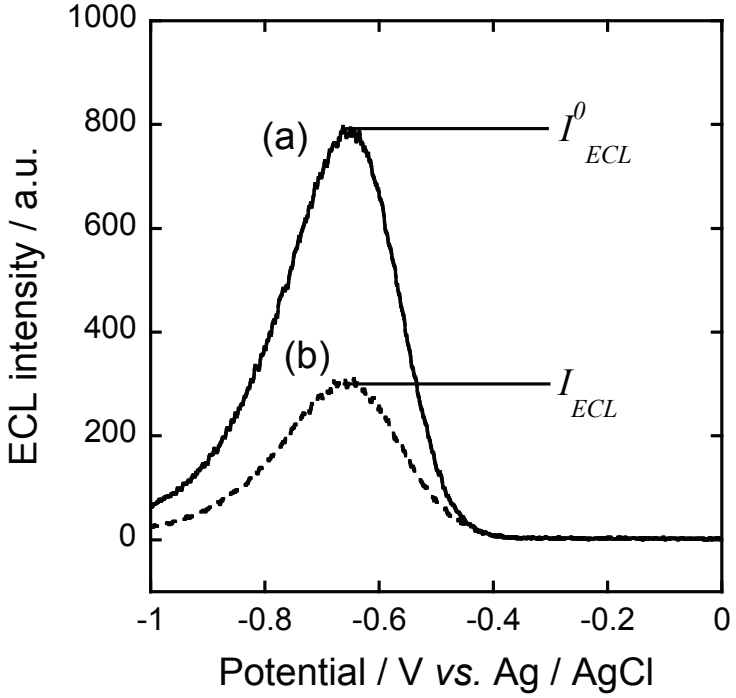

Figure 2-7 Inhibition of the ECL intensity by the addition of SOD. Solid line (a) without SOD; dotted line (b) in the presence of 0.1 U mL^{-1} SOD. Solution condition was the same as that in Fig. 2.3. Scan rate was 50 mV s^{-1}.

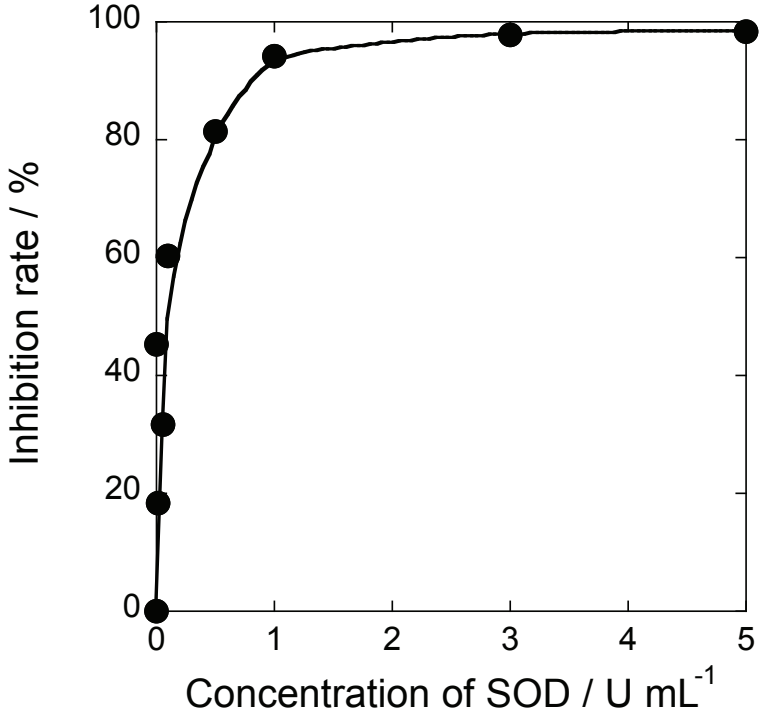

Figure 2-8 Dependence of SOD concentration on the ECL inhibition rate.

2.3.3 Quenching of the ECL signals by phenolic compounds

Typical phenolic compounds that possess the antioxidant activity can be naturally classified into two big groups, flavonoids and nonflavonoids. [26] In this study, the flavonoid compounds (quercetin, catechin and rutin) and some phenolic derivatives with different hydroxylated positions (caffeic acid, protocatechuic acid, catechol, 2, 3-DHBA, 2,4-DHBA, 2,5-DHBA, salicylic acid) were investigated as model compounds (Figure 2-9). Because some of flavonoids and phenolic derivatives undergo autoxidation, and are unstable under a higher pH condition, the experiments were conducted at pH 7 in this study [27].

Upon the addition of catechin into the Luc^{2+}/O_2 ECL system, we obtained a concentration-dependent inhibition of ECL similar to that for SOD (Figure 2-10). Apart from catechin (pK_{a1} = 8.85, pK_{a2} = 9.97), [28] other phenolic compounds, such as quercetin (pK_{a1} = 7.19, pK_{a2} = 9.36), [29] rutin (pK_{a1} = 4.47, pK_{a2} = 8.32), [30] catechol (pK_{a1} = 9.43), [29] caffeic acid (pK_{a1} = 4.47, pK_{a2} = 8.32) [28] and protocatechuic acid (pK_{a1} = 4.38, pK_{a2} = 8.74), [28] also exhibited a significant ECL inhibitory effect. Quenching of the ECL signals suggests that the phenolic compounds have potentials to scavenge $O_2\cdot^-$ produced at the electrode surface. The reaction of $O_2\cdot^-$ with the phenolic compounds, for example catechin, is suggested to be the scheme shown in Scheme 2-2.

Most flavonoids are not dissociated at pH 7. It can act as an antioxidant by donating an electron to the $O_2\cdot^-$ and produce a flavonoid phenoxyl radical (equation 2-2) through a proton-transfer process. The radical is subsequently deprotonated to a flavonoid anion radical because of a relatively low pK_a (=4.6) [30] of the flavonoid

phenoxyl radical (equation 2-3). The flavonoid anion radical can act as a secondary antioxidant by donating an electron to the $O_2\cdot^-$ to yield the corresponding quinone-type metabolites (oxidized form of catechin) according to the equation 2-4. The reaction mechanisms for the scavenging of $O_2\cdot^-$ by phenolic derivatives are considered to be the same as that for catechin, although caffeic acid and protocatechuic acid existed as monoanions at pH 7 due to deprotonation of the carboxylic acid group.

As shown in the reaction of the equation 2-4, the reaction can accompany some side reactions, such as a dimerization reaction, and is able to generate hydrogen peroxide (H_2O_2) due to an autoxidative behavior of the phenolic compound. The presence of H_2O_2 usually affects the results of the antioxidant activity in many chemiluminescence assays. [31] The ECL method, however, provides information about the radical scavenging effect specifically toward $O_2\cdot^-$. The relative capacity of phenolic compounds to scavenge $O_2\cdot^-$ could thus be evaluated from the degree of the inhibition rate of ECL signals.

I. Polyphenols

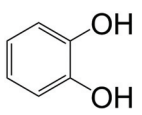

Catechol

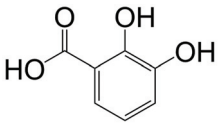

2,3-Dihydroxy benzoic acid (2,3-DHBA)

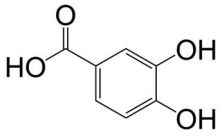

Protocatechuic acid (3,4-DHBA)

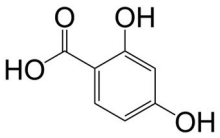

2,4-DHBA

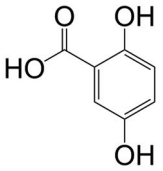

2,5-DHBA

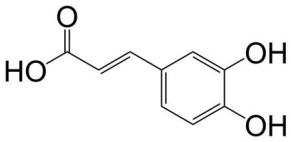

Caffeic acid

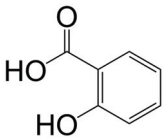

Salicylic acid

II. Flavonoids

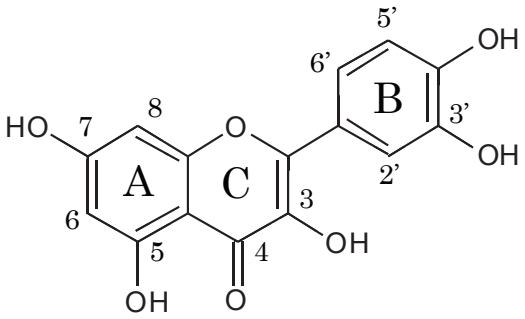

Quercetin

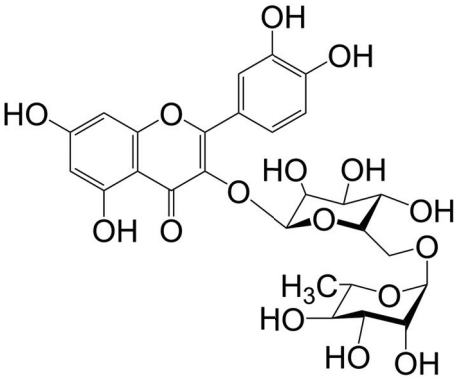

Rutin

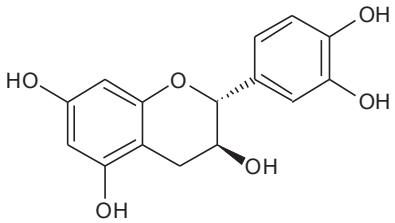

(+)-Catechin

Figure 2-9 Chemical structures of the phenolic compounds investigated in this study.

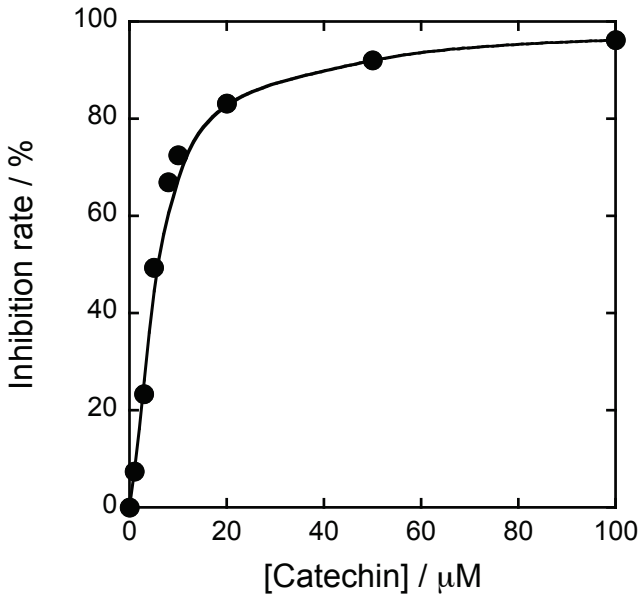

Figure 2-10 Dependence of the concentration of catechin on the ECL inhibition rate.

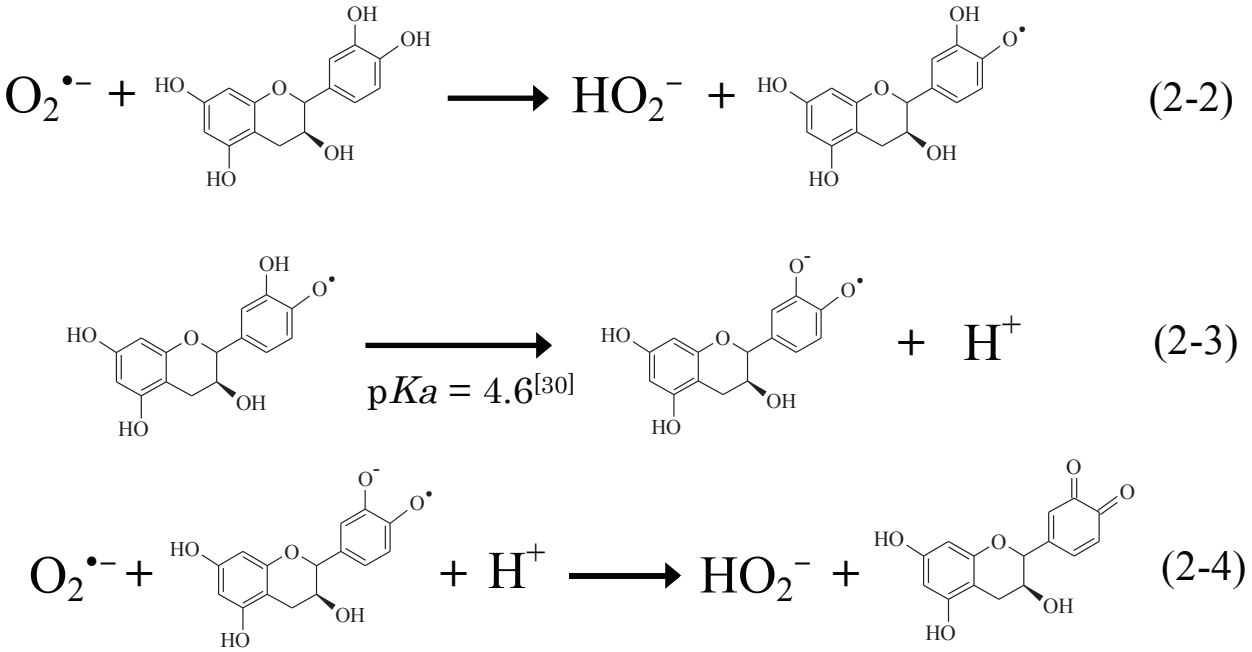

Scheme 2-2 Reaction scheme of antioxidant (catechin) against $O_2^{\cdot -}$.

2.3.4 Evaluation of the antioxidant capacity of phenolic compounds toward superoxide anion radicals

ECL inhibition rates (%) depended on both antioxidant capacity and the concentration of the phenolic compound, which were examined at different concentration levels for each phenolic compound. In this study, the ECL inhibition rate (%) measured at each concentration was compared against the SOD equivalent (U mL^{-1}) using the data in Figure 2-8. The relative antioxidant efficiency, K_{ao} (U $mmol^{-1}$ equivalent SOD), was used to evaluate the antioxidant activity of phenolic compounds. It is shown in Fig. 2-11 that good linear relationships between the SOD equivalent (U mL^{-1}) and the concentration of tested phenolic compounds were obtained in the range 0–50 μmol L^{-1} (only the data for quercetin, catechin, and salicylic acid are shown). The slopes of the plots are defined as the relative antioxidant efficiency, K_{ao} (SOD U $mmol^{-1}$), for each of the phenolic compounds; the larger the value of K_{ao}, the higher the antioxidant capacity. The 50%-inhibition concentrations (IC_{50}) are often used to evaluate antioxidant activity; the lower the IC_{50} value, the higher the activity of the phenolic compound. These values were easily calculated by linear regression of the plots in Fig. 2-11 and will be summarized in the next section along with the K_{ao} values. As expected, K_{ao} and IC_{50} depend on the position of the hydroxylation and on the chemical nature of the substituents present on the phenolic compound.

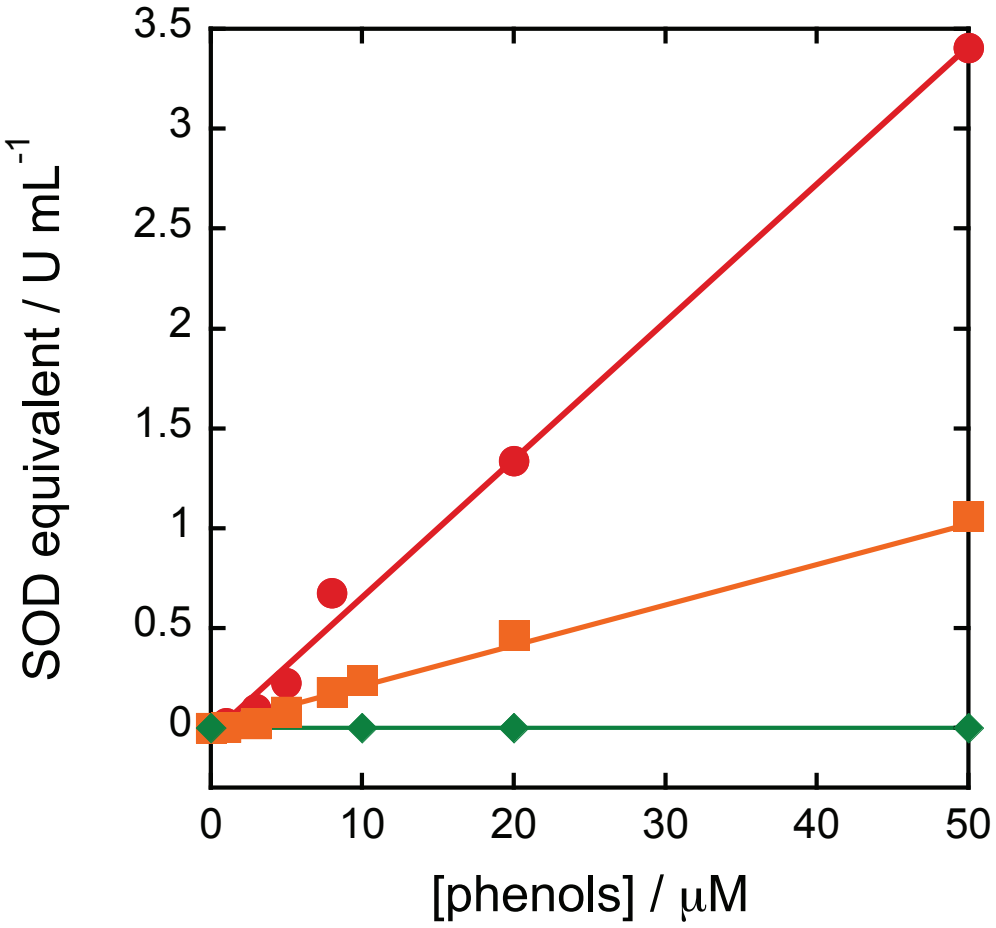

Figure 2-11 Relationship between the SOD equivalent and concentration of selected phenolic compounds. The slope of this plot is defined as the antioxidant efficiency, K_{ao} (U mmol^{-1}). (●) Quercetin, (■) catechin, and (◆) salicylic acid.

2.3.5 Comparison with other methods

We propose the Luc^{2+} ECL method for the evaluation of antioxidant capacity toward $O_2\cdot^-$. The results of the ECL method were compared with the chemiluminescence (CL) method and the DPPH method to determine its validity. Generally, $O_2\cdot^-$ was generated by the enzymatic reaction of hypoxanthine (HX)/xanthinoxidase (XOD), which can then be detected by Luc^{2+} CL [9]. In addition, the enhancement of the CL of Luc^{2+} has been reported in the micellar system using cationic and nonionic surfactants [32,33]. According to J. Stroch et al., the presence of Triton X-100 causes CL enhancement of Luc^{2+} in the XOD enzymatic system [34]. We then performed Luc^{2+} CL in a micellar system and attempted to evaluate the antioxidant capacity. Figure 2-12 shows the CL emission of Luc^{2+} in the HX/XOD system containing 12% Triton X-100. The CL was emitted when HX was mixed into the solution but no significant emission was observed when H_2O_2 was mixed into the solution. Therefore, this CL could be specific to $O_2\cdot^-$ generated by HX/XOD. The effect of the surfactant on the Luc^{2+} CL is summarized in Table 2.1. The CMC values of Triton X-100, Tween 20, and CTAB in aqueous neutral solution are 2.4×10^{-4} mol dm^{-3} [35] (~0.014 %); 4.88×10^{-5} mol dm^{-3} [35] (~0.0054 %); and 0.90–0.98 mM [36], respectively. Except for the data for systems without a surfactant, the values listed in Table 2.1 are much greater than the cmc. Luc^{2+} CL increased with the addition of cationic and nonionic surfactants. The enhancement of Luc^{2+} CL was greatest at 12% Triton X-100. This effect may originate from the hydrophobic environment in the micelle. The radicals ($Luc\cdot^+$, $HO_2\cdot$), intermediate (Luc(OO)), and excited species

generated in the Luc^{2+} CL reaction may be stabilized in the hydrophobic environment. Accordingly, light emission occurred in the micellar system. The difference between cationic and nonionic surfactants could be caused by electrostatic repulsion of Luc^{2+}. Next, the addition of SOD and antioxidants into the Luc^{2+} CL was examined. The intensity of Luc^{2+} CL decreased with the addition of SOD and antioxidant. As a result, we can obtain the inhibition rate curve, as shown in Fig. 2.13. As for ECL, K_{ao} can be calculated by comparing Fig. 2.13 (A) and Fig. 2.13 (B).

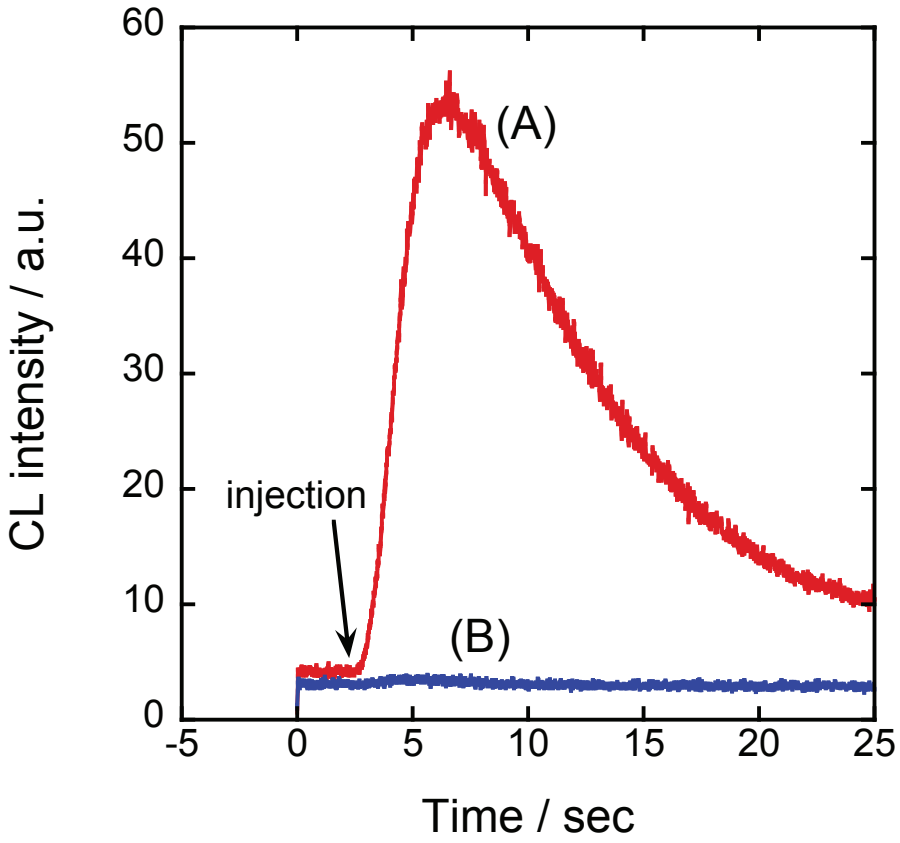

Figure 2-12 CL emission curves after injecting (A) 50 μM hypoxanthine or (B) 10 μM H_2O_2 into the solution containing 50 μM Luc^{2+}, 0.25 U/mL XOD, and 12% Triton X-100.

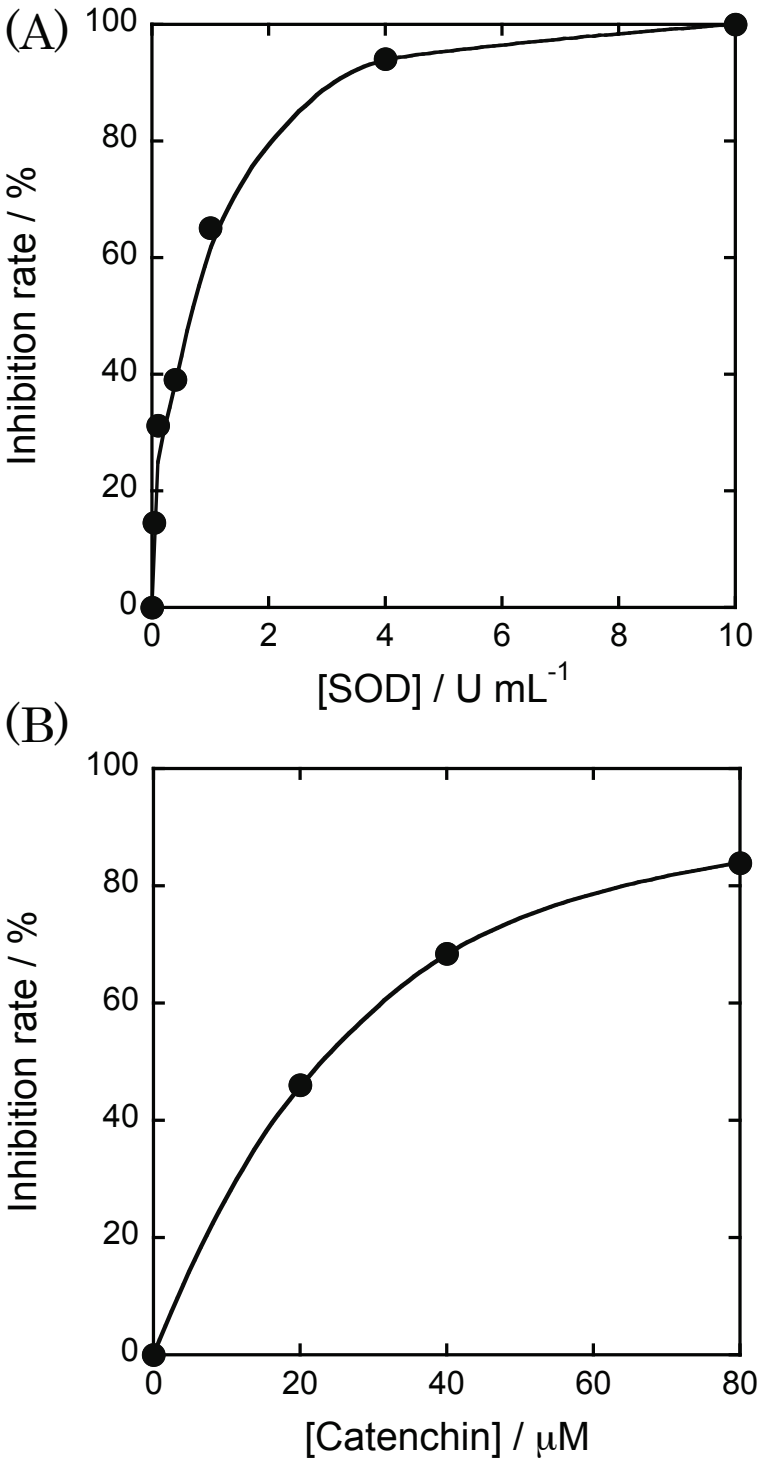

Figure 2-13 Dependence of the concentration of (A) SOD and (B) catechin on the CL inhibition rate. Solution condition is the same as that of Fig. 2.12.

Table 2-1 Effect of different surfactants on the Luc^{2+}−HX/XOD system.

Surfactant	Concentration	CL intensity / a.u.
without		0.00
Triton X-100	0 %	0.00
	1.2	7.94
	3	14.17
	6	36.88
	12	54.18
Tween 20	0 %	0.00
	1	6.88
	5	9.25
	10	17.72
	20	25.59
CTAB	0 mM	0.00
	1	2.52
	5	6.76
	10	3.40
	20	8.22

The DPPH method is a colorimetric method that uses the 2,2-diphenyl-1-picrylhydrazyl radical (DPPH·). The structure of DPPH· and its reaction with antioxidant (H-X) are shown in Fig. 2.14 (A). DPPH· has a dark purple color; however, it turns pale yellow after a hydrogen-transfer reaction with an antioxidant. The evaluation of antioxidant capacity is performed by recording the absorbance of DPPH· at 515 nm in ethanol solution; the lower the absorbance at a fixed time, the higher the antioxidant capacity. The concentration dependence of the color change of DPPH· after 24 h of reaction in a light-proof box is shown in Fig. 2.14 (B). We defined antioxidant capacity in the DPPH method as the slope of the plot of the absorbance decrease as a function of the concentration of antioxidant (mM^{-1}). A higher slope value indicates a higher antioxidant capacity.

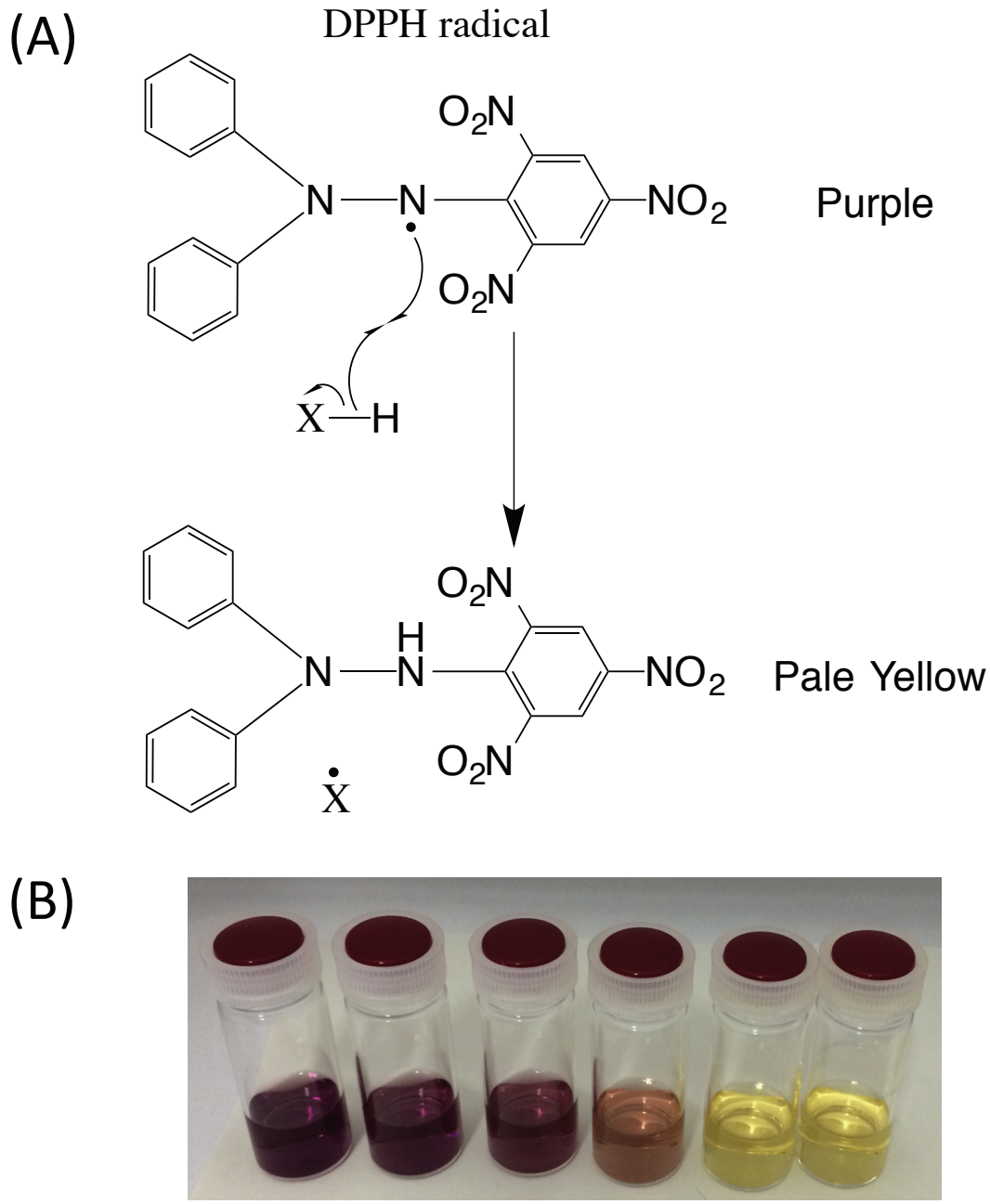

Figure 2-14 (A) Reaction scheme of an antioxidant (H-X) with DPPH·. (B) Color change of the 4.4 g L^{-1} DPPH· solution after 24 h of reaction with quercetin (from the left, the quercetin concentrations were 0, 3, 5, 10, 20, and 50 μM)

Table 2-2 Antioxidant capacity (K_{ao}, IC_{50}, and slope) of phenolic compounds

	ECL		CL		DPPH
Compound	K_{ao} / U $mmol^{-1}$	IC_{50} / mM	K_{ao} / U $mmol^{-1}$	IC_{50} / mM	Slope / mM^{-1}
Quercetin	0.0680	2.56	0.0626	26.5	0.065
Caffeic acid	0.0591	1.92	0.0178	54.0	0.051
Rutin	0.0284	5.80	0.0359	31.1	0.046
Catechin	0.0203	5.82	0.0400	22.4	0.050
Catechol	0.0170	14.10	0.0268	33.2	0.041
Protocatechuic acid	0.0236	6.90	0.0200	42.7	0.047
2,5-DHBA	0.0007	-	0.0014	-	0.033
2,4-DHBA	0.0005	-	0.0000	-	0.000
2,3-DHBA	0.0002	-	0.0007	-	0.062
Salicylic acid	0.0000	-	0.0000	-	0.000

Calculated antioxidant capacity (K_{ao}, slope) and IC_{50} are summarized in Table 2.2. The K_{ao} and slope values are also visualized as a bar graph in Fig. 2.16. Flavonoid compounds (quercetin, rutin, and catechin) exhibited relatively high antioxidant activities with K_{ao} values from 6.80×10^{-2} to 2.00×10^{-2} U $mmol^{-1}$ SOD equivalent. In general, the antioxidant activity of flavonoids depends on the structure and substitution pattern of the hydroxyl groups. The resulting antioxidant-derived radical is governed by its ability to stabilize and delocalize the unpaired electron of the semiquinone anion radical in reaction (2-4) in Scheme 2-2. [37-39] Rutin is a naturally occurring flavonol consisting of quercetin aglycone and a rutinoside moiety at position 3 of the C ring (Fig. 5). This may cause a loss of coplanarity of ring B in relation to the rest of the structure, [39] which, in comparison with quercetin, would result in a reduction of antioxidant activity. Indeed, quercetin has a structure like that of catechol in the B ring, and it also

has a 3-OH group attached to the 2,3-double bond adjacent to the 4-carbonyl in the C ring. With this structure, the hydrogen bond between the OH group in the B ring and the 3-OH group in the C ring would make the molecular structure planar. This planarity is expected to exhibit high electron delocalization, which would stabilize the π system of the flavonoid phenoxyl radical. Meanwhile, for catechin, electronic delocalization may occur separately on rings B and A because of the absence of a conjugated 2,3 double bond in the C ring. In comparison with quercetin and rutin, this may result in a reduction of the antioxidant activity.

Although flavonoids have been the focus of most dietary antioxidant studies, the antioxidant properties of nonflavonoid phenolic compounds have also been investigated in a number of radical scavenging assays. Phenolic compounds with a catechol moiety (e.g., caffeic acid, protocatechuic acid, catechol) present higher antioxidant activities. Caffeic acid is also known as cinnamic acid and is present in many plants. Caffeic acid exhibits a higher antioxidant activity because of additional conjugation in the propenoic side chain. Via resonance, this would facilitate electron delocalization between the aromatic ring and the propenoic group of the semiquinone anion radical ($Q\cdot^{-}$). However, for compounds without the catechol moiety (2,4-DHBA, 2,5-DHBA, salicylic acid), very low K_{ao} values were measured. Because the K_{ao} values for those compounds are extremely small, the IC_{50} could not be evaluated meaningfully. In the case of 2,3-DHBA, which has the catechol moiety but shows very low antioxidant activity, we considered that the steric effect caused by the COOH group interferes with the reaction at the catechol moiety, thereby reducing the antioxidant activity.

Comparing the result of the ECL method with that of the enzymatic CL method, the antioxidant capacities of caffeic acid and protocatechuic acid were relatively low. It is known that quercetin and rutin can inhibit the activity of XOD [10]; this effect gives additional antioxidant capacity to quercetin and rutin. Hence, these K_{ao} values become relatively high in comparison with those of other compounds. In addition, the hydrophobicity of catechin and catechol would affect K_{ao}. In neutral solution, caffeic acid (pK_{a1} = 4.47) and protocatechuic acid (pK_{a1} = 4.38) exist as monoanions due to deprotonation of the carboxylic acid group. However, catechin (pK_{a1} = 8.77) and catechol (pK_{a1} = 9.43) are not dissociated at pH 7. Catechin and catechol tend to exist in the hydrophobic environment formed within a micelle. This would accelerate the reaction with $O_2^{\cdot -}$ (or $HO_2^{\cdot}$) and result in a relatively high K_{ao} compared with caffeic acid and protocatechuic acid.

Except for 2,5-DHBA and 2,3-DHBA, the result of the DPPH method shows a similar tendency to that of ECL. A scavenging effect toward DPPH· by 2,5- and 2,3-DHBA has been reported, and this supports our results. [40] The difference between the reactivity of DPPH· and that of $O_2^{\cdot -}$ may cause the different tendencies in the results of the DPPH method.

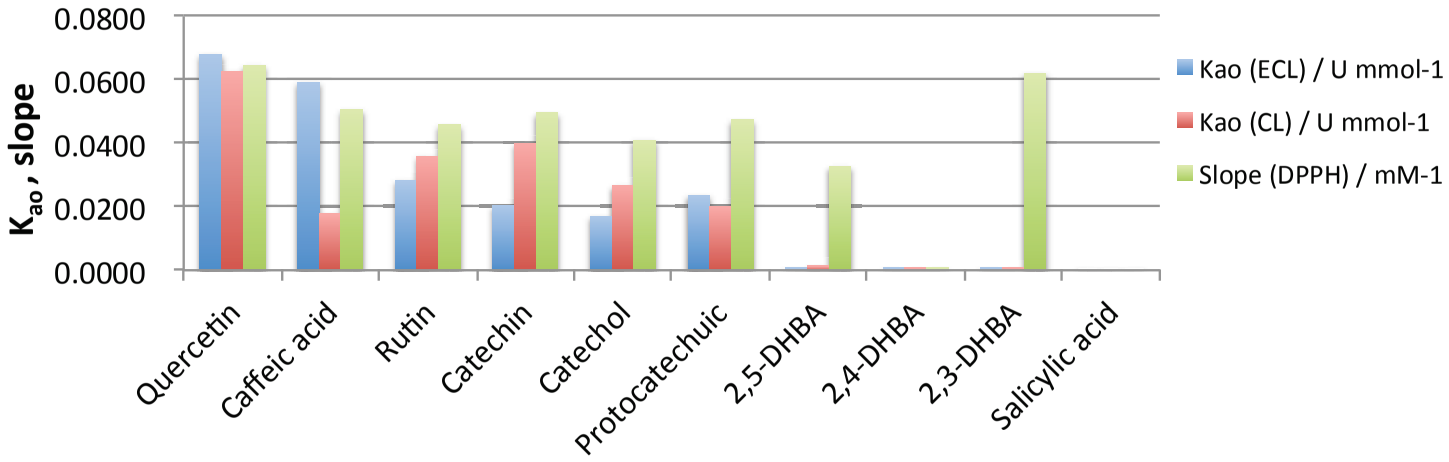

Fig. 2.15 K_{ao} (ECL and CL) and slope value of phenolic compounds.

2.4 Conclusions

In this chapter, we described the potential for determining antioxidant capacity using the ECL method. It has been demonstrated that the ECL signals of Luc^{2+} would be suppressed in the presence of phenolic compounds due to the elimination of $O_2\cdot^-$ by these compounds. The ECL inhibition rate (%) measured at each concentration was compared to the SOD equivalent (U mL^{-1}), and the relative antioxidant efficiency, K_{ao} (U $mmol^{-1}$ equivalent SOD), was used to evaluate the antioxidant activity of selected phenolic compounds. The results were compared with an enzymatic CL method and the DPPH method. The results showed similar tendencies. Differences in the comparison originated from the inhibition effect on the enzyme and differences in the reactivity of target radicals. It is notable that $O_2\cdot^-$ was electrogenerated by the one-electron reduction of dioxygen in the ECL method; therefore, its generation involves neither enzymes nor chelating metals, which are usually required in methods testing superoxide scavenging capacity. Consequently, this ECL method specifically measures the radical scavenging efficiency of phenolic compounds toward $O_2\cdot^-$ in aqueous solution.

References

[1] M. Carocho and I. C. F. R. Ferreira, A review on antioxidants, prooxidants and related controversy: natural and synthetic compounds, screening and analysis methodologies and future perspectives, *Food Chem. Toxicol* **51** (2013) 15.

[2] C. Kaur and H. C. Kapoor, Antioxidants in fruits and vegetables - the millennium's health, *Int. J. Food Sci. Technol.*, **36** (2001) 703.

[3] N. Balasundram, K. Sundram, and S. Samman, Phenolic compounds in plants and agri-industrial by-products: Antioxidant activity, occurrence, and potential uses, *Food Chem.* **99** (2006) 191.

[4] A. M. Pisoschi and G. P. Negulescu, Methods for Total Antioxidant Activity Determination: A Review, *Biochem. Anal. Biochem.*, **1** (2011) 106.

[5] C. A. Rice-Evans, N. J. Miller and G. Paganga, Structure-antioxidant activity relationships of flavonoids and phenolic acids, *Free Radic. Biol. Med.*, **20** (1996) 933.

[6] F. Auchère and F Rusnak, What is the ultimate fate of superoxide anion in vivo?, *J. Biol. Inorg. Chem.*, **7** (2002) 664.

[7] N. S. C. Gaulejac, C. Provost and G. Paganga, Comparative Study of Polyphenol Scavenging Activities Assessed by Different Methods, *J. Agric. Food Chem.*, **47** (1999) 425.

[8] S. Ignatov, D. Shinshniashvili, B. Ge, F. W. Scheller and F. Lisdat, Amperometric biosensor based on a functionalized gold electrode for the detection of antioxidants, *Biosens. Bioelectron,* **17** (2002) 191.

[9] S. Yamaguchi, N, Kishikawa, K. Ohyama, Y. Ohba, M. Kohno, T. Masuda, A. Takadate, K. Nakashima and N. Kuroda, Evaluation of chemiluminescence

reagents for selective detection of reactive oxygen species, *Anal. Chim. Acta,* **665** (2010) 74.

[10] P. Cos, L. Ying, M. Calomme, J. P. Hu, K. Cimanga, B. V. Poel, L. Pieters, A. J. Vlietinck and D. V. Berghe, Structure-activity relationship and classification of flavonoids as inhibitors of xanthine oxidase and superoxide scavengers, *J. Nat. Prod.*, **61** (1998) 71.

[11] C. Bourvellec, D. Hauchard, A. Darchen, J.-L. Burgot,and M.-L. Abasq, Validation of a new method using the reactivity of electrogenerated superoxide radical in the antioxidant capacity determination of flavonoid, *Talanta*, **75** (2008) 1098.

[12] A. René, M.-L. Abasq, D. Hauchard and P. Hapiot, How Do Phenolic Compounds React toward Superoxide Ion? A Simple Electrochemical Method for Evaluating Antioxidant Capacity, *Anal. Chem.*, **82** (2010) 8703.

[13] T. Okajima and T.Ohsaka, Chemiluminescence of lucigenin by electrogenerated superoxide ions in aqueous solutions, *Luminescence*, **18** (2003) 49.

[14] Y.-G. Sun, H. Cui and X.-Q. Lin, Study of electrochemiluminescence of lucigenin at glassy carbon electrodes in NaOH solution, *J. Lumin.*, **92** (2001) 205.

[15] K. D. Legg and D. M. Hercules, Electrochemically Generated Chemiluminescence of Lucigenin, *J. Am. Chem. Soc.*, **91** (1969) 1902.

[16] K. D. Legg, D. W. Shive and D. M. Hercules, Elctrochemistry of Lucigenin, *Anal. Chem.,* **44** (1972) 1650.

[17] Y. Li, H. Zhu, and P. Kuppusamy, Validation of lucigenin (bis-N-methylacridinium) as a chemilumigenic probe for detecting superoxide anion radical production by enzymatic and cellular systems, *J. Biol. Chem.*, **273**

(1998) 2015.

[18] M. Rost, E. Karge, and W. Klinger, What Do We Measure with Luminol-, Lucigenin- and Penicillin-amplified Chemiluminescence? 1. Investigations with Hydrogen Peroxide and Sodium Hypochlorite, *J. Biolumin. Chemilumin.,* **13** (1998) 355.

[19] S. I. Liochev and I. Fridovich, LUCIGENIN AS MEDIATOR OF SUPEROXIDE PRODUCTION : REVISITED, *Free Radic, Biol. Med.,* **25** (1998) 355.

[20] H. Qi, Z. Cao and L. Hou, Electrogenerated chemiluminesence method for the determination of riboflavin at an ionic liquid modified gold electrode, *Spectrochim. Acta, Part A*, **78** (2011) 211.

[21] H. Qi and C. Zhang, Electrogenerated chemiluminescence reaction of lucigenin with isatin at a platinum electrode, *Luminescence*, **19** (2004) 21.

[22] R. J. Taylor and A. A. Humffray, ELECTROCHEMICAL STUDIES ON GLASSY CARBON ELECTRODES III. OXYGEN REDUCTION IN SOLUTIONS OF LOW pH (pH<10), *J. Electroanal. Chem.*, **64** (1975) 85.

[23] B. H. J. Bielski and A. O. Allen, Mechanism of the Disproportionation of Superoxide Radicals, *J. Phys. Chem.*, **81** (1977) 1048.

[24] J. M. McCord and I. Fridovich, The reduction of Cytochrome c by Milk Xanthine Oxidase, *J. Biol. Chem.*, **243** (1968) 5753.

[25] J. M. McCord and I. Fridovich, Superoxide dismutase - an enzymic function for erytherocuprein (hemocuprein), *J. Biol Chem.*, **244** (1969) 6049.

[26] C. A. Rice-Evans, N. J. Miller and G. Paganga, Antioxidant properties of phenolic compounds, *Trends Plant Sci.,* **2** (1997) 152.

[27] M. Mochizuki, S. Yamazaki, K. Kano and T. Ikeda, Kinetic analysis and mechanistic aspects of autoxidation of catechins, *Biochim. Biophys. Acta,* **1569** (2002) 35.

[28] F. Z. Erdemgil, S. Şanli, N. Şanli, G. Özkan, J. Barbosa, J. Guiteras and J. L. Beltrán, Determination of pK_a values of some hydroxylated benzoic acids in methanol-water binary mixtures by LC methodology and potentiometry, *Talanta*, **72** (2007) 489.

[29] J. M. Herrero-Martinez, M. Sanmartin, M. Rosés, E. Bosch and C. Ràfols, Determination of dissociation constants of flavonoids by capillary electrophoresis, *Electrophoresis*, **26** (2005) 1886.

[30] S. V. Jovanovic, S. Steenken, M. Tosic, B. Marjanovic and M. G. Simic, Flavonoids as antioxidants, *J. Am. Chem. Soc.*, **116** (1994) 4846.

[31] R. Kahl, A. Weimann, S. Weinke and A. G. Hildebrandt, Detection of oxygen activation and determination of the activity of antioxidants towards reactive oxygen species by use of the chemiluminigenic probes luminol and lucigenin, *Arch. Toxicol.*, **60** (1987) 158.

[32] W. L. Hinze, T. E. Riehl, H. N. Singh and Y. Baba, Micelle-enhanced chemiluminescence and application to the determination of biological reductants using lucigenin, *Anal. Chem.*, **56** (1984) 2180.

[33] M. Asgher, M. Yaqoob, A. Waseem and A. Nabi, Flow injection methods for the determination of retinol and α-tocopherol using lucigenin-enhanced chemiluminescence, *Luminescence*, **26** (2011) 416.

[34] J. Storch and E. Ferber, Detergent-amplified chemiluminescence of lucigenin for determination of superoxide anion production by NADPH oxidase and xanthine oxidase, *Anal. Biochem.,* **169** (1988) 262.

[35] S. K. Hait, S. P. Moulik, Determination of Critical Micelle Concentration (CMC) of Nonionic Surfactants by Donor–Acceptor Interaction with Iodine and Correlation of CMC with Hydrophile–Lipophile Balance and Other Parameters of the Surfactants, *J. Surf. Deterg.*, **4** (2001) 303.

[36] A. Cifuentes, J. L. Bernal and J. C. Diez-Masa, Determination of critical micelle concentration values using capillary electrophoresis instrumentation, *Anal. Chem.*, **69** (1997) 4271.

[37] E. G. Bakalbassis, N. Nenadis and M Tsimidou, A Density Functional Theory Study of Structure–Activity Relationships in Caffeic and Dihydrocaffeic Acids and Related Monophenols, *J. Am. Oil Chem. Soc.*, **80** (2003) 459.

[38] M. Leopoldini, N. Russo and M. Toscano, The molecular basis of working mechanism of natural polyphenolic antioxidants, *Food Chem.*, **125** (2011) 288.

[39] S.A.B.E. Van Acker, M.J. De Groot, D.J. van den Berg, M.N.J.L. Tromp, G.D.O. den Kelder, W.J.F. van der Vijgh and A. Bast, A quantum chemical explanation of the antioxidant activity of flavonoid, *Chem. Res. Toxicol.*, **9** (1996) 1305–1312.

[40] Z. Sroka and W. Cisowski, Hydrogen peroxide scavenging, antioxidant and anti-radical activity of some phenolic acids, *Food Chem. Toxicol.*, **41** (2003) 753.

Chapter 3

Sonochemiluminescence (SCL) of lucigenin

3.1 Introduction

Ultrasonic irradiation of liquids provides a unique chemical environment originating from acoustic cavitation bubbles. [1,2] The extreme conditions in the bubbles can give rise to the phenomenon called sonoluminecence (SL), i.e., the light emission of acoustically driven bubbles [3,4], and can lead to the formation of reactive species such as •OH, H•, and H_2O_2 in aqueous liquids. These species are capable of inducing secondary oxidation or reduction reactions. [5] It has been known that an alkaline luminol solution emits light when irradiated with ultrasound of sufficient intensity. The phenomenon is called sonochemiluminescence (SCL), which is believed to occur through an oxidative chemiluminescence (CL) process induced by sonochemically generated •OH. The SCL of luminol has been used to investigate the mechanisms of acoustic cavitation under different sonication conditions. [6,7]

Lucigenin [Luc^{2+}: bis (N-methylacridiniumnitrate)] is a well-known CL probe and has been used for the determination of reactive oxygen species, especially those involved in the enzymatic production of hydrogen peroxide (H_2O_2) and superoxide radical anion ($O_2\cdot^-$). [8,9] Although both luminol and Luc^{2+} can react with H_2O_2 or $O_2\cdot^-$ to yield CL signals, the reaction mechanisms are fundamentally different. Luminol CL is the net result of the "oxidation" of luminol by reactive oxygen species, whereas Luc^{2+} CL involves an initial one–electron reduction of Luc^{2+} to a cation radical ($Luc^{\bullet+}$) that can react with $O_2\cdot^-$ to produce light, [10] *i.e.*, the "reductive" CL process. Unlike luminol, Luc^{2+} shows no SCL response in alkaline solution, and very

few studies compared SCL behavior between Luc^{2+} and luminol, especially in aqueous solutions.

In this chapter, we report the SCL behavior of Luc^{2+} from aqueous solutions using a small amount of alcohol as coreactant and discuss the probable mechanistic pathways for SCL. We suggested that the Luc^{2+} SCL reaction was driven by secondary sonochemical products, especially the generated $O_2\cdot^-$. Additionally, the spectroscopic properties as well as the spatial distribution of SCL in a microreactor were examined in this study.

3.2 Experimental section

3.2.1 Reagents

All reagents were of analytical grade and used as received. Luc^{2+} and superoxide dismutase (SOD) from bovine erythrocytes were purchased from Nacalai Tesque. Sodium hydroxide was purchased from Kanto Chemical. 2-Aminobenzenthiol and 2-pyridinecarboxaldehyde were purchased from Tokyo Chemical Industry. Alcohols, ethanol was purchased from Nacalai tesque; methanol, *n*-propanol and 2-propanol were purchased from Wako. Amines, propylamine, dipropylamine and tripropylamine were purchased from Wako; ethylamine diethylamine and triethylamine were purchased from Nacalai Tesque. 1 mM stock solutions of Luc^{2+} was prepared by dissolving appropriate amounts of the reagent in distilled water. The pH was carefully adjusted at an appropriate value by titrating with sodium hydroxide. All solutions were made with distilled water purified by a

WS200 distillation system (Yamato Scientific Co.).

The fluorescent probe 2-(2-pyridyl)benzothiazoline was synthesized in accordance with the method proposed earlier by Zhang et al.[11] Briefly, an appropriate amount of 2-pyridinaldehyde was mixed with 2-aminobenzenthiol at 1:1 molar ratio in benzene. The mixed solution was heated under reflux for about 3 h. After the solvent was removed at a low pressure, a yellow crude solid was obtained. It was then recrystallized from benzene and dried in vacuum. The stock solution of the fluorescent probe at 0.3 mM concentration was prepared by dissolving an appropriate amount of 2-(2-pyridyl)benzothiazoline in distilled water.

3.2.2 Instruments

Figure 3-1 shows a schematic diagram of the experimental setup for SCL measurement. The sonochemical reactor was made of a cylindrical acrylic chamber of 6 cm in inner diameter and was filled with distilled water. A lead zirconate titanate (PZT) transducer with 500 kHz was mounted on the stainless steel vibrational plate placed at the bottom of the reactor. The transducer was driven by an WF1974 function generator (NF Co., Japan) and amplified by a T145-5015 amplifier (THAMWAY Co., Japan). A cylindrical glass vessel of 3 cm in diameter was used as the sonochemical cell for SCL observation. In all experiments, the sample volume in the cell was 10 cm^3 and the top of the cell was capped with a rubber cap. Since the sonochemical efficiency is high near the liquid surface of the cylindrical chamber, [5] the cell was placed on the top of the chamber with a fixed position above the

transducer, and was irradiated indirectly with ultrasound from the PZT transducer. The light emitting from the sample solution was measured with a H6780 photomultiplier tube module (Hamamatsu Photonics, Japan) through a quartz glass window on the side of the sonochemical reactor. All experiments were conducted in a light-proof box. The SCL spectra and fluorescence spectra were recorded with a fiber optics spectrofluorophotometer USB2000 (Ocean Optics, USA) and a RF-5300PC spectrofluorophotometer (Shimadzu, Japan), respectively.

Fig. 3-2 shows a schematic diagram of a sonochemical microreactor for SCL observation. The reaction chamber had a size of 32 × 10 × 3 mm, which was assembled by stacking a stainless steel vibrational plate, a silicon rubber seal, a PEEK spacer, and a quartz glass plate. A 500 kHz PZT transducer was glued under the vibrational plate. A BS-40L cooled CCD camera (BITRAN, Japan) was placed on top of the reactor, and SCL images were recorded at a cooling temperature of 3 °C and a 60 s exposure time.

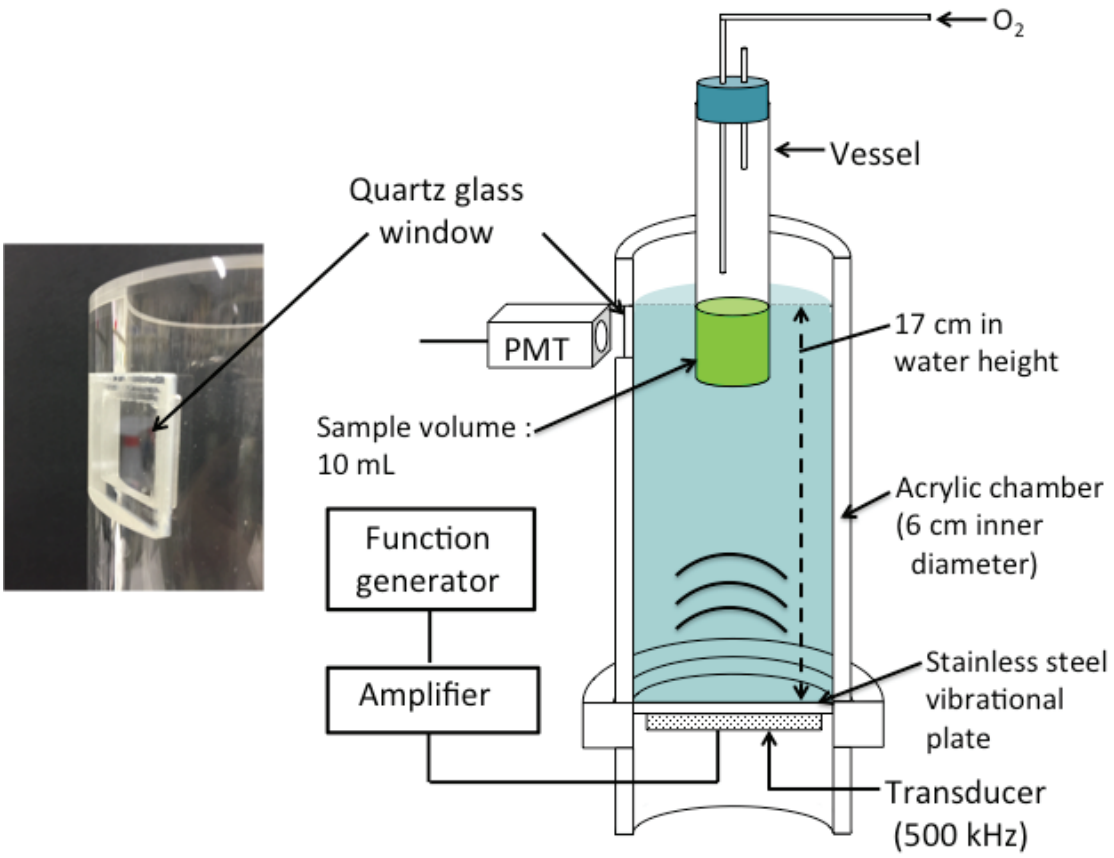

Figure 3-1 Sonochemical reactor for SCL measurement.

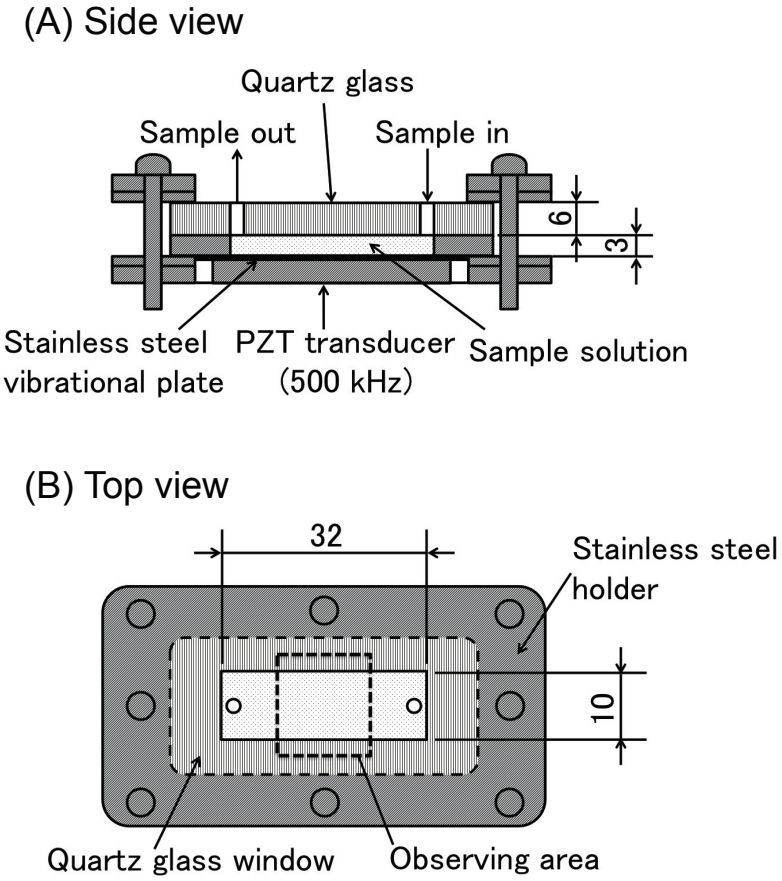

Figure 3-2 (A) and (B): The schematic diagram of sonochemical microreactor. (C): The photo image of microreactor.

3.3 Results and discussion

3.3.1 SCL of Luc^{2+} using alcohol as coreactant

Figure 3-3 shows the light emission from the samples sonicated with 500 kHz ultrasound. Very weak light emission could be observed from an O_2 saturated aqueous solution of pH 11 containing 50 mM Luc^{2+} (Fig.3-3(a)). As its intensity was mostly the same as that observed from Ar-saturated solution (Fig.3-3(b)), the emission was considered to be contributed from sonoluminescence (SL) of water. The light emission, however, was dramatically increased when 50 mM of 2-propanol ($CH_3CH(OH)CH_3$) was added in the solution as is shown in Fig.3-3(c).

The chemical effects of ultrasound originate from the acoustic cavitation. This high-energy microenvironment cleaves water molecules to generate high-energy species such as ·OH radicals and ·H atoms. [5,12] Under the condition we employed, as shown in Fig. 2, the electric output of ultrasound was 70 W, and the calorimetry power absorbed by water was 19 W. The sonochemical efficiency (*SE* value) based on $^{\bullet}OH$ yield was estimated as 0.7 nmol J^{-1}. In the ultrasonic field, 2-propanol molecules tend to adsorb onto the cavitation bubble / solution interface, where they can scavenge $^{\bullet}OH$ produced during cavitation. [13] The reaction of •OH with 2-propanol involves H-atom abstraction from C-H bonds, which leads to the production of a 2-propanol radical [$CH_3C^{\bullet}(OH)CH_3$] through the following reaction.

$$\cdot OH + CH_3CH(OH)CH_3 \rightarrow CH_3C\cdot(OH)CH_3 + H_2O \qquad (3\text{-}1)$$

The 2-propanol radical is a reductive one with a reduction potential of −1.39 V *vs.* NHE [14]; therefore, it more likely initiates the reduction reaction in bulk solution. [15] There are two possible reductive pathways for Luc^{2+} SCL that may be taken into account. One is the reduction of Luc^{2+} (with the reduction potential of −0.14 V *vs.* NHE) to a lucigenin cation radical ($Luc^{\bullet+}$) and the other is the reduction of molecular oxygen (with the reduction potential of -0.16 V *vs* NHE) to $O_2\cdot^-$ *via* a one-electron reduction process [reactions (3-2) and (3-3)], [16-18] respectively. Also the generation of $O_2\cdot^-$ by 2-propanol radical is reported in the photolysis [19] and pulse radiolysis [20]. In these studies 2-propanol radical react with O_2 to produce peroxy radical and decomposition of peroxy radical leads to the formation of $O_2\cdot^-$. The radical-radical coupling reaction between $Luc^{\bullet+}$ and $O_2\cdot^-$ is expected to initiate the light emission. [10,21]

$$CH_3C^{\bullet}(OH)CH_3 + O_2 \rightarrow O_2\cdot^- + CH_3COCH_3 + H^+ \quad (3\text{-}2)$$

$$CH_3C^{\bullet}(OH)CH_3 + Luc^{2+} \rightarrow Luc^{\bullet+} + CH_3COCH_3 + H^+ \quad (3\text{-}3)$$

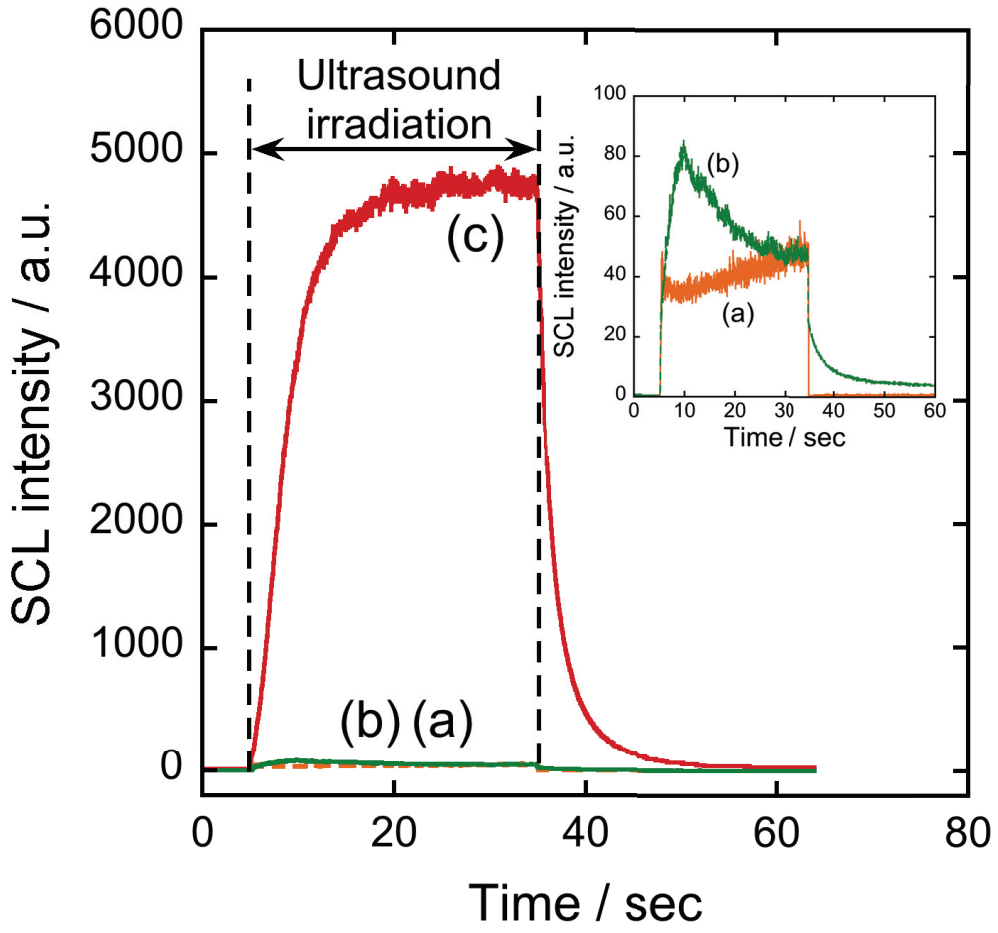

Figure 3-3 SCL and SL signals under the ultrasound irradiation by 500 kHz ultrasound in the pH 11 solution containing 50 μM Luc^{2+} (a) in the absence of 2-propanol with O_2-saturated and in the presence of 2-propanol with (b) Ar-saturated; (c) O_2-saturated.

In order to explain the observations seen in Fig. 3-3, the SCL of Luc^{2+}/2-propanol system was further examined by changing dissolved gasses and adding radical scavengers. The results are showed in Table 3-1. It can be seen that the SCL intensity strongly depended on dissolved oxygen concentration. The strongest SCL intensity was observed in an oxygen-saturated solution, but the intensity decreased considerably in the absence of oxygen (in N_2 or Ar saturated solutions), indicating that the molecular oxygen is required to generate SCL. Superoxide dismutase (SOD) is the enzyme that can catalyze the disproportionation of $O_2\cdot^-$ and can act as a scavenger against $O_2\cdot^-$ [22,23], whereas salicylic acid is known as the scavenger to $^{\bullet}OH$. [24] With the addition of SOD or salicylic acid into the system, the SCL from Luc^{2+} was almost completely quenched. Consequently we confirm the hypothesis that the generation of $O_2\cdot^-$ is crucial in Luc^{2+} SCL reaction.

Besides 2-propanol, methanol (CH_3OH), ethanol (C_2H_5OH) and *n*-propanol (C_3H_7OH) were also examined as coreactants in Luc^{2+} SCL system. The second order rate constants for the reaction of $^{\bullet}OH$ with methanol, ethanol, n-propanol and 2-propanol have been reported as 0.64×10^{12}, 2.4×10^{12}, 3.2×10^{12} and 3.3×10^{12} mol cm^{-3} s^{-1}, respectively (Table 3-2). [25] Then the reduction potential of methanol radical, ethanol radical and 2-propanol radical have been reported as -1.81, -1.93 and -2.10 V, respectively [14]. As can be seen in Table 3-2, the observed SCL intensity followed the order of 2-propanol > *n*-propanol > ethanol > methanol, which agreed with the rate constant for the reaction with •OH and the reduction potential of its radicals, indicating that $O_2\cdot^-$ generation was most efficient when 2-propanol was

used as a coreactant.

Table 3-1 SCL intensities observed in the solution containing 50 μM Luc^{2+} and 50 mM 2-propanol (pH 11) with various conditions.

Experimental Conditions	SCL Intensity/ a.u.
O_2 saturated	5440
Air saturated	3460
N_2 saturated	136
Ar saturated	290
O_2 saturated, with addition of 20 U mL^{-1} SOD	103
O_2 saturated, with addition of 10 mM salicylic acid	100

Table 3-2 SCL intensities observed in the solution containing 50 μM Luc^{2+} (pH 11) in the presence of different alcohols with the concentration of 10 mM and second order rate constants for the reaction of •OH with alcohols.

Alcohol	SCL Intensity/ a.u.	k /mol cm^{-3} s^{-1} [25]
No addition	70	
CH_3OH	915	0.64×10^{12}
C_2H_5OH	1620	2.4×10^{12}
C_3H_7OH	2861	3.2×10^{12}
$CH_3CH(OH)CH_3$	3930	3.3×10^{12}

3.3.2 Effect of output power and frequency

The sonochemical effects originate from the acoustic cavitation. The efficiency of cavitation depends on the ultrasound power and frequency. Therefore, we examined the effect of the applied power and frequency on Luc^{2+} SCL. The effect of ultrasound power on the SCL intensity is shown in Fig. 3-4. SCL intensity increased with increasing ultrasound power and saturated at 100 W. As can be seen in the low power area below 20W, no SCL was observed. This threshold is the cavitation threshold. When the sufficiently negative pressure is applied into the liquid, the cavitation will occur. However, the ultrasound power is below the cavitation threshold, the acoustic pressure is insufficient to the cavitation. Since the SCL signal could not been observed when the ultrasound power below its threshold to produce the cavitation, the SCL signals should be induced by the acoustic cavitation. We chose the ultrasound power of 80 W for other experiments to avoid the overload of the instruments. Fig. 3-5 shows the effect of ultrasound frequency on SCL intensity. The SCL intensity reached maximum at 500 kHz. It is reported that the sonochemical efficiency is most efficient in the range of frequency of 300 – 500 kHz [26]. Thus we chose ultrasound efficiency of 500 kHz for the experiments.

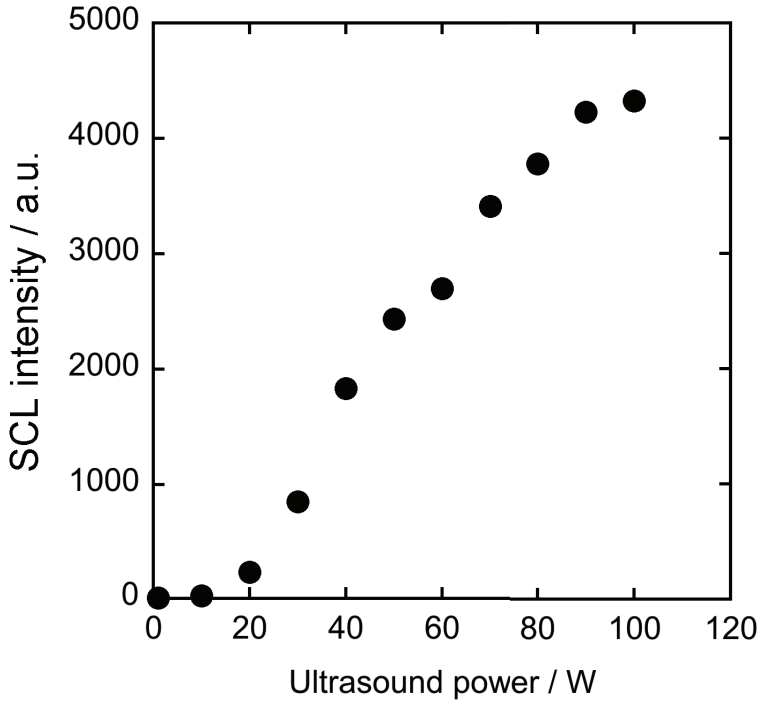

Figure 3-4 The dependence of ultrasound power on SCL intensity.

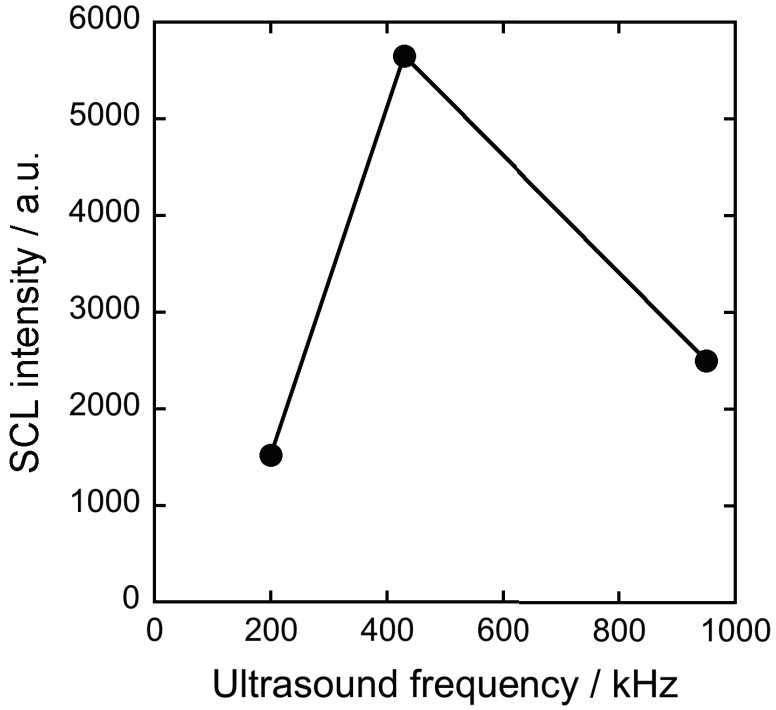

Figure 3-5 The dependence of ultrasound frequency on SCL intensity.

3.3.3 Effect of concentration of 2-propanol and pH

The concentration effects of 2-propanol as well as the pH effect on SCL were also investigated. Fig. 3-6 shows the effect of concentration of 2-propanol on SCL intensity. The higher the 2-propanol concentration in the system, the greater SCL intensity was observed. We suggest that it was owing to the increasing of $O_2\cdot^-$ concentration. The intensity, however, did not further increase when the concentration of 2-propanol was higher than 50 mM. This is probably due to the competition reactions by the 2-propanol radical recombination or the evaporation effect. 2-propanol can adsorb on the cavitation bubble / solution interface and evaporate into the cavitation bubble. Evaporation of 2-propanol caused temperature decrease of cavitation and it may suppress the sonochemical efficiency. [27] The effect of pH on SCL intensity is shown in Fig. 3-7. The SCL intensity was also examined in the pH range between 7 and 13. The SCL intensity could not be determined when pH was below 9, but increased monotonically in the pH range up to pH 12. This may be due to the reason that the $O_2\cdot^-$ is more stable in alkaline conditions. [28] Because Luc^{2+} exhibited the weak emission at an O_2 saturated solution when pH was above 12, pH greater than 12 was not suitable for the SCL study.

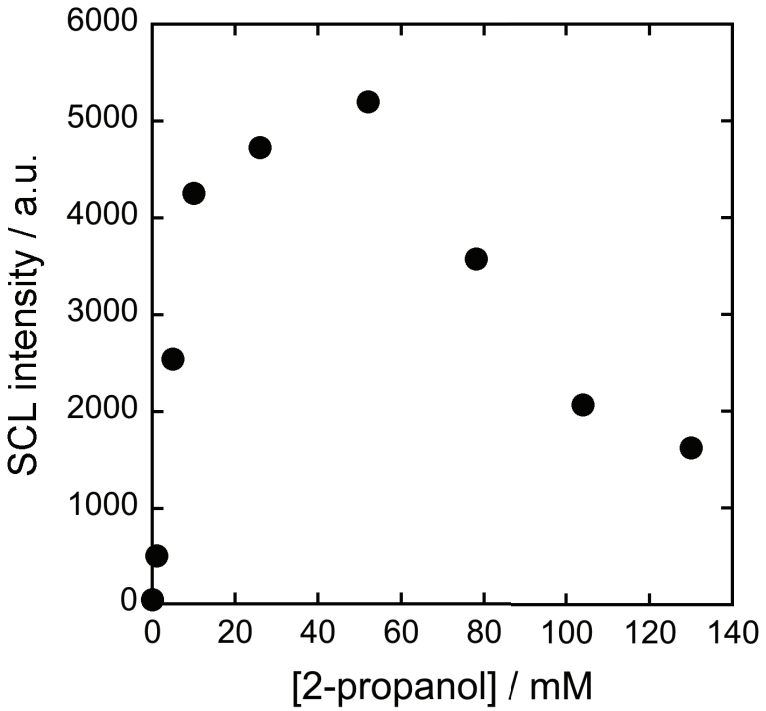

Figure 3-6 The concentration dependence of 2-propanol on SCL intensity at pH 11.

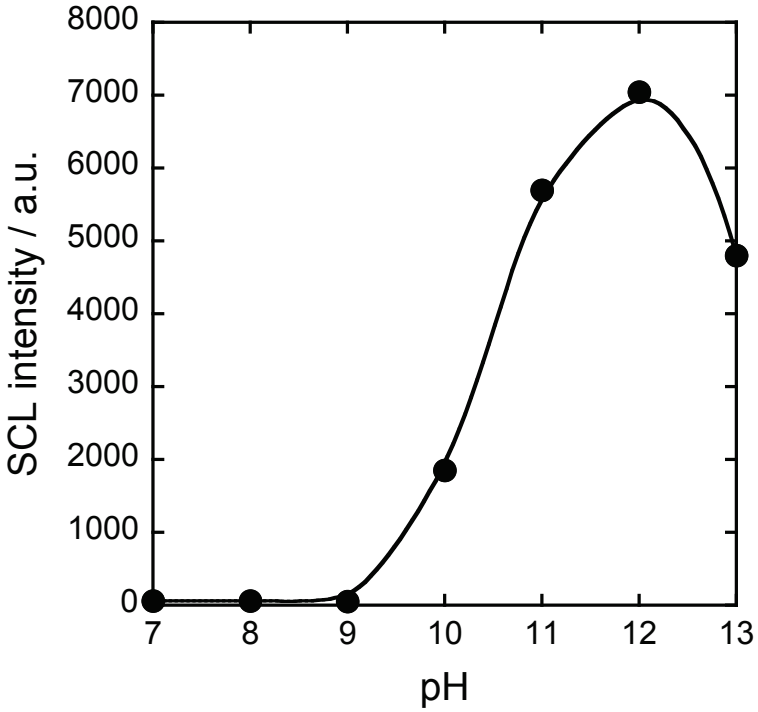

Figure 3-7 The pH dependence on SCL intensity in the solution containing 50 mM 2-propanol as a coreactant.

3.3.4 SCL of Luc^{2+} using amine as coreactant

Thus far it is discussed about the Luc^{2+} SCL using alcohol as a coreactant. In order to expand the application of SCL, we examined other compound as coreactant. Tri-*n*-propylamine (TPA) is one of aliphatic amines and known as a coreactant of anodic ECL [29]. When TPA is oxidized on the electrode, TPA radical cation ($TPA^{\cdot +}$) is generated. Subsequently it deprotonates and generates the reducing radical, TPA·[29]. TPA can produce the reducing radical species by the oxidative process. Therefore, we choose TPA and some aliphatic amines as coreactants in Luc^{2+} SCL.

Fig. 3-8 shows light emission signals upon 500 kHz ultrasound irradiation. The strong SCL emission was observed in the O_2-saturated solution (pH 11) containing 50 μM Luc^{2+} 1 mM TPA (Fig. 3-8 (a)). Similarly in the SCL using 2-propanol as coreactant, the lack of oxygen (Fig 3-8 (b)) or TPA (Fig 3-9 (c)) made the emission very weak. These weak emissions arise from the SL of water. Oxygen and TPA is necessary to gain the SCL. In ECL study, the emission from Luc^{2+} / TPA system in ethanol solution has been reported. [30] TPA was oxidized at anodic electrode potential and light emission has been observed. Authors concluded that TPA·, generated by electro-oxidation and deprotonation of $TPA^{\cdot +}$, acts as a reductant in the reaction with Luc^{2+} and O_2 and generated radicals, $Luc^{\cdot +}$ and $O_2^{\cdot -}$, initiate ECL emission. Similarly in SCL system, TPA was oxidized by ·OH and generated TPA· could reduce Luc^{2+} and O_2 to initiate emission reactions.

The effect of TPA concentration on SCL intensity is shown in Fig. 3-9. The

SCL intensity increased monotonically up to 0.8 mM and leveled off. This is due to the increase of $O_2 \cdot^-$ concentration with increasing concentration of TPA.

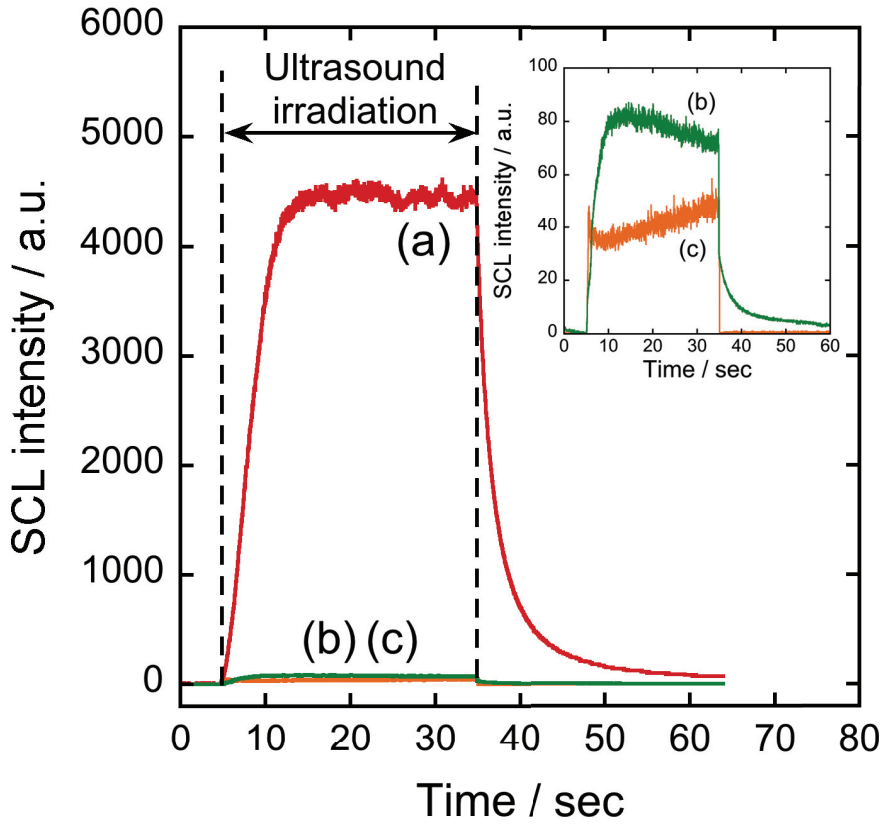

Figure 3-8 SCL and SL signals under the ultrasound irradiation by 500 kHz ultrasound in the solution containing 50 μM Luc^{2+} and 1 mM TPA (pH 11) with (a) O_2-saturated; (b) Ar-saturated. (c) In the absence of TPA.

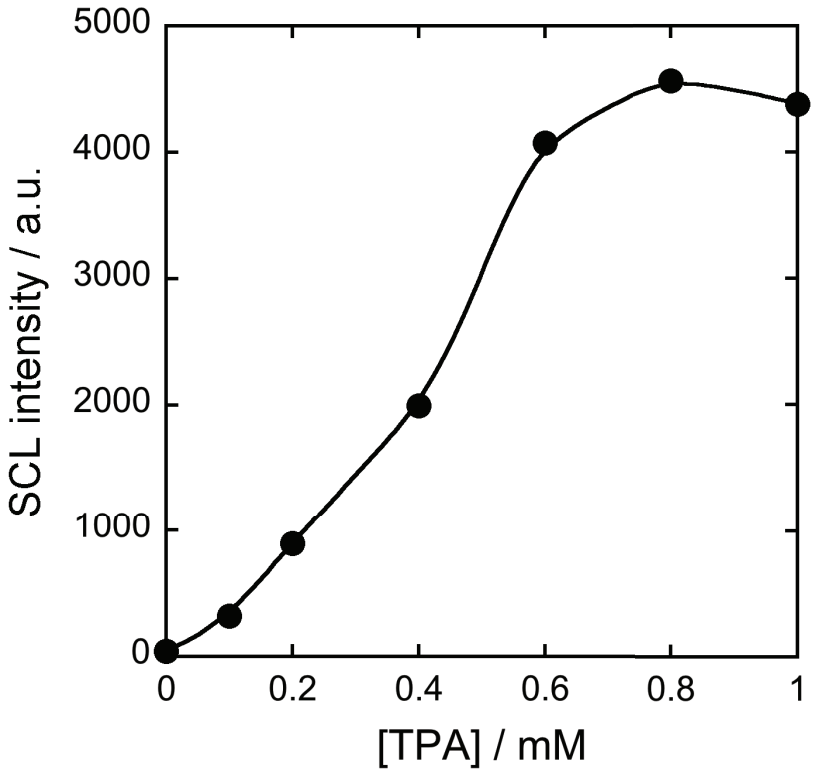

Figure 3-9 The dependence of the concentration of TPA on SCL intensity.

Fig. 3-10 shows the effect of various amines on luminol and Luc^{2+} SCL intensity. SCL intensities of the luminol system were inhibited by addition of the amines. Since the oxidation reaction by $^{\bullet}OH$ is needed for the luminol SCL emission, $^{\bullet}OH$ scavenged by the amines resulted in inhibition of luminol SCL. The second order rate constants for ethylamine and triethylamine are reported as 1.3×10^{10} and 1.1×10^{10} dm^3 mol^{-1} s^{-1}, respectively [31]. There is not great different between primary and tertiary amines. The second order rate constants of secondary amines and propylamines are probably similar values. Thus, the inhibition profiles were similar on luminol SCL. On the other hand, Luc^{2+} SCL intensities were greatly enhanced by dipropylamine, triethylamine and tripropylamine. The great

enhancement may be caused from radical stability. The first ionization potentials are reported for ethylamine (9.50 eV), propylamine (9.37 eV), dipropylamine (8.59 eV), triethylamine (8.08 eV) and tripropylamine (7.92 eV) [32]. The lower ionization potential means that oxidation of the amine is easier to occur and the generated radical ion is more stable. Therefore, the amines, which are tertiary and longer alkyl chain, enhanced the Luc^{2+} SCL intensities.

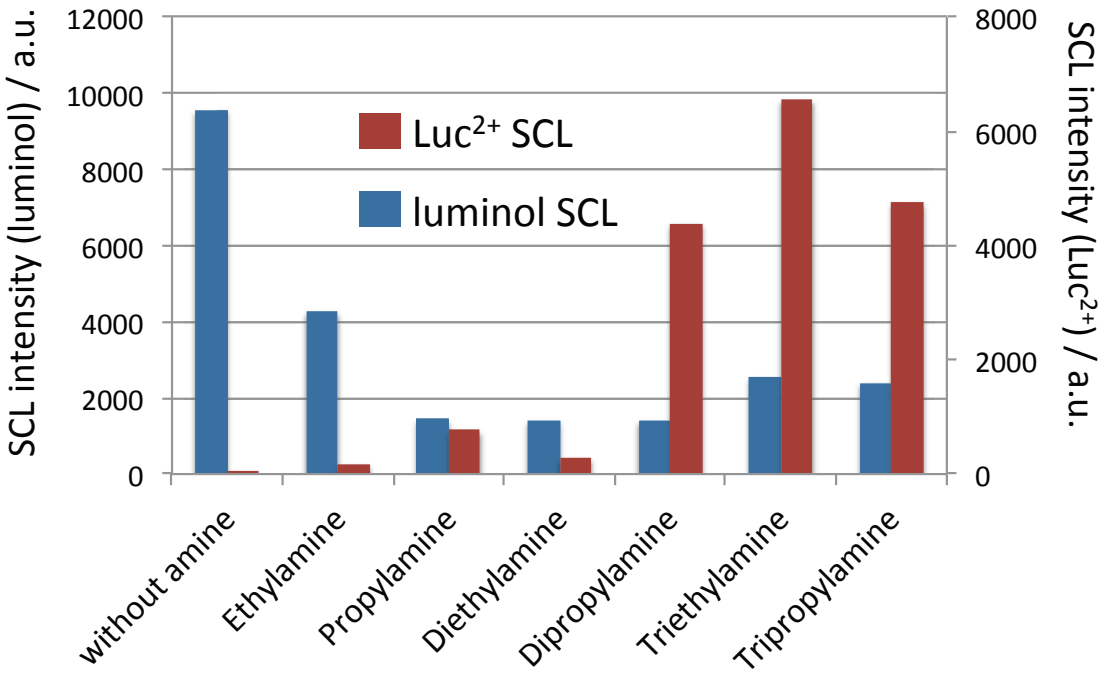

Fig. 3-10 The effect of the kind of amines on luminol SCL and Luc^{2+} SCL. The concentrations of amines are 1 mM.

3.3.5 Fluorescence probe used for detection of superoxide anion radical

To confirm the $O_2\cdot^-$ production in the reaction (3-2), $O_2\cdot^-$ was detected by a spectrofluorometric method using 2-(2-pyridyl)benzothiazoline as the fluorescent

probe. The probe can selectively react with $O_2\cdot^-$ by deleting hydrogen to yield 2-(2-pyridyl)-benzothiazole (Fig. 3-11), which exhibits strong fluorescence at 528 nm. [11] Figure 3-12(A) shows the fluorescence (FL) spectra of 30 μM 2-(2-pyridyl)benzothiazoline obtained by sonication of the O_2-saturated solution containing 10 mM 2-propanol. Before ultrasound irradiation, 2-(2-pyridyl)benzothiazoline itself exhibited no fluorescence. The FL intensity at 528 nm increased with increasing ultrasonic irradiation time, which demonstrated that $O_2\cdot^-$ was gradually produced in the solution. Figure 3-12(B) illustrates the FL intensity of 30 μM 2-(2-pyridyl)benzothiazoline as a function of ultrasound irradiation time in the (a) O_2-saturated solution and (b) N_2-saturated solution. Because the production rate of $O_2\cdot^-$ was higher in the O_2-saturated solution, it is confirmed that the 2-propanol radical can reduce oxygen to $O_2\cdot^-$, as shown in reaction (3-2).

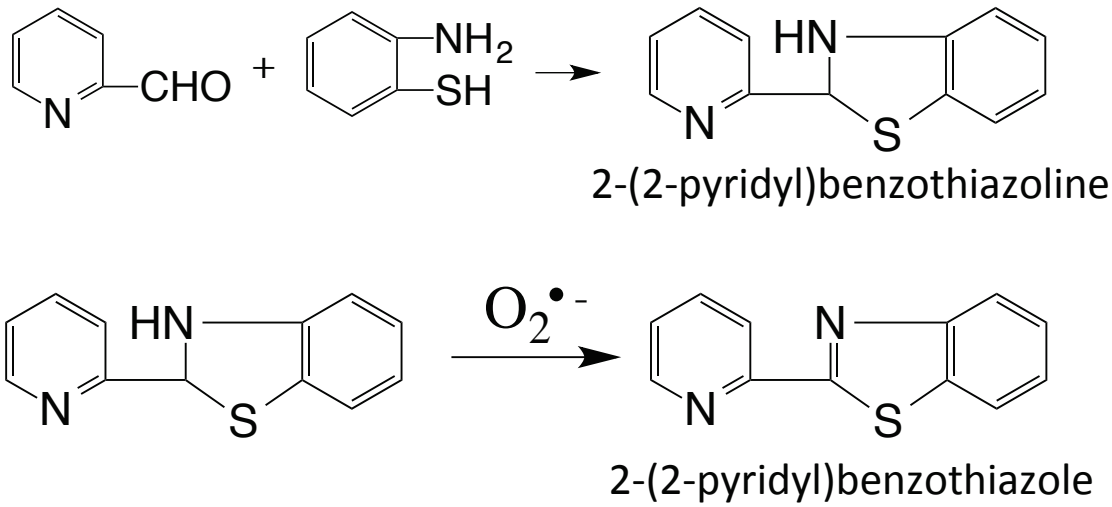

Figure 3-11 The reaction to synthesis of 2-(2-pyridyl)benzothiazoline and its reaction with $O_2\cdot^-$.

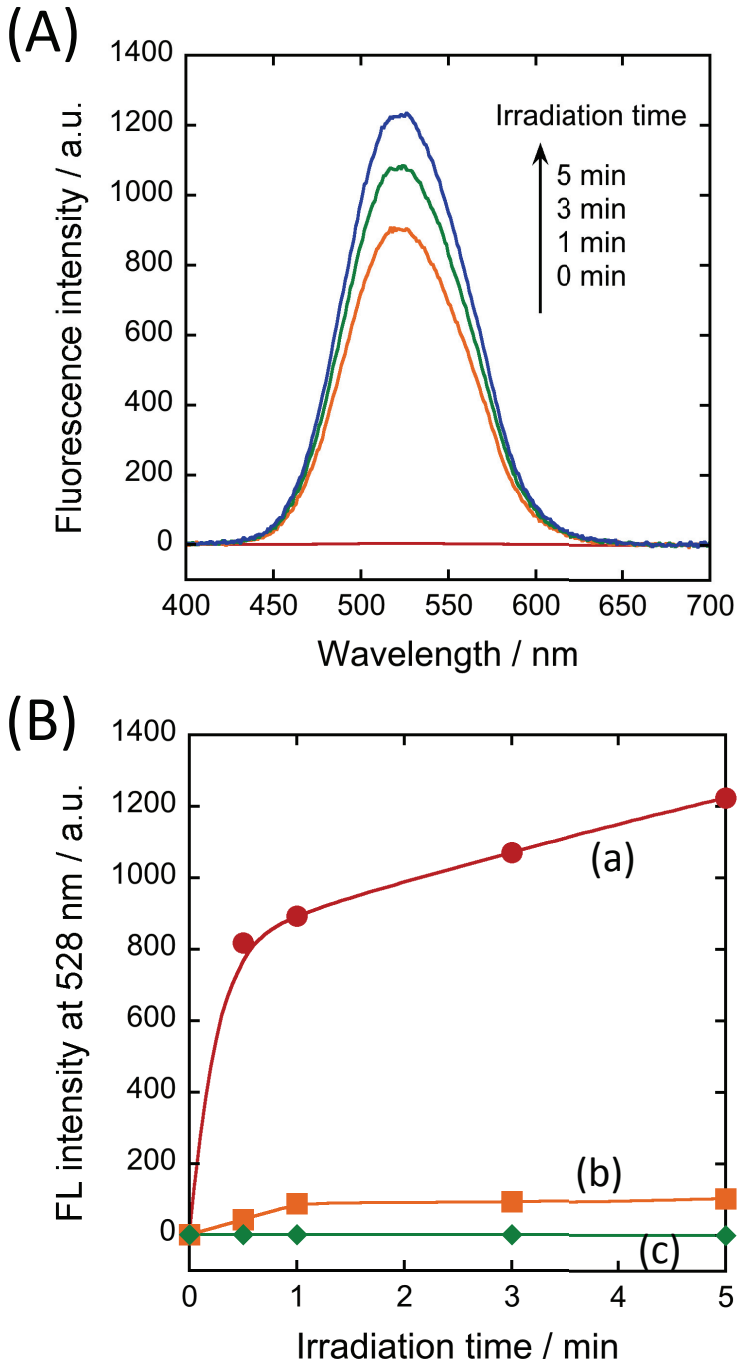

Figure 3-12 (A) Effect of ultrasonic irradiation time on fluorescence spectra of 30 μM 2-(2-pyridyl)benzothiazoline in O_2-satureted solution in the solution containing 10 mM 2-propanol (pH 11). (B) Relationship between the fluorescence intensity at 528 nm and ultrasonic irradiation time in (a) O_2-saturated solution; (b) N_2-saturated solution; (c) air-saturated solution without irradiation. λ_{ex} = 377 nm.

3.3.6 Calibration using hypoxanthine and xanthine oxidase

As mentioned in section 3.3.5, 2-(2-pyridyl)benzothiazoline can be used as a fluorescence probe for the detection of superoxide anion radical. However, the fluorescence intensity of this probe has not been connected to the concentration of superoxide. The calibration method of fluorescence intensity is necessary for quantitative analysis of superoxide. Usually, superoxide is generated in hypoxanthine (HX) / xanthine oxidase (XOD) system. If HX/XOD produces superoxide at a constant rate P (mol L^{-1} s^{-1}) and the superoxide decays in the pseudo-first order with a rate constant k (s^{-1}), the following equation is obtained:

$$\frac{d[O_2^{\bullet -}]}{dt} = P - k[O_2^{\bullet -}] \tag{3-5}$$

where $[O_2^{\bullet -}]_{ss}$ is the superoxide concentration.

Then rearrange and integrate Eq. (1), Eq. (2) is obtained:

$$[O_2^{\bullet -}] = \frac{P}{k}(1 - e^{-kt}) \tag{3-6}$$

When the reaction reaches the steady state, the left side of Eq. (3-5) equals to zero and Eq. (3-7) is obtained:

$$[O_2^{\bullet -}]_{SS} = \frac{P}{k} \tag{3-7}$$

where $[O_2^{\bullet -}]_{ss}$ means the superoxide concentration at the steady state. Substituting Eq. (3-7) to Eq. (3-6) and Eq. (3-8) is obtained:

$$[O_2^{\bullet -}] = [O_2^{\bullet -}]_{SS}(1 - e^{-kt}) \tag{3-8}$$

Rearrange and take the log of Eq. (4):

$$\ln\left\{\frac{[O_2^{\bullet-}]_{SS}}{[O_2^{\bullet-}]_{SS}-[O_2^{\bullet-}]}\right\}=kt \tag{3-9}$$

We assume that the superoxide concentration is proportional to the fluorescence intensity I, the calibration coefficient C (fluorescence intensity (a.u.) / μM) is given by

$$C=\frac{I}{[O_2^{\bullet-}]}=\frac{I_{SS}}{[O_2^{\bullet-}]_{SS}} \tag{3-10}$$

Substituting Eq. (3-10) to Eq. (3-9), we can obtain the fluorescence intensity form of Eq. (3-11):

$$F=\ln\left\{\frac{I_{SS}}{I_{SS}-I}\right\}=kt \tag{3-11}$$

When define the left-hand side of Eq. (3-11) as F, k can be obtained from the plot of F against t. The fluorescence response observed in HX/XOD system and transformed data following Eq. (3-11) are shown in Fig. 3-13. I_{SS} was determined to be 35.99 a.u. from average of the intensity values at the plateau of Fig. 3-13 (A) and k was 1.49×10^{-3} s^{-1} from the slope of Fig. 3-13 (B).

To determine P, we performed the Cytochrome c (Cyt c) reduction method. Cyt c is one of hemeprotein. This small protein has iron ion and shows redox activity. It is known that $O_2\cdot^-$ can reduce Cyt c (Fe^{III}) to Cyt c (Fe^{II}) [33]. Maximum absorbance of Cyt c (Fe^{II}) appears at 550 nm and its molar absorption coffecient at 550 nm is 0.028 M^{-1} cm^{-1} (from the data-sheet of Sigma-Aldrich Co.) Then we can calculate the concentration of $O_2\cdot^-$ by using the Cyt c method. Fig. 3-14 (A) shows absorbance at 550 nm in HX/XOD system and Fig 3.15 (B) shows the Cyt c (Fe^{II})

concentration plot calculated from Fig. 3-14 (A). As the amount of $O_2\cdot^-$ is equal to the amount of Cyt c (Fe^{II}), the generation rate of $O_2\cdot^-$ can be calculate from the initial generation rate of Cyt c (Fe^{II}) shown in Fig. 3-14 (B). The generation rate, P is 0.0106 μM s^{-1}. $[O_2^{\cdot-}]_{ss}$ is obtained from Eq. (3-7) and is 7.09 μM. Now substituting $[O_2^{\cdot-}]_{ss}$ and I_{SS} to Eq. (3-10), calibration coefficient C is calculated as 5.08 a.u. / μM.

Fluorescence intensities under ultrasound irradiation were already shown in Fig. 3-12. These intensities can be converted into $O_2\cdot^-$ concentration by using calibration coefficient. The $O_2\cdot^-$ concentration at 30 s irradiation time is calculated as 4.48 μM.

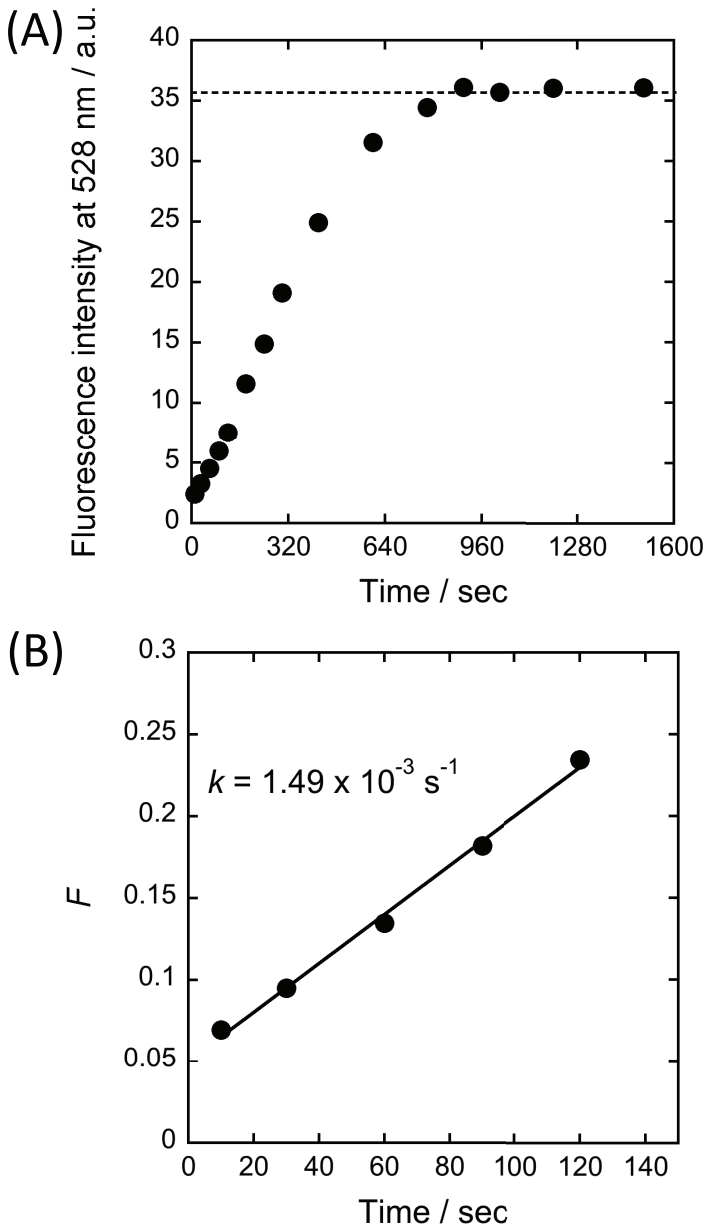

Figure 3-13 (A) Change of the fluorescence intensity at 528 nm with the reaction time in the solution containing 30 μM 2-(2-pyridyl)benzothiazoline, 20 U / L XOD and 120 μM HX. (B) The plot of F in Eq (3-11) *vs.* time.

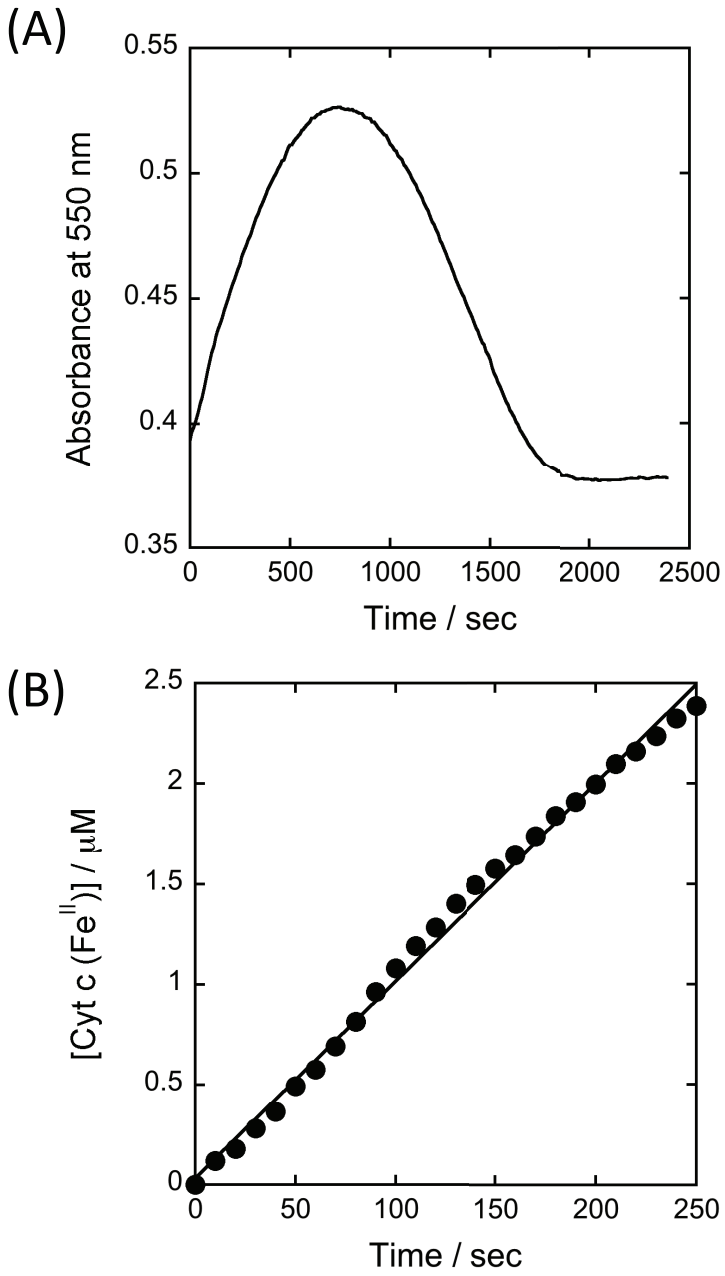

Figure 3-14 (A) Absorbance change at 550 nm with reaction time in the solution containing 180 μM Cyt c, 20 U /L XOD and 120 μM HX. (B) Initial generation rate of the reduced form of Cyt c.

3.3.7 Observation of SCL using a sonochemical microreactor

Recently, microreactors have been combined with ultrasound in order to better understand the physical and chemical aspects of sonochemistry. [7, 34, 35] We further studied the spatial distribution of SCL using a microreactor.

Figure 3-15(A) shows the SCL images for the luminol system. We found that stable bubbles or a bubble cloud was formed in the reactor during sonication, and luminol SCL was enhanced in the boundary between bubbles. These facts coincide with the results in a previous study. [36] On the other hand, however, no distinct spatial pattern was observed in the Luc^{2+} SCL system (Fig. 3-15(B)). It is, thus, suggested that the reactive species of 2-propanol radicals more likely initiate the reduction reaction in the bulk solution when they subsequently diffuse away from the cavitation bubble. Therefore, unlike the luminol SCL system, the SCL of Luc^{2+} arises from the secondary sonochemical reactions that occur in the bulk of solution.

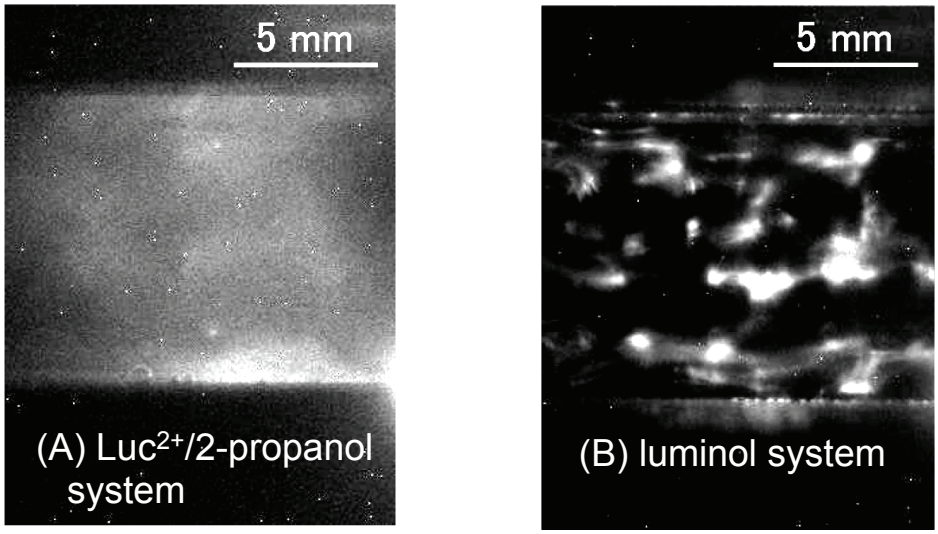

Figure 3-15 Photographic image of SCL observed in the sonochemical microreactor. (A) SCL observed in Luc^{2+}/2-propanol system; (B) in luminol system with exposure time of 60 s.

3.3.8 Possible pathways and spectroscopic properties of Luc^{2+} SCL system

An emission spectrum of Luc^{2+} ECL is shown in Figure 3-16. Maskiewicz et al. reported emission spectra of CL of Luc^{2+} with H_2O_2 in alkaline aqueous solution similar to Fig. 3-16. They considered that the emission spectrum resulted from absorption of NMA* emission by Luc^{2+}. [37] Legg and Hercules concluded that Luc^{2+} ECL in organic media (DMSO, DMF and Acetonitrile) was obtained from resonance singlet-singlet energy transfer in the NMA-Luc^{2+} system due to the fact that the rate of energy transfer is sufficiently faster than diffusion control. [38] Our experimental result shows that ECL was emitted from Luc^{2+} rather than NMA and the fluorescence spectrum of NMA is superimposable on the absorption spectrum of Luc^{2+} around 440 nm (Fig.3-17). This result is favorable situation for energy transfer.

Thus, Luc^{2+} SCL is emitted from exited Luc^{2+} (Luc^{2+}*) generated by energy transfer step. Support for the above interpretation comes from the formation of NMA due to the sonochemical reactions. Fig. 3-18(A) shows the fluorescent spectral changes during the sonication of an aqueous solution containing 10 μM Luc^{2+} and 50 mM 2-propanol (pH 11), which was saturated with oxygen. The first spectrum (red line) was measured before sonication. The fluorescence emission spectrum has two very closely located peaks at 495 nm and 510 nm, respectively. After the sonication, a new emission peak at about 430 nm appeared, and increased with increasing of the sonication time. On the other hand, the new peak could not observed in the sonicated solution in the absence of 2-propanol, as is shown in Fig. 3-18(B). Since the emission peak at 430 nm is identified with that of NMA, [37] NMA is thus suggested to be the product in the sonochemical reactions.

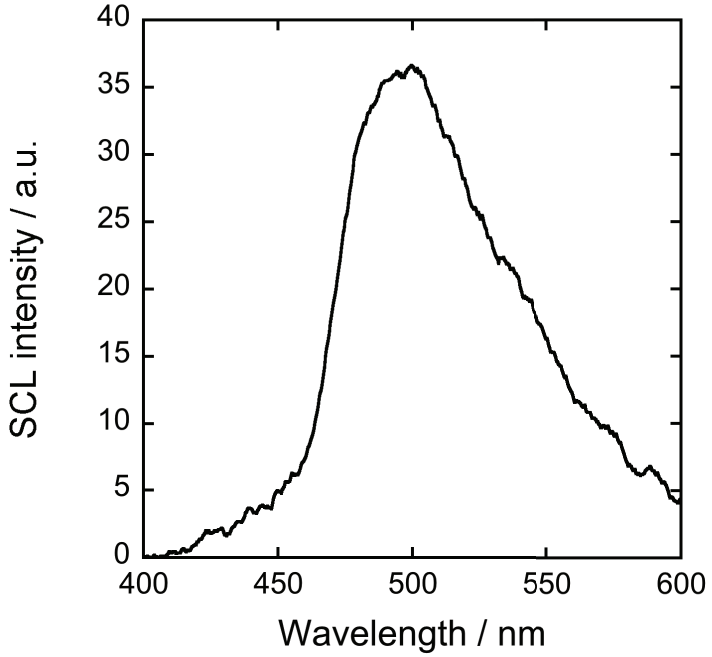

Figure 3-16 SCL emission spectrum of Luc^{2+} SCL system.

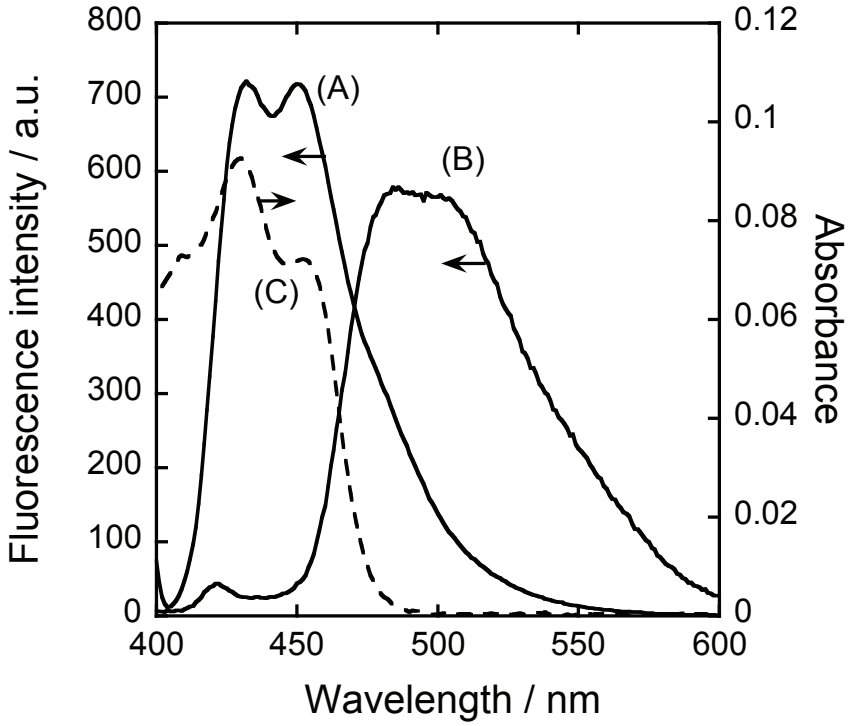

Figure 3-17 Fluorescence spectra of (A) 1.0 mM Luc^{2+} and (B) 0.5 mM NMA are shown in solid line. (C) Absorbance spectrum of 10 mM Luc^{2+} shown in dashed line.

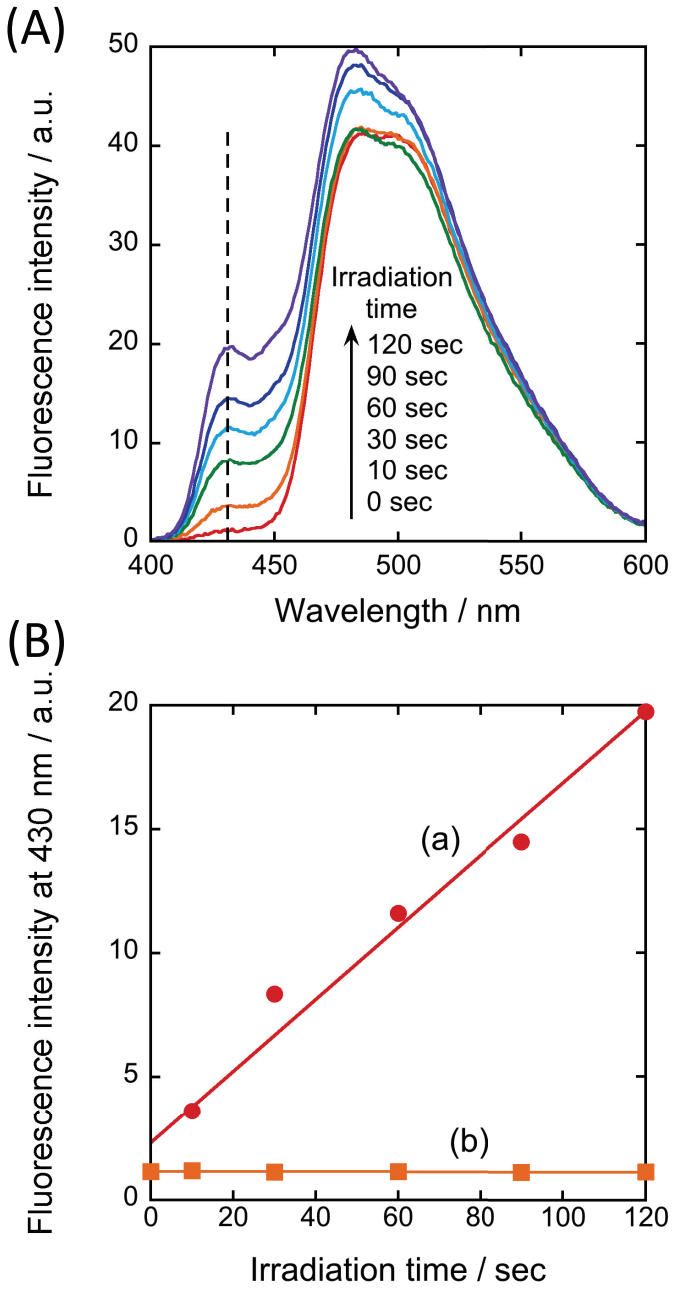

Figure 3-18 (A) Fluorescence spectra of the solution after ultrasound irradiation (λ_{ex} = 380 nm). Irradiation time: 0, 10, 30, 60, 90 s. The solution contained 10 μM Luc^{2+} and 50 mM 2-propanol (pH 11, O_2-saturated). (B) Dependence of irradiation time of fluorescence intensity at 430 nm: (a) in the present of 2-propanol; (b) in the absent of 2-propanol.

On the basis of the above experimental results, we suggest the possible pathways of the Luc^{2+}/propanol SCL system, as summarized in Scheme 3-1. The SCL reaction is considered to occur in two regions. In region I, H• and •OH are generated by cavitation near or inside the cavitation bubbles. 2-prapanol reacts with •OH near (or inside) a bubble to generate reducing radical species [$CH_3C^{\bullet}(OH)CH_3$]. In region II, radical species diffuse to the bulk solution where the secondary sonochemical reactions may be involved. In this region, the reducing radical species reacts with molecular oxygen and Luc^{2+} through one-electron transfer, producing both $Luc^{\bullet+}$ and $O_2\cdot^-$ species, and $Luc^{\bullet+}$ reacts with $O_2\cdot^-$ to yield an extremely unstable dioxetane-type intermediate Luc(OO), which finally decomposed to provide an excited state of NMA (NMA*). The energy of excited state of NMA transfers to Luc^{2+} and Luc^{2+} is excited. Accordingly, the emission will occur from excited state of Luc^{2+} generated by energy transfer step, which is shown as region III in Scheme 3.1.

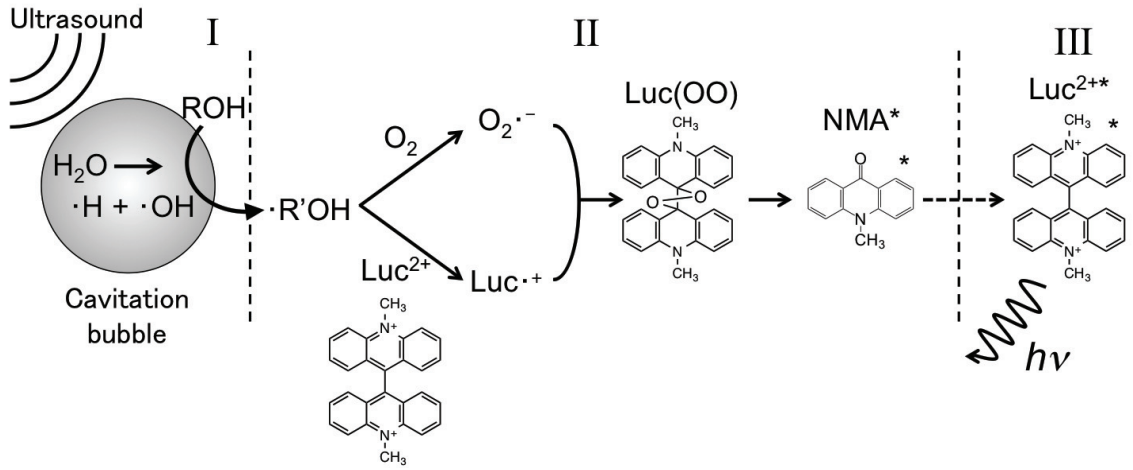

Scheme 3-1 Possible pathways of the Luc^{2+} SCL using 2-propanol as coreactant.· ROH represent the radical species CH_3C·$(OH)CH_3$ generated from the reaction of $CH_3CH(OH)CH_3$ (ROH) with ·OH.

3.4 Conclusions

A new SCL system using Luc^{2+} as a CL probe was investigated in this study. The experiment showed that Luc^{2+} gave SCL under 500 kHz ultrasound sonication when a small amount of alcohol was present as a coreactant. The SCL behavior was found to be strongly dependent on the presence of dissolved gases such as air, O_2, N_2, and Ar. The highest SCL intensity was observed in an O_2-saturated solution, but the intensity was very weak in the absence of O_2 (in N_2-saturated solution), indicating that molecular oxygen is required to generate SCL. Because the SCL intensity decreased in the presence of SOD, the generation of O_2·⁻ in the ultrasonic reaction field was important in light production in the Luc^{2+} SCL system. The evidence of O_2 ·⁻ production was validated by a spectrofluorometric method using 2-(2-pyridyl)benzothiazoline as the fluorescent probe. The results indicated that the

production of $O_2^{\cdot -}$ by ultrasound was more efficient in an O_2-saturated solution in the presence of 2-propanol, which is consistent with the results of SCL measurements. We suggest that the 2-propanol molecule in the interfacial region of a cavitation bubble reacts with a hydroxyl radical (•OH) to form a 2-propanol radical, $CH_3C^{\bullet}(OH)CH_3$, which can subsequently react with dissolved oxygen to generate $O_2^{\cdot -}$. We conclude that the generation of $O_2^{\cdot -}$ is crucial in Luc^{2+} SCL reactions. That is, the signal from Luc^{2+} SCL reflects the information on reductive species production in sonochemical reactions.

References

[1] H. N. McMurray and B. P. Wilson, Mechanistic and Spatial Study of Ultrasonically Induced Luminol Chemiluminescence, *J. Phys. Chem. A*, **103** (1999) 3955.

[2] S. Hatanaka, H. Mitome, K. Yasui, and S. Hayashi, Single-Bubble Sonochemiluminescence in Aqueous Luminol Solutions, *J. Am. Chem. Soc.*, **124** (2002) 10250.

[3] S. Hatanaka, S. Hayashi and P.-K. Choi, Sonoluminescence of Alkali-Metal Atoms in Sulfuric Acid: Comparison with That in Water, *Jpn. J. Appl. Phys.*, **49** (2010) 07HE01.

[4] K. Nozaki, S. Hatanaka and S. Hayashi, Dynamics of Single Sonoluminecsing Bubble in Concentrated Aqueous Alkaline Halide Solutions, *Jpn. J. Appl. Phys.*, **43** (2004) 6481.

[5] J. Jin, H. Kumeta, F. Takahashi and Y. Asakura, Sensitive Detection of Hydroxyl Radical Production in Ultrasonic Field with Electrochemiluminescence Optical Sensor, *Chem. Lett.*, **38** (2009) 292.

[6] T. Tsuziuti, K. Yasui, J. Lee, T. Kozuka, A. Towata and Y. Iida, Mechanism of Enhancement of Sonochemical-Reaction Efficiency by Pulsed Ultrasound, *J. Phys. Chem. A*, **112** (2008) 4875.

[7] D. F. Rivas, M. Ashokkumar, T. Leong, K. Yasui, T. Tuziuti, S. Kentish, D. Lohse and H. J. G. E. Gardeniers, Sonoluminescence and sonochemiluminescence from a microreactor, *Ultrason. Sonochem.* **19** (2012) 1252.

[8] S. I. Liochev and I. Fridovich, LUCIGENIN AS MEDIATOR OF SUPEROXIDE PRODUCTION: REVISITED, *Free Radic. Biol. Med.*, **25** (1998) 926.

[9] I. B. Afanas'ev, E. A. Ostrakhovitch, E. V. Mikhal'chik and L. G. Korkina, Direct enzymatic reduction of lucigenin decreases lucigenin-amplified chemiluminescence produced by superoxide ion, *Luminescence*, **16** (2001) 305.

[10] K. Faulkner and I. Fridovich, LUMINOL AND LUCIGENIN AS DETECTORS FOR $O_2 \cdot^-$, *Free Radic. Biol. Med.*, **15** (1993) 447.

[11] L. Zhang, B. Tang and Y. Ding, Study of 2-(2-Pyridyl)benzothiazoline as a Novel Fluorescent Probe for the Identification of Superoxide Anion Radicals and the Determination of Superoxide Dismutase Activity in Scallion Genus Foods, *J. Agric. Food Chem.*, **53** (2005) 549.

[12] K. Makino, M. M. Mossoba and P. Riesz, Chemical Effects of Ultrasound on Aqueous Solutions. Formation of Hydroxyl Radicals and Hydrogen Atoms, *J. Phys. Chem.*, **87** (1983) 1369.

[13] M. Ashokkumar, A. Crum, C. A. Frensley, F. Grieser, T. J. Matula, W. B. McNamara and K. S. Suslick, Effect of Solutes on Single-Bubble Sonoluminescence in Water, *J. Phys. Chem. A*, **93** (2000) 8462.

[14] H. A. Schwarz and R. W. Dodso, Reduction Potentials of CO_2^- and the Alcohol Radicals, *J. Phys. Chem.*, **93** (1989) 409.

[15] F. Grieser, R. Hobson, J. Sostaric and P. Mulvaney, Sonochemical reduction processes in aqueous colloidal systems, *Ultrasonics*, **34** (1996) 547.

[16] B. H. J. Bielski and J. M. Gebicki, Generation of Superoxide Radicals by Photolysis of Oxygenated Ethanol Solutions, *J. Am. Chem. Soc.*, **104** (1982)

796.

[17] I. Spasojević, S. I. Liochev and I. Fridovich, Lucigenin: Redox Potential in Aqueous Media and Redox Cycling with O_2^- Production, *Arch. Biochem. Biophys.*, **373** (2000) 447.

[18] P. M. Wood, The potential diagram for oxygen at pH 7, *Biochem. J.* **253** (1988) 287.

[19] M. S. McDowell, A. Bakac and J. H. Espenson, A Convenient Route to Superoxide Ion in Aqueous Solution, *Inorg. Chem.*, **22** (1983) 847.

[20] Y. Ilan, J. Rabani and A. Henglein, Pulse Radiolytic Investigations of Peroxy Radicals Produced from 2-Propanol and Methanol, *J. Phys. Chem.*, **80** (1976) 1558

[21] C. Lu, G. Song and J. Lin, Reactive oxygen species and their chemiluminescence-detection methods, *TrAC Trends in Anal. Chem.*, **25** (2006) 985.

[22] J. M. McCord and I. Fridovich, The reduction of Cytochrome c by Milk Xanthine Oxidase, *J. Biol. Chem.*, **243** (1968) 5753.

[23] J. M. McCord and I. Fridovich, Superoxide dismutase - an enzymic function for erytherocuprein (hemocuprein), *J. Biol Chem.*, **244** (1969) 6049.

[24] N. Shimizu, C. Ogino, M. F. Dadjour, K. Ninomiya, A. Fujihira and K. Sakiyama, Sonocatalytic facilitation of hydroxyl radical generation in the presence of TiO_2, *Ultrason. Sonochem.*, **15** (2008) 988.

[25] R. Overend and G. Paraskevopoulos, Rates of OH Radical Reactions. 4. Reactions with Methanol, Ethanol, 1-Propanol, and 2-Propanol at 296 K, *J. Phys. Chem.*, **82** (1978) 1329.

[26] S. Koda, T. Kimura, T. Kondo, H. Mitome, A standard method to calibrate sonochemical efficiency of an individual reaction system, *Ultrason. Sonochem.*, **10** (2003) 149.

[27] J. Rae, M. Ashokkumar, O. Eulaerts, C. Sonntag, J. Reisse and F. Grieser, Estimation of ultrasound induced cavitation bubble temperatures in aqueous solutions, *Ultrason. Sonochem.*, **12** (2005) 325.

[28] B. H. J. Bielski and A. O. Allen, Mechanism of the Disproportionation of Superoxide Radicals, *J. Phys. Chem.*, **81** (1977) 1048.

[29] W. Miao, J.-P. Choi and A. J. Bard, Electrogenerated Chemiluminescence 69: The Tris(2,2'-bipyridine)ruthenium(II), $(Ru(bpy)_3^{2+})$ / Tri-n-propylamine (TPrA) System Revisited - A New Route Involving $TPrA^{\cdot +}$ Cation Radicals, *J. Am. Chem. Soc.*, **124** (2002) 14478.

[30] H. Zhang, H. Cui, W. Wang, M.-J. Shi and J.-Z. Guo, Electrochemiluminescence of lucigenin/tributylamine system in ethanol solution, *J. Photochem. Photobiol. A Chem.*, **197** (2008) 55.

[31] M. Simić, P. Neta and E. Hayon, Pulse radiolytic investigation of aliphatic amines in aqueous solution, *Int. J. Radiat. Phys. Chem.*, **3** (1971) 309.

[32] J. B. Noffsinger and N. D. Danielson, Generation of Chemiluminescence upon Reaction of Aliphatic Amines with Tris(2,2'-bipyridine)ruthenium(III), *Anal. Chem.*, **59** (1987) 865.

[33] I. Fridovich, Quantitative Aspects of the Production of Superoxide Anion Radical by Milk Xanthine Oxidase, *J. Biol. Chem.*, **245** (1970) 4053.

[34] T. Kozuka, K. Yasui, S. Hatanaka, T. Tuziuti, J. Lee and A. Towata, Study of an Acoustic Field in a Microchannel, Jpn. *J. Appl. Phys.*, **49** (2010) 07HE14.

[35] D. F. Rivas, P. Cintas and H. J. G. E. Gardeniers, Merging microfluidics and sonochemistry: towards greener and more efficient micro-sono-reactors, *Chem. Commun.,* **48** (2012) 10935.

[36] T. Tuziuti, K. Yasui, T. Kozuka, A. Towata and Y. Iida, Enhancement of Sonochemical Reaction Rate by Addition of Micrometer-Sized Air Bubbles, *J. Phys. Chem. A*, **110** (2006) 10720.

[37] R. Maskiewikz, D. Sogah and T. Bruice, Chemiluminescent Reactions of Lucigenin. 1. Reactions of Lucigenin with Hydrogen Peroxide, *J. Am. Chem. Soc.*, **101** (1979) 5347.

[38] K. D. Legg and D. M. Hercules, Electrochemically Generated Chemiluminescence of Lucigenin, *J. Am. Chem. Soc.*, **91** (1969) 1902.

Chapter 4

Antioxidant Activity Analysis with Sonochemiluminescence

4.1 Introduction

Oxygen-derived free radicals such as singlet molecular oxygen, superoxide anion radical ($O_2^{\cdot -}$), and hydroxyl radical (•OH) are very highly reactive species. Much attention has been paid to antioxidative activities [1,2] and their effect on human health; therefore, methods for the estimation of antioxidant activities are required. However, the identification of radical species is not easy due to their short lifetimes and differing chemical properties. Over the past few years, a variety of methods has been developed, including colorimetric [3, 4], fluorimetric [5, 6], electrochemical [7, 8], and chromatographic assays [9]. Of particular interest are chemiluminescence based tests, which offer a simple but sensitive means of monitoring low antioxidant levels [10, 11]. Both luminol and Luc^{2+} can emit luminescence when ROS are present. Consequently, the decrease in CL intensity derived from luminol or Luc^{2+} CL reactions has been investigated as a screening method for the determination of antioxidants in real samples [10].

A system for the determination of antioxidant activity has two components: 1) a generator of free radicals, e.g., ROS, and 2) a detector allowing quantification of the generated species and indicating changes in the measured signal in response to the presence of antioxidative compounds. It is well recognized that acoustic cavitation in liquids give rise to very intense local physicochemical effects that could lead to the hemolytic cleavage of covalent bonds between the oxygen and hydrogen atoms comprising the water molecules present. As a result, when liquid is irradiated by an ultrasonic wave, water and oxygen molecules inside the bubble are dissociated and

reactive radical species are created in the bubble. Thus, ultrasonic irradiation is considered an effective source for ROS generation. It was indicated in Chapter 3 that the intensity of Luc^{2+} SCL is essentially due to the generation of $O_2\cdot^-$ in the ultrasonic fields. That is to say, the SCL system permits the quantification of antioxidant activity without using an enzyme for $O_2\cdot^-$ production. The potential use of SCL in determining antioxidant activity has not been well investigated, and published literature in this area is very scarce. In this chapter, the SCL of the Luc^{2+}/2-propanol system is proposed for the evaluation of antioxidant activity against $O_2\cdot^-$ for the first time. The kinetic aspects of the SCL reactions are discussed.

4.2 Experimental section

4.2.1 Reagents

All chemicals used were of analytical grade. Luminol (5-amino-2,3-dihydro-1,4-phthalazinedione), lucigenin (bis-N-methylacridiniumnitrate), and superoxide dismutase (SOD) of bovine erythrocytes (5140 U/mg) were purchased from Nacalai Tesque (Kyoto, Japan). Protocatechuic acid, catechin, and rutin were purchased from Nacalai Tesque (Kyoto, Japan). Caffeic acid, Trolox, and quercetin were purchased from Tokyo Chemical Industry Co. (Tokyo, Japan). All solutions were prepared with distilled water purified by a WS200 distillation system (Yamato Scientific Co., Tokyo, Japan). 1 mM stock solutions of luminol and lucigenin were prepared by dissolving appropriate amounts of reagent in distilled water. The pH was carefully adjusted to an appropriate level by titration with sodium hydroxide. A series of

antioxidant standard solutions were prepared by sequentially diluting the standard stock solutions.

4.2.2 Instruments

The apparatus used in this study has been described in Chapter 3. Briefly, the sonochemical reactor was a cylindrical acrylic chamber of a 6 cm in internal diameter, which was filled with distilled water. A 500 kHz PZT transducer was mounted on a stainless steel vibrational plate placed at the bottom of the reactor. The transducer was driven by a WF 1974 function generator (NF Co., Japan) and amplified by a T145-5015 amplifier (THAMWAY Co., Japan). A cylindrical glass vessel of 3 cm in diameter was used as a sonochemical cell for SCL observation. In all experiments, the sample volume in the cell was 10 cm^3, and the top of the cell was sealed with a rubber cap. Since the sonochemical efficiency became larger near the liquid surface of the cylindrical acrylic chamber, the cell was placed at the top of the chamber at a fixed position above the PZT transducer and was irradiated indirectly by ultrasound from the transducer. The light emitting from the sample solution was measured with a H6780 photomultiplier tube module (Hamamatsu Photonics, Japan) through a quartz glass window on the side of the sonochemical reactor. All experiments were conducted in a light-proof box.

4.2.3 Measurement of the $O_2 \cdot^-$ scavenging properties of samples

The SCL intensity was recorded as a function of time. An aqueous solution at pH 11 containing 50 μM Luc^{2+} and 50 mM 2-propanol was used as a blank. For each

sample, the average SCL intensity of three measurements was calculated.

4.3 Results and discussion

4.3.1 Features of SCL profiles

In analytical CL methodology, the CL dynamic profile (a plot of CL intensity *vs.* time) is a kinetic response curve that corresponds to the generation of the light emitting products and the formation of the final product. Luminescence kinetic measurements are usually performed with a stop-flow apparatus to quickly mix the samples and reagents. The solution is analyzed in a flow cell for the measurement of CL intensity over time. However, kinetic measurements with SCL are much simpler. The SCL signal can be recorded after sonication of the solution without the mixing reagents. Figure 4-1 shows typical SCL profiles observed for samples of the luminol and Luc^{2+} solutions, respectively. The SCL of luminol was initiated by the radical species generated sonochemically, and the intensity rapidly reached its maximum (within 2 s). However, the intensity then gradually decreased and reached a steady state after 30 s ((A) in Fig.4.1). In the presence of 50 mM 2-propanol, the initial portion of the SCL profile (<2 s) decreased due to the scavenging of •OH by 2-propanol, but the intensity in the steady state portion remained unchanged. In the case of Luc^{2+}, only very weak light emission was observed in the O_2-saturated aqueous solution (pH 11) containing 50 μM Luc^{2+} [(C) in Fig. 4.1]. After the addition of 50 mM 2-propanol to the solution, significantly increased light intensity was observed. Unlike the case for luminol SCL, the light intensity gradually increased and reached its maximum (steady state) after 15 s of

sonication [(D) in Fig. 4.1]. It was suggested in Chapter 3 that SCL from Luc^{2+} could be due to the formation of $O_2\cdot^-$ when a small amount of 2-propanol is present as a co-reactant, and the generation of $O_2\cdot^-$ is considered as the rate determining step in the Luc^{2+} SCL reaction.

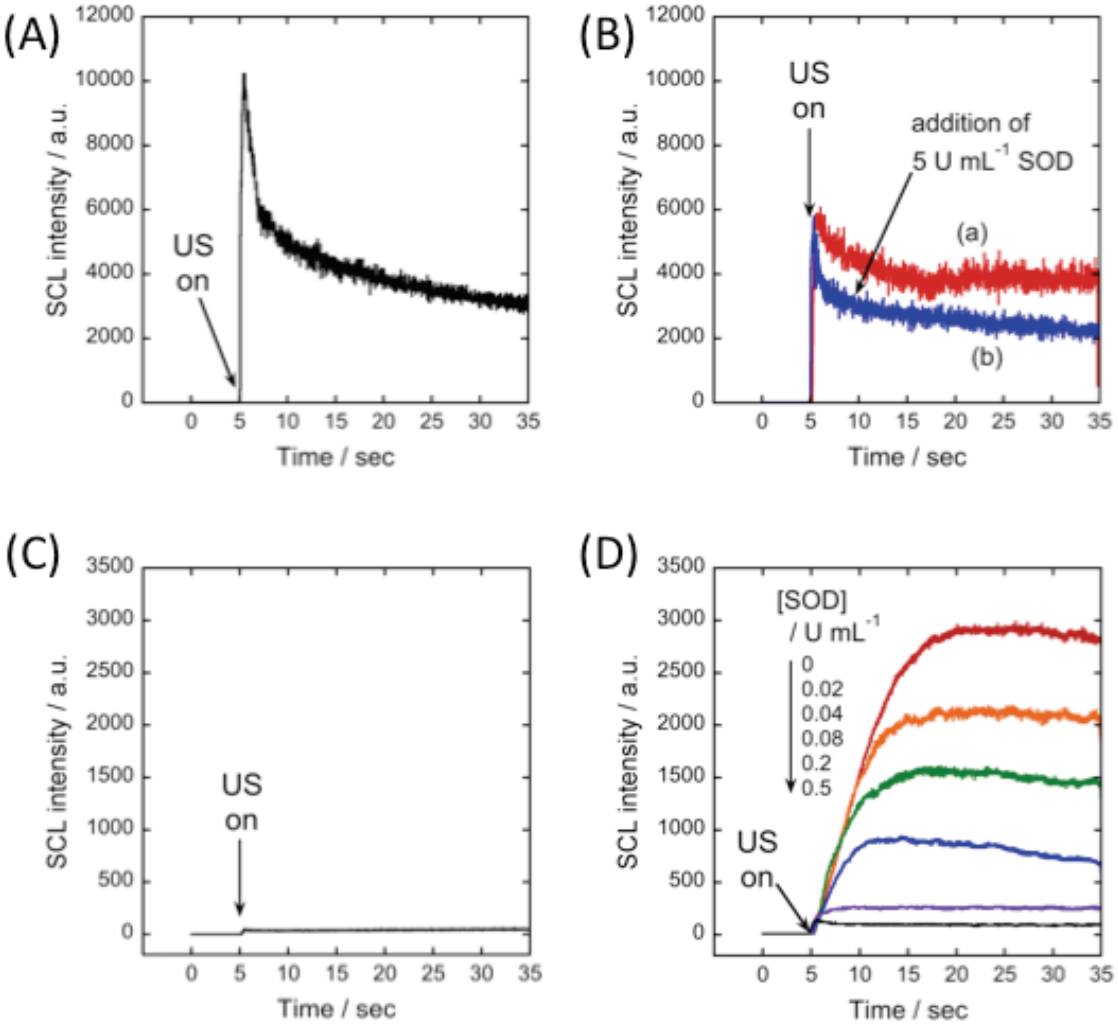

Figure 4-1 SCL dynamic profiles observed in luminol and Luc^{2+} SCL systems under 500 kHz ultrasound irradiation (with an output power of 80 W): (A) an air-saturated aqueous solution containing 50 μM luminol (pH 11); (B) solution (A) in the presence of 50 mM 2-propanol; (C) 50 μM Luc^{2+} in O_2-saturated aqueous solution (pH 11); and (D) solution (C) in the presence of 50 mM 2-propanol. In (B) and (D), the SCL responses in the presence of SOD at different concentration levels are also presented.

There are three possible steps in the sonochemical reactions; these lead to the formation of $O_2\cdot^-$:

I. $H_2O))) \cdot OH + H\cdot$ (4-1)

II. $\cdot OH + CH_3CH(OH)CH_3 \rightarrow CH_3C^{\bullet}(OH)CH_3 + H_2O$ (4-2)

III. $CH_3C^{\bullet}(OH)CH_3 + O_2 \rightarrow O_2\cdot^- + CH_3COCH_3 + H^+$ (4-3)

The SCL intensity *vs*. time profile of (D) in Fig. 4.1 is a kinetic response curve that corresponds to the $O_2\cdot^-$ generating rate. The 'plateau' portion in the curve (after 15 s sonication) indicates that the concentration of $O_2\cdot^-$ reached a steady state.

4.3.2 Quenching of the SCL signals

Superoxide dismutase (SOD) is an enzyme that can catalyze the disproportionation of $O_2\cdot^-$ and act as a scavenger of $O_2\cdot^-$. With the addition of 5 U mL^{-1} of SOD to the solution, the intensity of the SCL signal from luminol was quenched by about 30%, whereas the SCL from Luc^{2+} was completely quenched. It is therefore suggested that the SCL of Luc^{2+} is due to the formation of $O_2\cdot^-$, whereas the SCL of the luminol system might be induced by other radical intermediates besides $O_2\cdot^-$; that is to say, the assay based on the Luc^{2+} SCL system is more specific to $O_2\cdot^-$. The reaction scheme for luminol SCL might be more complicated, but we cannot presently offer a more reasonable interpretation.

It is a remarkable characteristic of the Luc^{2+} SCL system that the signal intensity reaches steady state after a sonication time of 15 s. This provides an opportunity for the detection of antioxidant activity against $O_2\cdot^-$. Figure 4-1(D) demonstrates the effect of SOD concentration on the SCL of Luc^{2+}. The effect is characterized by an inhibition of the chemiluminescence intensity. The evaluation parameter of the measurement is the inhibition of SCL, which can be calculated with the following equation.

$$\text{SCL inhibitation rate}(\%) = \frac{(I_{SCL}^{0} - I_{SCL}^{x})}{I_{SCL}^{0}} \times 100 \qquad (4\text{-}4)$$

Here, $I_{SCL}{}^{0}$ is the SCL intensity observed in the absence of antioxidant, whereas $I_{SCL}{}^{x}$ is the SCL intensity yield in the presence of antioxidant at differing concentrations (Fig. 4-2). As shown in Fig. 4-3, the decrease in SCL depended on the concentration of SOD.

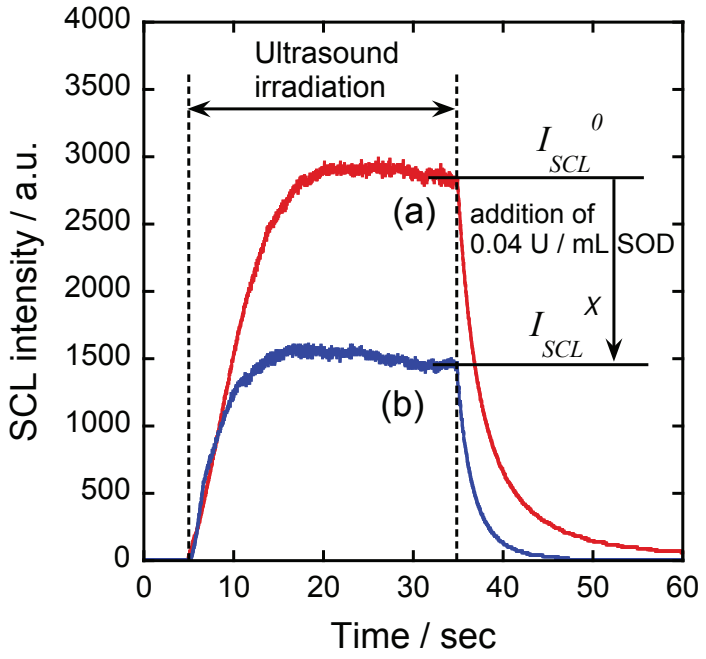

Figure 4-2 Inhibition of SCL intensity by the addition of SOD. SCL intensities in the solution containing 50 μM Luc^{2+}, 1 mM NaOH, and 50 mM 2-propanol (O_2 saturated) (a) without or (b) with 0.04 U/mL SOD.

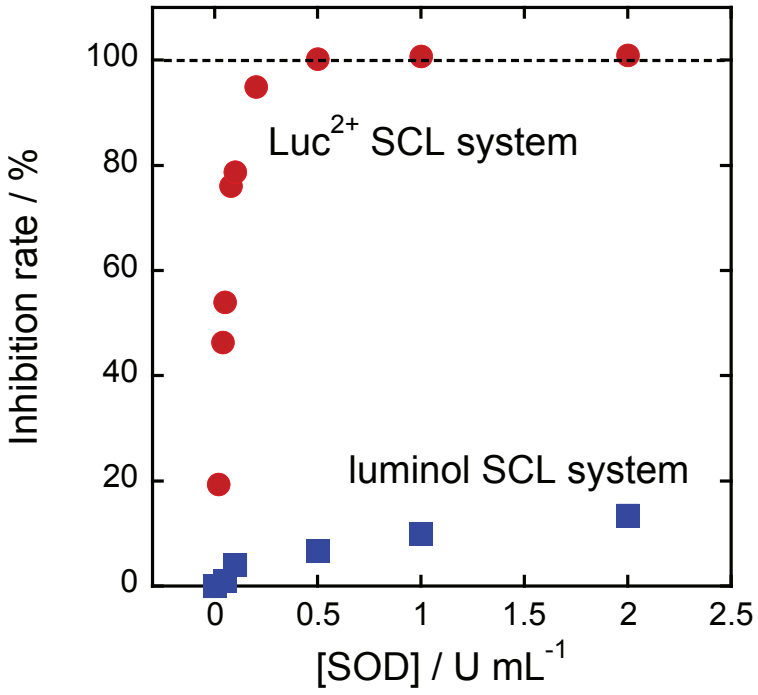

Figure 4-3 Dependence of SOD concentration on the SCL inhibition rate (%).

The presence of other water-soluble antioxidants, such as ascorbic acid, caffeic acid, Trolox, and quercetin, produced the same effect. The main feature of the SCL method is the combining of the simple and reliable sonochemical method for $O_2\cdot^-$ generation with a sensitive chemiluminescence detection.

4.3.3 Kinetic aspects involved in the Luc^{2+} SCL system

In this study, a sonochemical system was used as a source of $O_2\cdot^-$ generation. When $O_2\cdot^-$ is generated in the Luc^{2+} and antioxidant (X) system, two competitive reactions occur: the light emitting reaction of Luc^{2+} with $O_2\cdot^-$ and the scavenging reaction of $O_2\cdot^-$ by X. The scheme of the competitive reaction is shown in Fig. 4-5.

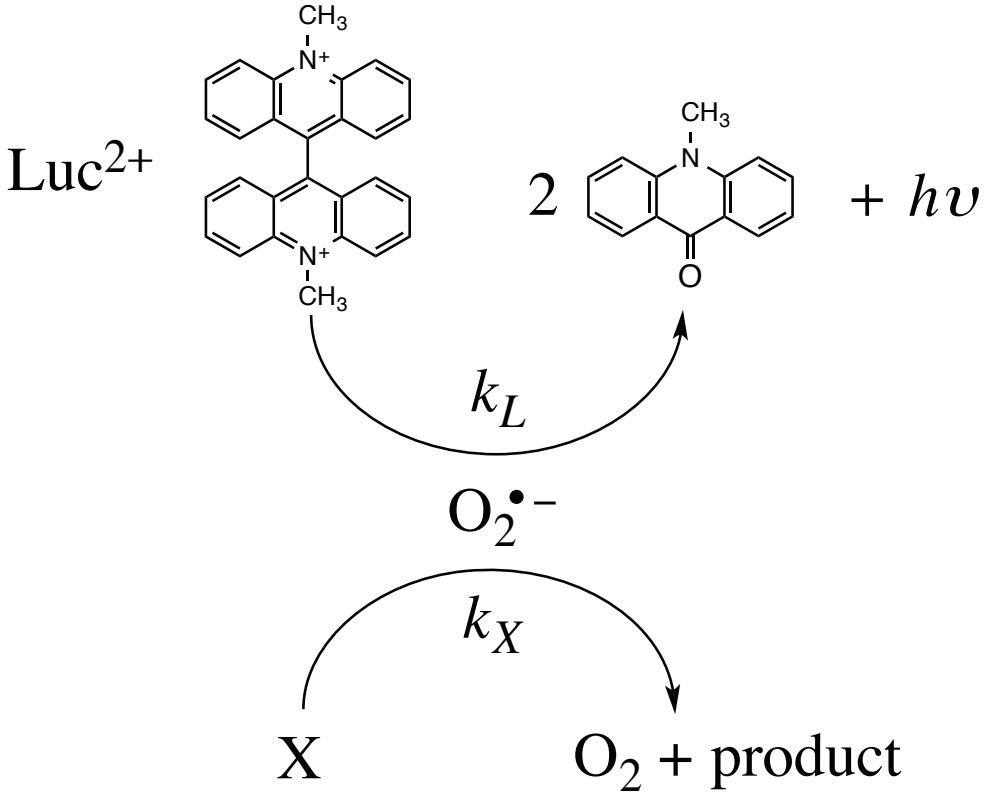

Fig. 4-4 Scheme of competitive reaction around $O_2\cdot^-$ by Luc^{2+} and X. X denotes the antioxidant.

The method of kinetic competition was used to determine the rate constant, which is also one of the evaluation methods for antioxidant capacity. In the scheme shown in Fig.4-4, the rate equations for the removal of $O_2\cdot^-$ and the consumption rate of Luc^{2+} are expressed by Eqs. 4-5 and 4-6, respectively [12].

$$-\frac{d[O_2^{\cdot-}]}{dt} = k_L[O_2^{\cdot-}][Luc^{2+}] + k_x[O_2^{\cdot-}][X] \quad (4\text{-}5)$$

$$-\frac{d[Luc^{2+}]}{dt} = k_L[O_2^{\cdot-}][Luc^{2+}] \quad (4\text{-}6)$$

where k_L and k_x are the second order reaction rates of the reaction of Luc^{2+} and antioxidant X with $O_2\cdot^-$.

Dividing Eq. 4-5 by Eq. 4-6, one obtains Eq. 4-7.

$$\frac{d[O_2^{\cdot-}]/dt}{d[Luc^{2+}]/dt} = 1 + \frac{k_x[X]}{k_L[Luc^{2+}]} \quad (4\text{-}7)$$

The SCL intensity was found to be proportional to the Luc^{2+} concentration (up to 50 μM). At a sufficient level of Luc^{2+}, and in the absence of antioxidant X, the consumption rate of $O_2\cdot^-$ is equal to the rate of superoxide generation $d[O_2\cdot^-]/dt$, which is the consumption rate of Luc^{2+} $d[Luc^{2+}]/dt$. SCL intensity from the Luc^{2+} system is proportional to the consumption rate of Luc^{2+}. Thus, if I_{SCL}^0 and I_{SCL}^X represent SCL intensity in the absence and presence of X, respectively, Eq. 4-7 becomes

$$\frac{I_{SCL}^0}{I_{SCL}^x} = 1 + \frac{k_x[X]}{k_L[Luc^{2+}]} \quad (4\text{-}8)$$

When we plot I_{SCL}^0/I_{SCL}^x as a function of the concentration ratio $[X]/[Luc^{2+}]$, the plot becomes linear with a slope of k_X/k_L and an intercept of unity. The plot for Trolox

is shown in Fig. 4.5. We also plotted the other antioxidants but these plots became curved at high antioxidant concentrations; therefore, we approximated these as linear at low concentration. We used a k_L value of 1.054×10^6 mol^{-1} L s^{-1}, as obtained from a non-enzymatic CL study [13].

The rate constants for the reaction of $O_2^{\bullet -}$ with a test antioxidant were obtained by competitive kinetic analysis as follows. The slope k_X/k_L was 4.396, and the k_X of Trolox was calculated as 4.63×10^6 mol^{-1} L s^{-1}. The k_X values of the other antioxidants were calculated by plotting in the same manner as for Trolox. These results are summarized in Table 4.1.

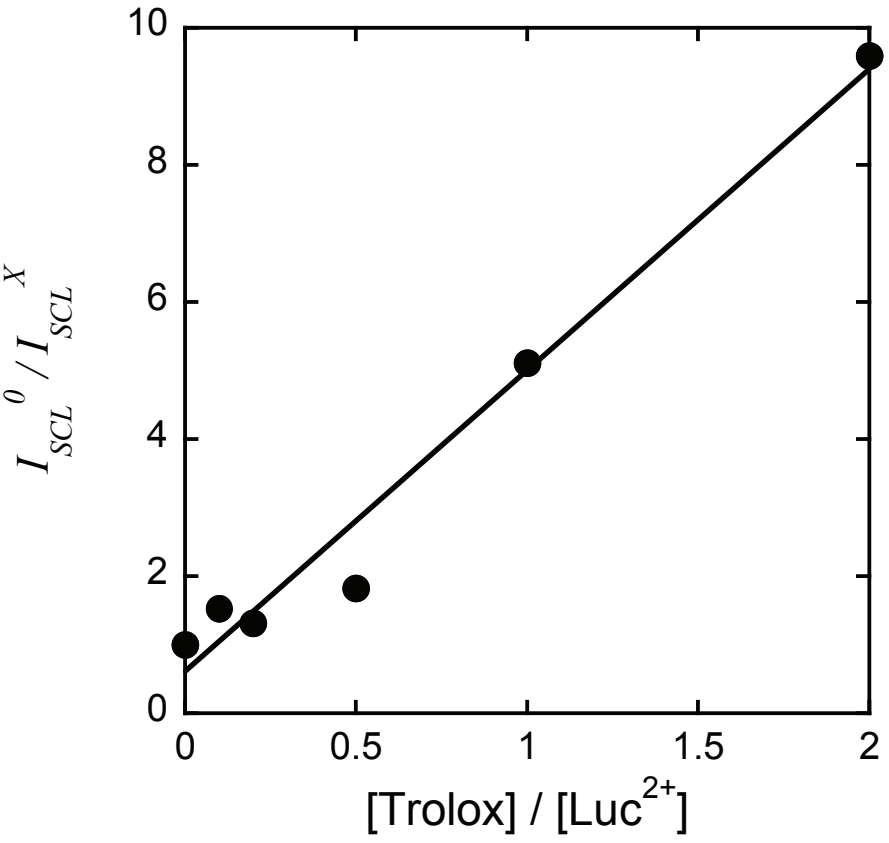

Fig. 4-5 Plot and approximate linear regression of ($I_{SCL}^{\ 0}/I_{SCL}^{\ x}$) vs. ([Trolox]/[$Luc^{2+}$]). Concentration of Luc^{2+} was 50 μM.

Table 4.1 Calculated k_X and K_{ao} values from the SCL method

Compunds	k_x / mol^{-1} L s^{-1}	K_{ao} / U $mmol^{-1}$
Caffeic acid	2.58×10^7	0.021
Protocatechuic acid	8.15×10^6	0.008
Quercetin	3.89×10^6	0.007
Rutin	2.16×10^6	0.003
Trolox	4.63×10^6	0.002

4.4 Conclusions

Based on the data obtained in this Chapter, the described Luc^{2+} SCL method provides some potentially interesting findings: (1) *in situ* and reagentless ROS generation shows the promise of a homogeneous reaction between an antioxidant and ROS without mixing or diffusion processes; (2) simultaneous SCL detection contributes fast and sensitive signal measurements; (3) using the steady state portion of the SCL dynamic curve, it is possible to obtain kinetic information on the reaction between the antioxidant and $O_2\cdot^-$; and 4) analyses are achieved with simple instrumentation and common reagents. In conclusion, the developed SCL method provides an alternative for antioxidant capacity analysis, especially for the high-throughput screening of potential antioxidants.

References

[1] H. E. Seifrieda, D. E. Andersonb, E. I. Fishera and J. A. Milnera, A review of the interaction among dietary antioxidants and reactive oxygen species, *J. Nutr. Biochem.* **18** (2007) 567.

[2] M. Carocho and I. C.F.R. Ferreira, A review on antioxidants, prooxidants and related controversy: Natural and synthetic compounds, screening and analysis methodologies and future perspectives, *Food Chem. Toxicol.*, **51** (2013) 15.

[3] J. M. McCord and I. Fridovich, Superoxide dismutase an enzymic function for erytherocuprein (hemocuprein), *J. Biol. Chem.*, **244** (1969) 6049.

[4] C. Beauchamp and I. Fridovich, Superoxide dismutase: Improved assays and an assay applicable to acrylamide gels**,** *Anal. Biochem*., **44**, 276 (1971).

[5] H. Zhao, S. Kalivendi, H. Zhang, J. Joseph, K. Nithipatikom, J. Vásquez-Vivar and B. Kalyanaraman, Superoxide reacts with hydroethidine but forms a fluorescent product that is distinctly different from ethidium: potential implications in intracellular fluorescence detection of superoxide, *Free Radic. Biol. Med.*, **34** (2003) 1359.

[6] B. Tang, L. Zhang and L.-L. Zhang, Study and application of flow injection spectrofluorimetry with a fluorescent probe of 2-(2-pyridil)-benzothiazoline for superoxide anion radicals, *Anal. Biochem.*, **326** (2004) 176.

[7] A. Renè, M. L. Abasq, D. Hauchard, and P. Hapiot, How do phenolic compounds react toward superoxide ion? A simple electrochemical method for evaluating antioxidant capacity, *Anal. Chem.*, **82** (2010) 8703.

[8] C. Bourvellec, D. Hauchard, A. Darchen, J. L. Burgot and M. L. Abasq, Validation of a new method using the reactivity of electrogenerated superoxide radical in the antioxidant capacity determination of flavonoids, *Talanta*, **75** (2008) 1098.

[9] A. Ogawa, H.Arai, H. Tanizawa, T. Miyahara, and T. Toyo'oka, On-line

screening method for antioxidants by liquid chromatography with chemiluminescence detection. *Anal. Chim. Acta*, **383**, 221-230 (1999).

[10] X. Wei, C. Liu and Y. Tu, Microemulsion-enhanced electrochemiluminescence of luminol-H_2O_2 for sensitive flow injection analysis of antioxidant compounds, *Talanta*, **94** (2012) 289.

[11] M. M. J. Oosthuizen, M. E. Engelbrecht, H. Lambrechts, D. Greyling and R, D. Levy, The effect of pH on chemiluminescence of different probes exposed to superoxide and singlet oxygen generators, *J. Biolumin. Chemilumin.*, **12** (1997) 277.

[12] E. Finkelstein, G. M. Rosen and E. J. Rauckman, Spin Trapping. Kinetics of the Reaction of Superoxide and Hydroxyl Radicals with Nitrones, *J. Am. Chem. Soc.*, **102** (1980) 4994.

[13] D. Taubert, T. Breitenbach, A. Lazar, P. Censarek, S. Harlfinger, R. Berkels, W. Klaus and R. Roesen, Reaction rate constants of superoxide scavenging by plant antioxidants, *Free Radic. Biol. Med.*, **35** (2003) 1599.

Chapter 5

Conclusions and Future Prospects

As was described in Chapter 1, excessive amounts of ROS may be harmful because they can attack biological macromolecules, giving rise to protein, lipid, and DNA damage. Recently, antioxidants have attracted considerable attention because of their tissue protecting effects via the neutralization of ROS. Phenolic antioxidants are important classes of natural antioxidants. Antioxidant activity evaluation has therefore attracted much interest in many fields, not only in food chemistry, but also in nutrition research and clinical medicine. In this thesis, fundamental studies on ECL and SCL systems for Luc^{2+} were carried out for the purpose of developing a reliable analytical tool for antioxidant activity evaluation. This study provides chemical information about methods for clarifying the reaction mechanisms, scavenging efficiency, and kinetic scavenging rates of antioxidants. Moreover, it will aid in the identification of reactive species and allow quantification of the extent of antioxidant scavenging using various assays. In addition, this study will improve the comparability of the results and make them more understandable, as well as bringing a more rational basis to the evaluation of these assays. To expand our understanding of the ECL reaction, analyses of the detailed reaction mechanism and its application to the determination of selected co-reactants were carried out.

In Chapter 2, a novel and non-enzymatic method for studying the free radical-scavenging properties of the phenolic compounds against superoxide ion ($O_2 \cdot^-$) by using cathodic electrochemiluminescence (ECL) of lucigenin (Luc^{2+}) was reported for the first time. The ECL of Luc^{2+} at a glassy carbon (GC) electrode was observed in an aeration electrolytic solution (pH 7). This was considered to be due to the reaction of the one-electron reduced form of Luc^{2+} (i.e., a radical cation, $Luc \cdot^+$) with *in situ* electrogenerated $O_2 \cdot^-$. It was demonstrated that the ECL signals of Luc^{2+} would be

suppressed in the presence of phenolic compounds due to the elimination of $O_2\cdot^-$ by these compounds. The ECL inhibition rate (%) measured at each concentration was compared against the SOD equivalent (U mL^{-1}), and the relative antioxidant efficiency, K_{ao} (U $mmol^{-1}$ equivalent SOD), was used to evaluate the antioxidant activity of phenolic compounds. Because $O_2\cdot^-$ was electrogenerated by the one-electron reduction of dioxygen, the method involves neither enzymes nor chelating metals (which are usually required in methods for testing superoxide scavenging capacity). Consequently, this method was proven to be able to specifically measure the radical scavenging efficiency of phenolic compounds toward $O_2\cdot^-$ in aqueous solution.

In Chapter 3, the SCL behavior of lucigenin (Luc^{2+}) was studied in aqueous solutions irradiated with 500 kHz ultrasound. Compared with the SCL of a luminol system, a markedly increased SCL intensity was observed in 50 μM Luc^{2+} aqueous solution (pH 11) when small amounts of co-reactants such as 2-propanol coexsisted. It has been shown that SCL intensity strongly depends on the presence of dissolved gases such as air, O_2, N_2, and Ar. The highest SCL intensity was obtained in an O_2 saturated solution, indicating that molecular oxygen is required to generate SCL. Since SCL intensity is quenched completely in the presence of superoxide dismutase (SOD) (an enzyme that can catalyze the disproportionation of $O_2\cdot^-$), the generation of $O_2\cdot^-$ in the ultrasonic reaction field is important in the SCL of Luc^{2+}. In this work, the evidence for $O_2\cdot^-$ production was examined by a spectrofluorometric method using 2-(2-pyridyl) benzothiazoline as the fluorescent probe. The results indicated that the yield of $O_2\cdot^-$ was markedly increased in O_2-saturated solutions when a small amount of 2-propanol coexists, which was consistent with the results of the SCL measurements. 2-propanol in the interfacial region of a cavitation bubble reacts with a hydroxyl radical ($^{\bullet}OH$) to form

a 2-propanol radical, $CH_3C^{\bullet}(OH)CH_3$, which could subsequently react with dissolved oxygen to generate $O_2^{\bullet -}$. The most likely pathways for SCL, as well as the spatial distribution of SCL in a microreactor, were discussed in this Chapter.

In Chapter 4, the application of the SCL method to antioxidant activity analysis was described. Based on the data obtained in this Chapter, ROS generated by ultrasonic irradiation can react with Luc^{2+} or luminol to produce SCL. The presence of an antioxidant, such as SOD or Trolox, quenched the ROS, which in turn quenched the SCL. The Luc^{2+} SCL system was found to be more specific and sensitive for $O_2^{\bullet -}$. By using the steady state portion of the SCL dynamic curve, it was also possible to obtain kinetic information on the reaction between the antioxidant and $O_2^{\bullet -}$. The main feature of the SCL method is the combination of a simple and reliable sonochemical method for $O_2^{\bullet -}$ generation with very sensitive chemiluminescence detection.

Both ECL and SCL provided potential benefits: (1) *in situ* and reagentless ROS generation shows the promise of a homogeneous reaction between an antioxidant and ROS without mixing or diffusion processes; (2) simultaneous SCL detection provides fast and sensitive signal measurement; and 3) analysis can be achieved with simple instrumentation and common reagents. To address the problem of the pH dependence of radical scavenging antioxidant activity, future work will focus on the combination of ECL or SCL detection systems with a flow injection analysis system so that ROS generation and detection can be performed at different pH values.

List of Publications

I Original papers

1. Application of Electrochemiluminescence for the Evaluation of the Antioxidant Capacity of Some Phenolic Compounds Against Superoxide Anion Radicals
   Masanori Matsuoka and Jiye Jin, *Analytical Sciences*, 31 (2015) 629.

2. Sonochemiluminescence from Lucigenin in an Aqueous Solution Using Alcohols as Coreactant
   Masanori Matsuoka and Jiye Jin, *Chemistry Letters*, 44 (2015) 1759.

3. Sonochemiluminescence of lucigenin: Evidence for superoxide radical anion formation by ultrasound irradiation
   Masanori Matsuoka, Fumiki Takahashi, Yoshiyuki Asakura and Jiye Jin, *The Japanese Journal of Applied Physics*, 55 (2016) 07KB01.

4. ルシゲニン水溶液におけるソノケミルミネッセンスの観測
   松岡聖典, 高橋史樹, 朝倉義幸, 金継業, *日本ソノケミストリー学会誌*, 10 (2016) 8.

5. ルシゲニンのソノケミルミネッセンス: 超音波によるスーパーオキシドラジカルアニオンの生成反応
   金継業, 松岡聖典, *超音波テクノ*, Vol. 28(3-4), 印刷中.

II. International Symposium (oral)

1. Electrochemiluminence Method for Evaluating Antioxidant Capacity Of Phenolic Compounds Toward Superoxide Radical Ion
   Masanori Matsuoka and Jiye Jin, 3rd International Young Scientists Conference on Analytical Sciences (IYSCAS III), Andalas Univ., Indonesia, 2014 (Sep. 23)

2. Sonochemiluminescence of Lucigenin in an Aqueous Solution Using Alcohol as Coreactant
   Masanori Matsuoka, Yoshiyuki Asakura, and Jin Jiye, The 36th Symposium on Ultrasonic Electronics (USE2015), Tsukuba, Japan, 2015 (Nov. 05)

II. Domestic Symposium

1. ナノ構造を有する金電極におけるルシゲニンの電気化学発光挙動
   松岡 聖典, 金 継業, 日本分析化学会第 62 年会, 近畿大学, 2013 年 9 月 10 日-12 日 (9 月 12 日)

2. 活性酸素種の電気化学発光を利用したフェノール類化合物の抗酸化能評価法の開発
   松岡 聖典, 金 継業, 日本分析化学会第 63 年会, 広島大学, 2014 年 9 月 17 日-19 日 (9 月 18 日)

3. ルシゲニンのミセル増感化学発光法によるフェノール類化合物の抗酸化能評価

   松岡 聖典, 金 継業, 第 75 回分析化学討論会, 山梨大学, 2015 年 5 月 23 日-24 日 (5 月 24 日)

4. ルシゲニン水溶液におけるソノケミルミネッセンスの観測

   松岡 聖典, 髙橋 史樹, 朝倉 義幸, 金 継業, 第 24 回ソノケミストリー討論会, 大阪府立大学, 2015 年 10 月 23 日-24 日 (10 月 23 日)

Acknowledgements

I express my sincere gratitude and appreciation to **Professor Jiye Jin**, Department of Chemistry, Faculty of Science, Shinshu University, for his continuous instruction with large support, important advice, and fruitful encouragement thorough my doctoral course in Shinshu University.

I also express my earnest thankfulness to **Professor Teruo Hinoue**, **Associate Professor Hirosuke Tatsumi**, **Assistant Professor Fumiki Takahashi,** Department of Chemistry, Faculty of Science, Shinshu University, and **Dr. Yoshiyuki Asakura,** Honda Electronics Co., for their valuable discussions and precious suggestions.

The contributions of colleagues of Professor Jiye Jin's laboratory for carrying out some experiments in this work are sincerely acknowledged.

I would like to express my thanks to the member of the section of the academic situation that improved the school life in my study of Shinshu University.

Finally, I would like to extend my gratitude and appreciation to my father, **Takao Matsuoka**, my mother, **Kimiko Matsuoka**, my grandmother, **Mitsuko Sekiguchi**, my brother, **Hiroyuki Matsuoka** and my sister **Yui Matsuoka** for their kind supports at any time.

May 2016

Matsuoka Masanori